Role of HIV-1 Nef dimerization in SERINC5 restriction factor antagonism and Src-family kinase recruitment

by

Ryan Staudt

B.S., Pennsylvania State University, 2014

Submitted to the Graduate Faculty of the

School of Medicine in partial fulfillment

of the requirements for the degree of

Doctor of Philosophy

University of Pittsburgh

2020

UNIVERSITY OF PITTSBURGH

SCHOOL OF MEDICINE

This dissertation was presented

by

Ryan Staudt

It was defended on

July 17, 2020

and approved by

Robert Binder, Ph.D., Associate Professor, Department of Immunology, School of Medicine

Lori Emert-Sedlak Ph.D., Research Assistant Professor, Department of Microbiology and Molecular Genetics, School of Medicine

Lawrence Kane, Ph.D., Professor, Department of Immunology, School of Medicine

Nicolas Sluis-Cremer, Ph.D., Professor, Department of Medicine, Division of Infectious Diseases

Dissertation Director: Thomas E. Smithgall, Ph.D., Professor and Chair of Microbiology and Molecular Genetics, School of Medicine

Copyright © by Ryan Staudt

2020

For Shirley Staudt

Role of HIV-1 Nef dimerization in SERINC5 restriction factor antagonism and Src-family kinase recruitment

Ryan Staudt, PhD

University of Pittsburgh, 2020

The HIV-1 Nef accessory protein plays a prominent role in viral pathogenesis, immune evasion of HIV-infected cells, and AIDS progression. Nef lacks intrinsic biochemical activity, and instead functions through interactions with multiple host cell effector proteins. Previous studies have shown that Nef homo-dimerizes at a hydrophobic interface between two Nef molecules. As Nef dimerization has been implicated in several Nef functions, it may represent a novel and effective target for antiretroviral drug development. Research that further expands our understanding of Nef dimerization may aid in the development of future therapeutics.

Therefore, for the first part of my dissertation, I explored the role of Nef dimerization in Nef antagonism of the host restriction factor SERINC5. We showed that Nef homodimers are required for the AP-2 dependent downregulation of SERINC5, trafficking to late endosomes, and exclusion from newly synthesized viral particles. Disruption of Nef dimerization impaired antagonism of SERINC5, rescuing SERINC5 inhibition of viral infectivity. In addition, dimerization-defective Nef mutants retained interaction with both SERINC5 and AP-2 by fluorescence complementation assay, suggesting that the Nef dimer bridges SERINC5 with AP-2 to drive endocytosis of cell-surface SERINC5.

For the second part of my dissertation, I examined the dynamics and individual contribution of predicted dimer-stabilizing residues towards dimerization and complex formation in solution. Crystal structures have revealed distinct orientations of the Nef dimer interface within

complexes of Nef bound to Src family kinase SH3 domain vs. Nef complexes bound to SH3-SH2 domain. I was able to validate the orientation of the dimer interface captured in each structure using biophysical and biochemical studies. As part of a collaborative study, I was able to confirm that Nef Asp123 contributes to Nef dimerization within the SH3-bound but not the SH3-SH2 bound structure of Nef. I also identified a Nef residue (Tyr115) that stabilizes Nef dimerization within both complexes, suggesting that it is a consistent feature of Nef dimerization across two potential stages of kinase domain engagement. Taken together, this dissertation helps to further illuminate the mechanics of Nef dimerization, and implicates Nef dimerization in one of the more recently discovered Nef functions: Nef antagonism of SERINC5.

Table of Contents

List of Figures

Acknowledgements

It's been a strange experience wrapping up my dissertation over the last few months, spending all day writing about one virus while our lives are influenced by the activity of another. The graduate school and research environment I'll be rejoining after my defense is very different from the environment that I left in March, and it's difficult to not feel the weight of finality which accompanies that fact. But with that sense of finality is a great deal of nostalgia, and strong gratitude for everything and everyone that helped me reach this point in my graduate school career.

I'd first like to thank my advisor Dr. Thomas Smithgall for creating an endlessly supportive and engaging research environment. You've taught me so much about life and science over the last few years, and I've always appreciated how you constantly make yourself available to your students and staff. While research is always marked by frustrating results and roadblocks, your positive and hopeful attitude always helped rejuvenate me and keep me motivated. I also really appreciate how much you supported my various attempts to develop myself professionally and explore new opportunities.

I'd like to thank my committee- my dissertation chair and first lab rotation mentor, Dr. Lawrence Kane, as well as Dr. Robert Binder, Dr. Lori Emert-Sedlak, and Dr. Nicolas Sluis-Cremer. Your expertise over the few last years has been essential for this project, and I sincerely appreciate the feedback, guidance, and time you've shared with me.

Thank you to Dr. John Engen and Dr. Jamie Moroco at Northeastern University for letting me collaborate on our previous study. I am also grateful to everyone on the 5th floor of Bridgeside Point II who has supported me in some way- Kristin DiGiacomo, Jamie Huffman, Zhou Zhong, Chris Kline, Joe Llaneza, Joanne Polk, JV, Mary Lou Meyer. Thank you to the School of Public

Health for funding me on the Pittsburgh AIDS Research Training Grant. And thanks to the faculty and staff of the Molecular Pharmacology Training Program including Shannon Granahan, Dr. Bruce Freeman, Dr. Patrick Pagano, Dr. Tija Jacob, and Dr. Guillermo Romero. I am also grateful to the Sluis-Cremer and Ambrose labs for helping to expand my HIV knowledge and perspective through our joint lab meetings.

Of course, many thanks to members of the Smithgall lab (past and present), which often felt like a surrogate family for me throughout my time in Pittsburgh. Their scientific contributions and emotional support to my graduate career cannot be overstated. Dr. Lori Emert-Sedlak- thank you for your mentorship and letting me "darken your door" with questions, I would not be half the scientist I am without your support and expertise. Dr. John Jeff Alvarado- thank you for supporting me and for always brightening up the lab with a joke or a song (you ask everyone about their "rock star scientist", but you showed me what one looks like). Dr. Sherry Shu- I've always looked up to your hard work and intelligence, and your advice and "deer stories" were important parts of my graduate school experience. Dr. Haibin Shi- thank you for teaching me everything I know about SPR, and for your constant and cheerful presence in the lab. Dr. Li Chen- thank you for everything you do to keep the lab running, and I appreciate your virology advice and the occasional Tzm-bl passage. Dr. Shoucheng Du- I admire your work ethic and contributions to the lab, and it's been a pleasure getting to know you over the last few years. To Kiera Regan- thank you for everything you do for the lab, you have a bright career ahead of you. To Manish Aryal and Ari Selzer- I'm so glad I could go through the lab with you guys, and I appreciate being able to always bounce first draft experimental ideas and hypotheses off you, since you both offer such thoughtful feedback. It's been an honor to celebrate and commiserate our research highs and lows together (hopefully we can shoot pool again once we get out of this).

Thank you to my former labmates, especially Winson Fai Li and Dr. Jerrod Poe, who helped me get acquainted with BiFC and confocal microscopy. A big thank you to Dr. Ravi Patel for your constant friendship and advice, it was so helpful to move through the Pharmacology program and lab at the same time as you. Additional thanks to Dr. Heather Rust, Dr. Prerna Grover, Dr. Mark Weir, Kindra Whitlach, Kecey Shen, Eleanor Johnston, Julia Reece, and my former mentees in the lab (Sarah Colon, Richard Potter, and Austin Summers).

Thank you to everyone who at Penn State who set me on this path, especially Dr. Pamela Hankey Giblin for giving me my first start in research, and to Mike Quickel for sharing your knowledge and enthusiasm for research with me at a critical time in my life. Also, thanks to Dr. Nicole Wilski for your friendship, I'm glad that we could go on our scientific journeys at the same time and learn from each other's experiences.

Outside of the academia, I'd like to thank all my friends and family for being a part of my life- and for being understanding when the occasional experiment intruded on set plans. A huge thanks to my parents and stepdad for their support and inspiration- your hospital conversations around the dinner table helped spark my interest in biomedical science. I'd also like to thank the friends I've made in graduate school for six years of friendship and inspiration, especially Dr. Dillon Kunkle, Dr. Emily Beckwitt, Dr. Tiffany Bernardo, and Dr. Josh Lorenz. My gratitude towards Larry Hailsham, Michael McDaniels, and James McKay for being fantastic neighbors and friends.

And greatest thanks to my partner Amy Del Rio for being my biggest supporter, especially during these last few challenging months. I can't imagine my life without you, and while I am grateful I came to Pittsburgh due to the education and experience I've received, meeting you was

absolutely the most important and consequential result of that decision. As uncertain as the future is right now, it is a constant comfort to know that I'll be spending it with you.

-Ryan Staudt

1.0 Introduction

1.1 Human Immunodeficiency Virus (HIV-1)

1.1.1 History and Global Burden of HIV/AIDS

The shadows of the human immunodeficiency virus (HIV) epidemic first appeared in 1981 within a corner of the Center for Disease Control's *Morbidity and Mortality Weekly Report (MMWR)*. One article within the June 5th report recounted the appearance of *Pneumocystis carinii* pneumonia within five men in the Los Angeles area, a diagnosis commonly found within severely immunosuppressed patient populations (*1*) but unexpected for healthy men in their 20s and 30s (*2*). This localized outbreak of *P. carinii* pneumonia was unique enough to warrant reporting within the medical literature, and so a case report outlining the symptoms, medical history, and outcomes of these patients was written and published within the MMWR. Without realizing it, the authors penned the first description of what would become HIV/AIDS in the medical literature, suggesting *"*the possibility *of a cellular-immune dysfunction related to a common exposure that predisposes individuals to opportunistic infections."*

That "common exposure" continued to spread across the United States, manifesting as opportunistic infections, the rare cancer Kaposi's Sarcoma, non-Hodgkin's lymphoma (*3*). In 1982, the CDC settled on a term to describe this mysterious immunosuppression and the assortment of opportunistic conditions that characterized it - Acquired Immunodeficiency Syndrome or AIDS (*4*). The causative agent of AIDS, the Human Immunodeficiency Virus (HIV),

would be identified just one year later by the laboratory of Dr. Luc Montagnier (*5*), providing researchers a definitive target to combat AIDS.

HIV transmission peaked in the United States during 1984-1985, with nearly 130,000 new cases reported each year (*6*). This number began to recede as HIV testing and prevention efforts became more widespread (*7, 8*). Today, the number of new HIV infections within the US has dropped to 37,000 each year (*9*), but the disease burden of HIV is still keenly felt across the world. There are almost 38 million people infected with HIV worldwide, and each year brings over 700,000 HIV-related deaths and 1.7 million new infections (*10*). HIV has particularly devasted regions of southern and eastern Africa, where over half of current HIV infections currently exist (*10*).

1.1.2 Background on human and simian retroviruses

> *"HIV hasn't happened to humanity just once. It has happened at least a dozen times—a dozen that we know of, and probably many more times in earlier history. It wasn't a singular piece of vastly unlikely bad luck, striking humankind with devastating results—like a comet come knuckleballing across the infinitude of space to smack planet Earth and extinguish the dinosaurs. No. The arrival of HIV in human bloodstreams was, on the contrary, part of a small trend. Due to the nature of our interactions with African primates, it seems to occur pretty often."*
>
> — David Quammen, Spillover: Animal Infections and the Next Human Pandemic (*11*)

The global HIV pandemic can be linked primarily to viruses within the main group (Group M) of HIV-1, and it is this lineage that is responsible for over 97% of HIV infections around the world today (*12*). Group M can be further broken down into at least 9 subtypes or clades-A, B, C, D, F, G, H, K, and potentially a newly discovered L subtype (*13*). The most prevalent subtype is clade C, which makes up nearly half of HIV infections and circulates within Eastern and Southern Africa. However, most HIV research has centered around HIV-1 Clade B, which represents only 11% of global HIV-1 infections, and is found within the Americas, Western Europe, East Asia, and Oceania (*14, 15*). Initial human transmission of HIV-1 Group M can be traced to a region of Central Africa within the Democratic Republic of Congo during the early 20th century (*16*), and the earliest evidence of human HIV-1 infection is a 1959 sample from this area (*17*). Although it is unclear when and where HIV-1 Group M first crossed over from non-human primate hosts, the high similarity of HIV-1 Group M to a simian immunodeficiency virus (SIV) strain that infects chimpanzees (SIVcpz) within southeast Cameroon suggests the initial zoonotic transmission occurred within that region (*18, 19*).

HIV-1 Group M has rightfully commanded scientific attention over the last forty years, but the existence of other pathogenic lineages of HIV demonstrates that the arrival of HIV is the product of a consistent zoonotic interplay between humans and other primates (*20*). Over 40 primate species have been shown to harbor SIV infections, and each species typically harbors their own strain of the virus without the onset of pathogenesis (*21*). However, instances of cross-species transmission of SIV into humans has led to the creation of over a dozen different lineages of pathogenic HIV. In addition to Group M, there are three viral lineages from three separate transmission events that encompass HIV-1- Groups N (new), O (Outlier) and P (Pending)(*18*). Group N is also believed to have originated from chimpanzees within Cameroon, however, its

origin is distinct from Group M, and fewer than 20 human infections have been identified to date (*22*). The final two groups of HIV-1, Group O and P, appear to be closely related to strains of SIV native to Western lowland gorillas (*23*). Group O is the second most common lineage of HIV-1 to infect humans, however, it represents fewer than 1% of total HIV-1 infections (*23*). Group P is the rarest form of HIV-1, and has been isolated from only two patients to date (*20*).

While HIV-1 is the product of four separate instances of zoonotic transmission between humans and primates, the distantly related HIV-2 is believed to be comprised of nine separate transmission events (Groups A to I). HIV-2 is responsible for the final 1 to 2 million of the world's HIV infections (*24, 25*), and though it causes AIDS in infected humans, it consistently displays reduced transmission and a lower rate of AIDS progression compared to HIV-1 (*25*). Overall nucleotide sequence homology hovers around 40% between both viruses (*26*), and early characterization of HIV-2 showed that it was serologically dissimilar enough to strains of HIV-1 to warrant its own classification (*27*).

In contrast, HIV-2 has a greater degree of sequence homology with SIV, a link which served as one of the earliest pieces of evidence that HIV was of simian origin (*28*). Around the time that HIV-2 was initially isolated, the first strain of SIV was discovered from a research colony of rhesus macaques suffering from simian AIDS (SIVmac)(*29*). Serologic analysis of HIV-2 showed greater reactivity for serum isolated from SIVmac-infected macaques than for serum isolated from HIV-1 infected humans, suggesting a close relationship between HIV-2 and SIVmac (*27*). Interestingly, SIVmac is not endemic to rhesus macaques, but derives from a lineage of SIV that infects sooty mangabeys (SIVsmm). SIVmac was itself the product of a cross-species transmission between research primates used during the 1970s (*30*). It is a fascinating coincidence

that both HIV-2 and SIVmac, two separate zoonotic transmissions of SIVsmm into two distinct primate species, were discovered within the span of just three years.

1.1.3 HIV-1 Genome

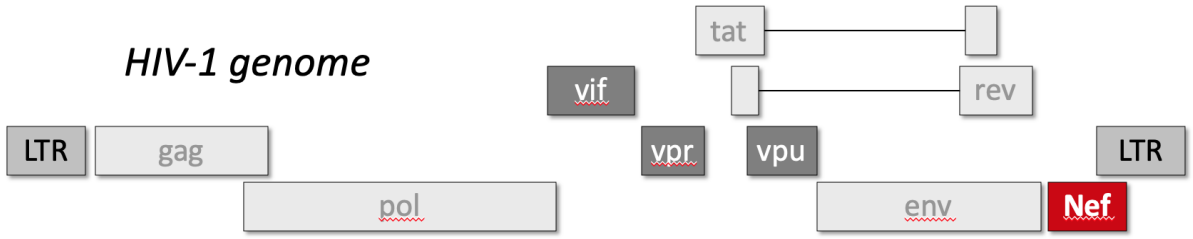

Figure 1: Organization of the HIV-1 Genome

Schematic illustrating the 9kb HIV-1 genome, which is organized into nine open reading frames encoding 15 proteins. Highlighted in dark gray (Vif, Vpr, Vpu) and red (Nef) are the HIV-1 accessory proteins.

The HIV-1 genome (Figure 1) is comprised of a 9 kb single-stranded positive sense RNA, and encodes fifteen proteins across nine open reading frames (*31*).These open reading frames are flanked on either side by the 5' and 3' Long Terminal Repeats (LTR), which contribute to viral transcription and insertion of the HIV-1 proviral DNA into the genomes of infected cells (*32*, *33*).The three fundamental genes common to HIV-1 and all retroviruses are those that encode Pol, Gag, and Env, the polyprotein precursors to all structural and enzymatic HIV proteins.

The Gag polyprotein (p55) bundles together the major structural proteins of HIV-1 and is recruited to the host cell membrane of infected cells via a myristoylated N-terminus. At the host cell membrane, Gag directs recruitment of the viral genome and coordinates budding of the viral lipid membrane. Cleavage of Gag by the HIV protease (PR) initiates virion maturation, and results in the creation of individual structural proteins required to form the viral capsid core (overviewed

in the virion structure section). The primary Gag products are the matrix protein (MA), capsid (CA or p24), and nucleocapsid (NC); however, cleavage by PR also creates two spacer proteins (SP1 and SP2) and the p6 peptide (*34*).

The Pol gene encodes the critical enzymatic machinery that drive HIV replication- the viral protease (PR), reverse transcriptase (RT), and integrase (IN). RT, the enzyme for which the retrovirus family is named, converts single-stranded viral RNA into double-stranded cDNA (*35*). Following reverse transcription, the Pol-derived IN protein catalyzes the insertion of viral cDNA into the host cell genome (*36*), driving viral replication. PR is involved in the processing and maturation of viral proteins, especially the Pol and Gag polyproteins (*37*).

The Env gene expresses the gp160 polyprotein, which in contrast to Gag and Pol is cleaved by the cellular protease Furin instead of PR. Cleavage of gp160 by Furin produces the transmembrane glycoprotein 41 (gp41) and the surface glycoprotein 120 (gp120), which work in tandem to direct viral recognition of host cell receptors (CD4 and CCR5 or CXCR4) and viral fusion with the host cell membrane (*38*).

The HIV genome also encodes two regulatory proteins, the transactivator protein (Tat) and the regulator of virion expression (Rev). Tat amplifies the transcription of integrated viral DNA, accelerating viral replication within infected cells (*39*). The regulator Rev also plays an important role in viral replication, and hijacks the host nuclear export machinery to transport unspliced viral RNA out of the nucleus and into the cytoplasm (*40*).

The final four proteins encoded by HIV are the accessory proteins Vif, Vpr, Vpu, and Nef. These accessory proteins are not required for viral replication but play an important role in viral pathogenesis, immune escape, and viral spread in vivo (*41*). The accessory protein Nef is the major focus of this thesis project and will be explored thoroughly within Section 2 of the introduction.

1.1.4 HIV-1 Structure

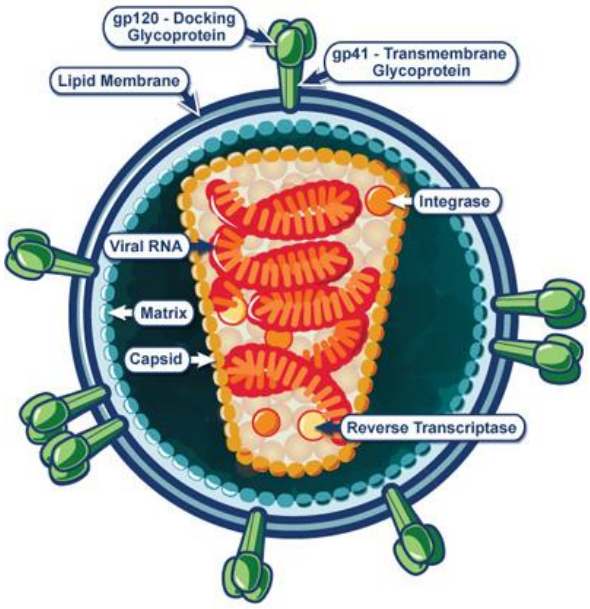

Figure 2: Structure of the HIV-1 Virion

Cartoon illustration of the HIV virion, and a depiction of the structural (MA, CA, gp120/gp41) and enzymatic proteins (RT, IN) that are incorporated into the virus. Figured is adapted from the NIH NIAID website, and is licensed under the Creative Commons Attribution 4.0 International License.

The HIV virion is encapsulated by a lipid envelope roughly 100-120 nm in diameter, and contains two copies of the single-stranded RNA genome surrounded by a conical protein core (*42*). The lipid envelope of HIV originates from the cellular membrane of infected cells, as virions bud off from the host cell membrane following assembly. While budding, HIV inherits any host cell membrane proteins that reside within the borrowed lipid bilayer, some of which have been shown to have a direct impact on HIV infectivity and attachment (*43*, *44*). Env glycoprotein complexes are also incorporated into the viral membrane, which control viral receptor recognition and fusion during viral spread. Three molecules of the gp120 surface protein associate with three molecules of the transmembrane protein gp41 to form the HIV Env spike, and around 72 of these spikes dot the surface of the newly synthesized virion (*38*, *42*).

Directly inside the viral membrane is a shell comprised of 2000-5000 monomers of the matrix (MA) protein, which associate with the viral membrane via an N-terminal myristoylation group and positively charged residues (*45*). Tucked within the MA lattice shell is the conical viral core comprised of 1000-1500 copies of the p24 capsid (CA) protein (*46*). Inside the capsid core lies both copies of the RNA viral genome, which are coated and chaperoned by the nucleocapsid (NC) protein into a stable and tight conformation (*47*). The viral core also incorporates several non-structural viral proteins, including components of the viral replication machinery (RT, PR, and IN) and the accessory proteins Nef, Vpr, and Vpu (*48*).

1.1.5 HIV Life Cycle

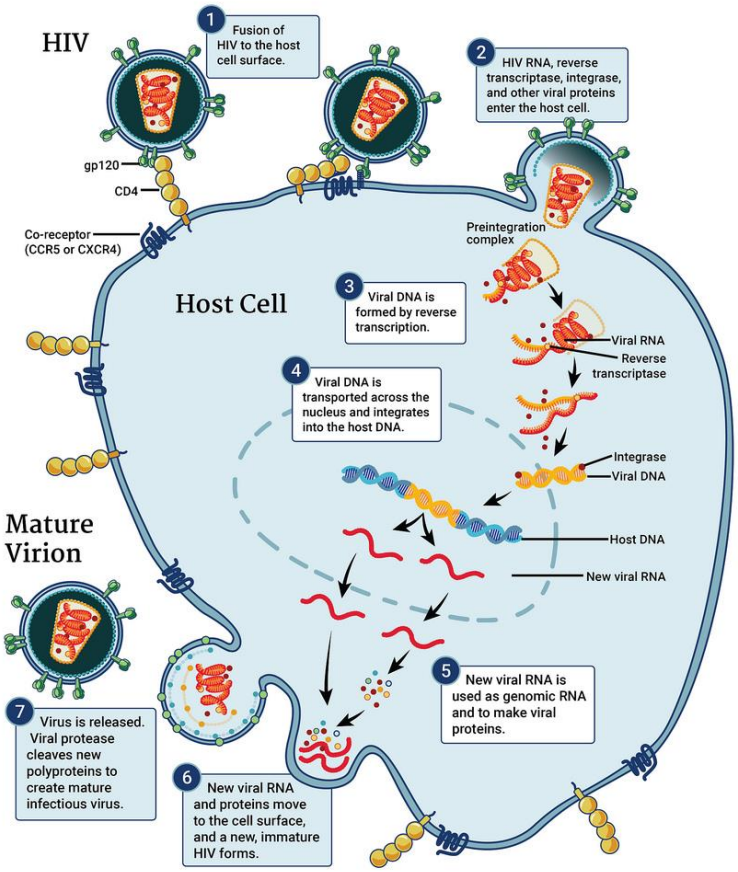

Figure 3: Illustration of the HIV-1 Life Cycle

Depiction of the major stages of the HIV-1 life cycle. 1) Env spike proteins bind to viral receptors and co-receptors on the surface of target cells. Fusion is initiated between the viral membrane and target cell membrane following insertion of the gp41 fusion peptide. 2) The viral core is delivered into the cytoplasm after fusion, and the capsid begins to uncoat. 3) RT is initiated during or after capsid uncoating, viral RNA is transcribed into viral DNA. 4) Integrase mediates the insertion of viral DNA into the host cell genome. 5) Host machinery initiates transcription of proviral DNA, production and export of viral RNA is aided by Tat and Rev. 6) Viral proteins and genome assemble at the cell surface of the infected cell. 7) HIV-1 virion (with host-derived membrane) buds off from infected cells, PR activity processes the immature virion into a mature virus. Figured is adapted from the NIH NIAID website, and is licensed under the Creative Commons Attribution 4.0 International License.

HIV primarily infects CD4+ T lymphocytes and macrophages, but can also infect several other myeloid lineage cells including dendritic cells, osteoclasts, and microglia (*49*). Host cell recognition and viral entry require the receptor CD4, with viral tropism directed by the co-receptor

CXCR4 or CCR5. HIV tropism can be split into three categories- viruses with a preference for CCR5 are classified as R5 or macrophage (M-tropic), CXCR4-preferring viruses are known as X4 or T-lymphocyte tropic (T-tropic), and viruses that can bind to both co-receptors are labeled as X4/R5 viruses (*50*).

Initiation of the viral life cycle begins with the first step of viral entry and fusion- the binding of infectious HIV-1 virions to CD4 through the gp120 component of HIV Env (Figure 2). Engagement of gp120 by CD4 reveals the co-receptor binding site within gp120, allowing for the virion to associate with its preferred co-receptor. Receptor and co-receptor binding by gp120 induce a conformational change within gp41, which initiates the insertion of the gp41 fusion peptide into the cell membrane. The gp41 fusion peptide, now anchored on either side by the viral and cellular membrane, bends into a six-helix bundle that serves as a mechanical lever to trigger membrane fusion. Expansion of the resulting fusion pore between the HIV and cell membranes then allows for the release of the viral core into the cytoplasm (*38*), and begins the next stage of viral infection.

Following fusion and entry, the viral capsid disassembles, and reverse transcription of viral RNA begins within the cytoplasm. Reverse transcription may initiate while the capsid uncoats or immediately following disassembly, however, the exact timing of the two processes is contentious (*51*). During reverse transcription, viral RNA is converted from single-stranded RNA into double-stranded cDNA by reverse transcriptase/RNase H in preparation for nuclear transport and integration. First, RT utilizes host tRNA to synthesize a complementary strand of DNA using the RNA genome strand as a template, forming a DNA-RNA complex which is processed by RNase H. RT then initiates synthesis of the second complementary strand of DNA, resulting in a dsDNA copy of the viral genome that is amenable to insertion into the host cell genome (*35*).

The double-stranded DNA product then associates with viral and cellular proteins to form the pre-integration complex (PIC)(*52*), and is transported into the nucleus of the infected cell. Once inside the nucleus, IN orchestrates the processing and integration of the viral genome into host DNA, starting with the hydrolytic digest of the 3' termini of each strand of viral DNA to create a two-nucleotide overhang. The 3' overhangs within the viral DNA then attack and infiltrate target DNA in a process known as strand transfer, creating an integration intermediate that connects the viral DNA to host chromosomal DNA. Overhangs and nicks created by this process are then resolved by host cell enzymes to yield a single integrated proviral product within host chromosomes (*36*).

In the presence of cellular activation, transcription of the integrated proviral DNA is initiated at the 5' LTR by RNA Polymerase II (RNAPII) and host cell transcription factors. However, efficient generation of full-length transcripts requires engagement of the viral Tat protein with a region within the LTR referred to as the trans-activation response (TAR) element. Tat association with TAR aids transcription elongation, and serves to boost the rate of viral transcription within infected cells (*32, 53*). Transcription yields unspliced full-length transcripts of the HIV-1 genome, as well as spliced and partially spliced mRNAs for viral proteins. While the fully spliced mRNA transcripts are transported into the cytoplasm to initiate early translation of Rev, Tat, and Nef, partially spliced and unspliced viral transcripts (including the viral genome) require the recruitment of the viral Rev protein to be transported out of the nucleus (*54*).

Following translation and post-translational modification within the Golgi, the Gag polyprotein directs assembly of the HIV virion using the uncleaved Gag domains (*55*). The myristoylated MA domain stabilizes Gag association with the cell membrane, and promotes but is

not required for Env incorporation into the virion (*46, 56*). Both copies of the RNA genome are recruited by the NC domain of Gag, and the other domains within Gag drive protein-protein interactions required for assembly of the immature viral particle at the cell membrane, as well as budding. Critically, the p6 domain of Gag recruits the cellular ESCRT (endosomal sorting complexes required for transport) machinery, which mediates budding and eventual fission of the HIV membrane from the infected cell (*55*). During or immediately after budding, viral maturation initiates with PR cleavage of the Gag polyprotein, yielding an infectious virion that can begin the viral life cycle anew.

1.1.6 HIV-1 Transmission and Pathogenesis.

Most HIV infections occur through sexual transmission, wherein mucosal surfaces within the male or female genital tract or rectum are exposed to HIV-contaminated fluids (*57*). However, alternative and less frequent modes of transmission exist, including vertical transmission from an infected mother, and exposure to infected blood (commonly from shared needles used for intravenous drug use) (*58*). Following exposure, the virus infiltrates the lamina propria, and within hours infects resident CD4+ lymphocytes, macrophages, and dendritic cells (*59, 60*). The virus then establishes an initial seeding population of infected cells over the order of several days, before being transferred into draining lymph nodes and lymphoid tissues.

Once HIV-1 is disseminated into lymphoid tissue, the virus takes advantages of abundant and heavily concentrated CD4+ T cells to replicate at high levels, which produces a burst of viremia about 10-14 days following initial infection (*61*). It is during this acute phase that flu-like symptoms of HIV infection emerge, which include fever, swelling of lymph nodes, nausea, muscle aches, sore throat, headache, and diarrhea (*62*). An initial and dramatic depletion of CD4+ T cells

occurs during this phase, particularly within the gut-associated lymphoid tissue (GALT)(*63*), and the viral reservoir is firmly established at this point. Toward the end of the acute phase, antibodies and cytotoxic CD8+ T-lymphocytes mount a futile response against viral replication, which along with the depletion of viral target cells contribute to a reduction in plasma viral loads to a stable set level known as the viral set point (*58, 61*).

As viral load reaches its set point, CD4+ T cell levels partially rebound, and the virus reaches the chronic or "clinical latency" stage. This is the longest stage of HIV infection, wherein HIV replicates steadily and asymptomatically over a span of anywhere from 1-20 years, gradually infecting and depleting the body's supply of CD4+ T cells (*64*). The final stage of HIV infection is the onset of AIDS, which is marked by a decline in CD4+ levels to under 200 cells/μL of blood. At this depleted level, the immune system is unable to mount a response against replicating HIV, and viral levels spike as CD4 T cell counts continue to plummet. Symptoms from opportunistic infections emerge, which typically prove fatal to the late-stage AIDS patient (*64*).

If left untreated, most patients will progress towards AIDS within 8-10 years, and succumb to AIDS by 10 years following initial infection (*65*). However, a small number of infected patients maintain CD4+ T cell levels in the presence of detectable viral loads without progressing to AIDS. Patients who maintain this activity for at least 10 years are referred to as long-term non-progressors (LTNPs)(*66*). An even smaller subset of LTNPs are Elite Controllers (ECs), which make up only 1% of HIV-infected individuals. ECs do not only fail to develop AIDS, but are able to control viral loads below detectable levels in the absence of antiretroviral therapy (*67*). While some LTNPs and ECs may simply benefit from being infected with competent viruses that display poor viral fitness (e.g., defects in the viral Nef gene as described in more detail below), it is likely that there

are host attributes that may explain the robust protective responses against HIV that these patients exhibit (*58, 68*).

1.1.7 HIV-1 Treatments and Curative Strategies

Immediately following the identification of HIV as the causative agent of AIDS, work began to identify pharmacological treatments for this viral infection. The first class of therapeutics developed against HIV were nucleoside reverse transcriptase inhibitors (NRTI), which are nucleoside/nucleotide analogs that impair reverse transcription by causing early chain termination following incorporation into viral cDNA (*69*). The first antiretroviral drug and first NRTI was the thymidine analog zidovudine (ZDV, also known as 3′-azido-2′,3′-dideoxythymidine/AZT), which was initially synthesized in the 1960s during a failed effort to develop novel anti-cancer therapeutics. ZDV received a second life in the mid-70s when it was found to inhibit retroviral replication for the murine leukemia virus (MLV) (*70, 71*). After HIV was identified and isolated, ZDV was incorporated into a screen of potential antiretroviral compounds, and was confirmed in 1985 by the National Cancer Institute (NCI) to be a bona-fide inhibitor of HIV-1 replication (*70, 72*). ZDV quickly moved through clinical trials over the next two years, where it demonstrated sufficient clinical efficacy to be granted FDA approval in 1987 (*73, 74*).

For four years, ZDV was the sole therapeutic option for HIV/AIDS, and was administered as monotherapy (*75*). But while patients on a ZDV regimen saw an increase in survival and delayed AIDS progression (*76*), ZDV monotherapy was marred by the onset of viral resistance and unfavorable toxicity profiles (including nausea, anemia, and bone marrow suppression) (*77*). The appearance of additional NRTIs, including zalcitabine (ddC) and didanosine (ddI), allowed for initiation of combination NRTI therapy that markedly delayed AIDS progression compared to

ZDV monotherapy (*78*). However, AIDS-related fatalities in the United States would continue to climb until 1995, when two new classes of antiretroviral compounds would arrive on the scene: non-nucleoside reverse transcriptase inhibitors (NNRTIs) and protease inhibitors (PI) (*3, 79*). NNRTIs also target HIV RT, but allosterically bind to the enzyme and impair reverse transcriptase without being incorporated into viral cDNA (*80*). Most protease inhibitors, as their name implies, target HIV's ability to form mature virions via the proteolytic cleavage of Gag and GagPol precursors via PR (*81*). Introduction of the protease inhibitor saquinavir in 1995, followed by the NNRTI nevirapine in 1996, led to the introduction of a triple-drug regimen, referred to as highly active antiretroviral therapy (HAART). The use of three drugs from two different classes of inhibitors (commonly 2 NRTIs + 1 PI or 2NRTIs + 1 NNRTI) resulted in dramatic suppression of viral replication and restored CD4+ T cell counts with a lower incidence of resistance (*79*). The efficacy of HAART was soon reflected in epidemiologic data, as the following years brought the first decrease in US AIDS-related deaths since the start of the epidemic 10 years prior (*82*).

HAART therapy has continued to improve over the last 25 years through the development of drugs with greater efficacy and tolerability, and today there are over 30 antiretroviral compounds across six classes (*69, 83*). Newer classes of antiretroviral drugs include integrase inhibitors, viral fusion inhibitors, and coreceptor antagonists (*84*). However, while HAART has forever altered the clinical implications of contracting HIV-1, there is no cure for individuals infected with HIV. HIV infection still manifests as a chronic condition requiring lifelong adherence to an antiretroviral regimen. Also, despite the widespread distribution of effective antiretroviral compounds to people infected within the developed world, only 60% of people currently infected with HIV today receive antiretroviral therapy worldwide (*85*).

Unfortunately, development of effective curative strategies for HIV-1 has proven to be an even more difficult challenge than developing drugs to control infection. For example, while six vaccine strategies have entered clinical trials, five out of the six showed no efficacy (*86*). The sixth vaccine candidate, which combined recombinant HIV-1 Env along with a Canarypox viral vector expressing Gag, PR, and Env, only achieved 31% efficacy in humans (*87*). Ongoing work has also encompassed a search for a therapeutic cure for HIV infection, which represents either complete clearance of the latent viral reservoir from infected patients ('sterilizing cure') or competent immune suppression of viral replication following termination of antiretroviral therapy ('functional cure')(*88*). One potential sterilizing cure lies in the concept of "shock and kill", wherein HIV+ patients managing infection through HAART are treated with latency reversal agents (LRAs) to induce viral transcription and translation of viral proteins. While HAART should suppress further infection and replication, induction of viral transcription could potentially allow for immune recognition and clearance of latently infected cells (*89*). However, while current LRA candidates have demonstrated varying degrees of reactivation of latent virus in vivo (*90-92*), legitimate questions remain as to whether these agents achieve full reactivation of the latent viral reservoir, as well as whether effective clearance can be obtained following reactivation (*93*).

Successful development of new therapies to achieve HIV-1 cure may involve drugs that target HIV-1 accessory proteins. The Nef protein is particularly attractive in this regard, because of its central role in helping HIV-infected cells avoid detection by the host immune system. The structure and function of Nef is described in detail in the next few sections, along with progress in the discovery and development of Nef inhibitors.

1.2 HIV-1 Nef

1.2.1 Role of HIV Nef in viral pathogenesis

The viral *nef* genes encode a relatively small (27-34 kDa, depending on the lentivirus), myristoylated, non-enzymatic accessory proteins that are one of the first proteins expressed during the viral life cycle. The ORF for HIV Nef is located at the 3' end of the genome and overlaps with the ORF for Env and the 3' LTR. Nef was initially mischaracterized based on early evidence that it was a "Negative Factor" of HIV-1 replication (*94*). To the contrary, Nef plays prominent roles in HIV pathogenesis by promoting viral replication and spread in vivo, and in AIDS progression by enabling immune escape of HIV-infected cells. Patients infected with HIV harboring deleted or defective Nef often display slow or stalled progression towards AIDS (*95, 96*), while deletion of Nef within SIV has similarly been shown to impair both HIV replication and simian AIDS progression in rhesus macaques (*97*). In addition, expression of HIV Nef alone within CD4+ cells induces an AIDS-like disease in a transgenic mouse model, suggesting a direct role for Nef in AIDS progression (*98*).

1.2.2 General Structure of Nef

Nef is composed of a flexible and myristoylated N-terminal arm, a conserved folded core with a large internal loop, and an unstructured C-terminal tail (Figure 4). As the dynamic nature of the N-terminal arm renders it suboptimal for crystallization, nearly all X-ray crystal structures of HIV-1 Nef to date have focused on the folded core region. NMR studies of the N-terminal anchor confirm that this region has little higher order structure (*99*), and current models of

unbound, full-length Nef have only been possible through computational assembly of the anchor domain with established Nef core structures (*100*). However, while full resolution of the N-terminal arm region has remained elusive, partial density for the arm has been resolved in a structure of full-length Nef fused to a binding partners, and are described in greater detail in Section 1.2.5 (*101*). The same holds true for the internal flexible loop, the structure of which is only observed in crystal structures of Nef in complex with host cell proteins.

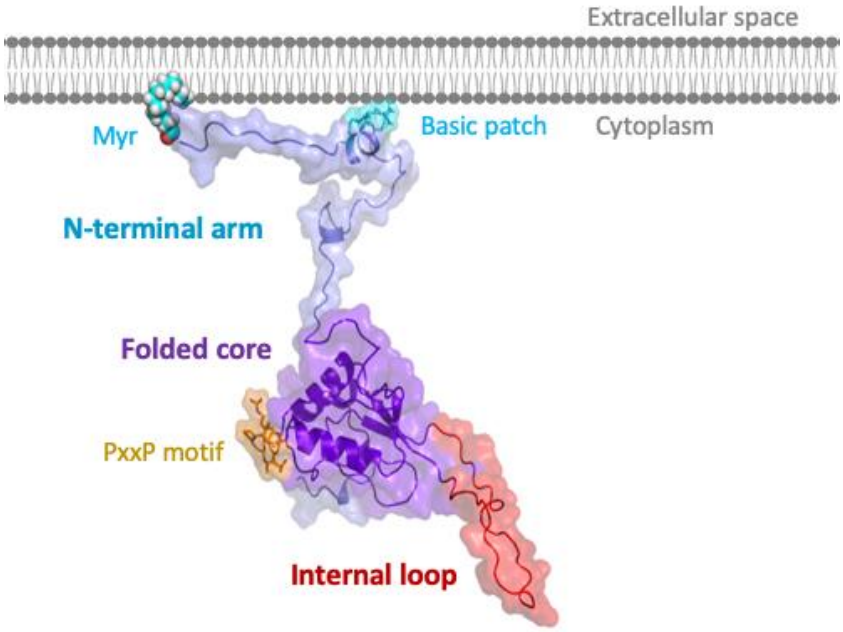

Figure 4: Structural Model of HIV-1 Nef at the Plasma Membrane

1.2.3 Key Functions of Nef

1.2.3.1 Promotion of viral infectivity

One of the more elusive aspects of Nef function involves the mechanism behind the long-running observation that Nef promotes the inherent infectivity of viral particles. HIV infectivity

typically refers to the signal from in vitro HIV reporter cell assays, including the HeLa-based TZM-bl reporter cell system (*102*). TZM-bl cells express the viral receptors CD4 and CXCR5/CCR5, as well as an integrated copy of the Tat-regulated HIV-1 LTR fused to luciferase or β-gal reporter genes (*103, 104*). A single round of HIV infection and integration within TZM-bl reporter cells results in Tat-dependent induction of luciferase or β-gal activity, and the degree of the reporter signal normalized to the quantity of input virus provides a quantitative measure of "infectivity".

In 1994, it was first reported that deletion or disruption of full-length Nef expression severely impairs the infectivity of the resulting virus (*105*), implying a positive contribution of Nef towards the infectivity of viral particles. Subsequent studies showed consistent Nef enhancement of viral infectivity across various viral subtypes and producer cells, although the degree of that enhancement varied anywhere from 3- to 40-fold (*106*). New features and requirements of Nef promotion of infectivity were continually reported, including a dependence on Nef myristoylation, AP-2 association and clathrin-mediated endocytosis, an enhanced phenotype in lymphoid cells (*107*), and a conservation of infectivity enhancement within SIV Nef and other retroviral proteins (*108*). Despite these breakthroughs, the key mechanism behind Nef promotion of infectivity eluded researchers until 2015, when the existence of a novel host cell restriction factor known as SERINC5 was identified. A major focus of my thesis research involved the mechanisms of Nef interaction with SERINC5, which is reviewed in detail in Section 3.

1.2.3.2 Alteration of host cell protein trafficking

Nef has no known inherent enzymatic activity, and functions instead through a wide network of interactions with host cell proteins (*109*). Among the 70 host cell proteins that Nef has been reported to engage are essential components of the intracellular trafficking machinery, which

Nef hijacks to modulate the expression and trafficking of host proteins to the cell surface (*110*). HIV-1 Nef induces the downregulation of a wide variety of host cell immune receptors and other membrane proteins, including CD4, MHC-I/-II, CD28, CXCR4/CCR5, CD1, CD80, CD86, and SERINC5 (*111-117*). Nef expressed by SIV and HIV-2 can also downregulate CD3, and SIV Nef (as well as some rare subtypes of HIV-1 Nef) can downregulate the restriction factor tetherin (*118*). Nef can also increase the surface expression of host cell proteins to improve viral pathogenesis, notably the transmembrane lectin protein DC-SIGN (*119*). Two of the best-characterized Nef functions are downregulation of MHC-I and CD4, which are directed by unique Nef interactions and pathways described below.

Downregulation of CD4 is conserved across virtually all HIV-1 subtypes (*120*), and while this function may seem counterintuitive due to CD4's role as the viral receptor, it is in full alignment with the role of Nef in cell survival and immune escape. Cell surface expression of CD4 within already infected cells can lead to cytotoxic superinfection. Furthermore, interactions between CD4 and Env on the surface of infected cells expose HIV to antibody-dependent cell-mediated cytotoxicity (ADCC), which is driven by anti-Env antibodies that recognize otherwise cryptic Env epitopes (*121, 122*). In the absence of infection, downregulation of cell-surface CD4 is mediated through phosphorylation-dependent engagement of the cytosolic tail of CD4 by the adaptor protein 2 (AP-2) complex, which drives clathrin-mediated endocytosis of CD4 into the endolysosomal pathway (*123*). Nef accelerates this endocytic process, engaging both the cytosolic tail of CD4 (*124*) and the α and σ2 subunits of AP-2 to promote clathrin-mediated endocytosis (*111, 125*). This critical viral function is also performed by the viral accessory protein Vpu, although Vpu is expressed later during infection and targets CD4 through a distinct ubiquitination-dependent process (*126*).

The major histocompatibility complex I (MHC-I) antigen presentation pathway is another critical target for Nef, as it is a key component of the adaptive immune response to viral infection. Antigenic peptides derived from proteolytically digested viral proteins are loaded onto MHC-I within the ER and are then presented on the surface of infected cells. Recognition of viral peptides presented by MHC-I serves as an alarm of infection for CD8+ cytotoxic T lymphocytes, which kill the infected cell. Several viruses have developed means of downregulating MHC-I in order to evade immune detection (*127*), but the immune system counters that activity with a mechanistic fail-safe performed by natural killer (NK) cells. NK cells monitor expression of MHC-I on the surface of cells, and destroy any cells with suspiciously low levels of MHC-I surface expression (*128*). Fascinatingly, Nef manages to evade both NK and CD8+ T cell killing through selective downregulation of MHC-I molecules of the HLA-A and HLA-B classes (*129*). However, Nef does not affect MHC-I molecules monitored by NK cells (HLA-C and HLA-E), allowing Nef to antagonize immune recognition of HIV infection without exposing infected cells to cytotoxic clearance by NK cells.

In contrast to CD4, MHC-I downregulation by Nef is driven by Nef association with the endocytic adaptor protein complex 1 (AP-1). There are two current models for Nef downregulation of MHC-I. In the first model, known as the "signaling model", Nef is recruited by the phosphofurin acidic cluster 2 (PACS) protein into the trans-Golgi network (TGN), where Nef drives the activation of Src-family kinases. Activation of the Src kinases initiates a signaling cascade that results in increased levels of membrane PIP3 via PI-3K, driving activation of the small GTPases Arf1 and Arf6 followed by endocytosis of cell surface MHC-I. Once internalized, MHC-I is trapped in vesicles with Nef and AP-1, preventing recycling back to the plasma membrane (*130*). In the second model, known as the stoichiometric model, Nef associates with AP-1 and its

activator Arf1 to trap newly synthesized MHC-I within the TGN, and inhibit anterograde trafficking towards the plasma membrane (*131, 132*). In both models, intracellularly sequestered MHC-I is led into late endosomes and eventually lysosomes through the activity of the coatomer protein complex subunit β (β-COP).

Endosomal and lysosomal targeting of internalized MHC-I and CD4 are directed through a β-COP-dependent processes, and Nef appears to associate directly with β-COP in vitro (*133*). Nef-directed intracellular retargeting is also reliant upon Nef association with the ESCRT machinery, which drives the sorting of intracellular cargo into late endosomal multivesicular bodies. Nef interacts with the ESCRT protein ALIX in late endosomes and lysosomes (*134*), an interaction proposed to control Nef-mediated targeting of endosomal cargo into lysosomes (*135*).

1.2.3.3 Nef-dependent kinase activation

Cytoplasmic kinases represent another major class of Nef binding partners, several of which are activated by Nef and appear to contribute to HIV replication and pathogenesis. This group includes members of the Tec and Src families of non-receptor protein-tyrosine kinases, phosphatidylinositol 3-kinase (PI-3K) (*136*), and the p21-activated kinase 2 (Pak2) (*137*). Nef binding and activation of Src-family kinases is the one of the best-characterized functions of Nef and has been the focus of many structural, cellular, and in vitro studies. Early work demonstrated that Nef preferentially binds to the SH3 domains of Hck and Lyn, two of the eight mammalian Src-family kinases (*138*). Subsequent studies established that Nef binding displaces the SH3 domain from its regulatory position on the back of the kinase domain, resulting in constitutive kinase activation both in vitro and in cell-based systems (*139-141*). Nef-dependent Hck activation has been shown to play an important role in HIV replication, infection, and MHC-I downregulation (as described above), and activation of Hck is conserved across all HIV-1 Nef M-group subtypes

(*142*). Hck is expressed primarily in macrophages, and knockdown of Hck expression has been shown to compromise HIV-1 replication in this cell type (*143*). Compared to Hck, Lyn, and c-Src, Nef engagement of other Src-family members is less definitive, including the Src family kinase Lck. The Lck kinase is a critical component of T cell receptor signaling, and though Nef expression within T cell lines results in intracellular retargeting of Lck, there are conflicting reports on whether Nef binds directly to Lck within cells (*139, 144, 145*).

More recent studies have linked Tec-family kinases to the HIV-1 life cycle and established a role for Nef in activation of this kinase family. HIV-1 target cells express the Tec family kinases Itk and Btk, both of which play important roles in antigen receptor signaling, as well as lymphocyte activation and development (*146*). Functional Itk activity has been shown to be essential for HIV-1 replication, and pharmacological inhibition or knockdown of Itk impairs nearly every step of the viral life cycle (*147*). Subsequent studies showed that both Itk and Btk interact with Nef at the cell membrane, and that Itk inhibitors impair Nef-dependent enhancement of infectivity and replication (*148, 149*). Nef-dependent interaction with Itk is highly conserved across major subtypes of HIV-1, further supporting an essential mechanistic role (*148*).

1.2.4 Nef Binding Partners- Description and Structure.

As described in the preceding sections, host cell tyrosine kinases and endocytic adaptor proteins represent two major classes of binding partners essential for Nef functions related to enhancement of viral replication and immune escape. The next few sections describe the structural features important for the natural regulation of these Nef effectors, followed by details of the molecular mechanisms used by Nef to hijack these proteins for the benefit of the virus.

1.2.4.1 Src family kinases

The Src kinase family is a well-studied group of non-receptor protein-tyrosine kinases that play diverse roles in signal transduction. There are eight members of the Src family expressed in mammals (Src, Hck, Lck, Fyn, Lyn, Yes, Fgr, and Blk). While several family members exhibit ubiquitous expression across multiple cell lineages (Fyn, Src, Yes), others are confined to particular cell types (Blk, Fgr, Hck, Lck, Lyn) (*150*). Despite having distinct expression patterns, all Src-family kinases are similarly organized with respect to structured domains. At the N-terminus of all Src family kinases is the myristoylated and sometimes palmitoylated SH4 domain, which anchors the kinase to the cell membrane. Downstream of the SH4 domain is the "Unique" domain, the amino acid sequence of which differs for each family member and regulates interactions and functions specific to each kinase (*151*). Next are the SH3 and SH2 domains, which are key regulators of kinase activity, and mediate protein-protein interactions with substrates and other cellular proteins. The SH3 domain is made up approximately 60 residues arranged into five beta strands within two anti-parallel beta sheets, and is a common structural feature found within nearly 200 cellular proteins (*152*). The SH3 domain recognizes and binds to poly-proline type II helices within target proteins, often referred to as PxxP motifs. While all SH3 domains recognize a PxxP motif, they harbor unique preferences for the individual amino acids surrounding that motif (*153, 154*). SH2 domains recognize specific motifs centered around phosphotyrosine (pTyr), and electrostatically engage with pTyr through a conserved arginine (*155*). Like the SH3 domain, SH2 recognition is conferred by the surrounding amino acids, which in the case of Src family kinases is typically a pTyr-Glu-Glu-Ile motif (*156*). In addition to mediating protein-protein interactions, both domains play a prominent regulatory role for all Src-family members, as intramolecular association of these regulatory domains lock the overall kinase into an inactive,

'assembled' conformation (*157, 158*). More specifically, the SH3 domain binds to a poly-proline type-II helix formed by the linker between the kinase and SH2 domains, and the SH2 domain binds to a pTyr located within the C-terminal tail of the kinase. Release of this auto-inhibitory regulation, for example through engagement of SH2 or SH3 by a binding partner, frees the kinase into an open partially active state. This allows the catalytic kinase domain to undergo autophosphorylation at a conserved Tyr within the activation loop, opening the kinase active site to allow for entry of ATP and substrate required for phosphorylation of kinase targets (*159*). One interesting exception to this general regulatory paradigm is Fgr, which is expressed primarily in myeloid leukocytes. While Fgr can adopt the 'assembled' conformation associated with inactive Src, this family member is constitutively active and not under regulatory control of its SH3 and SH2 domains (*157*).

1.2.4.2 Adaptor protein complexes

Transmembrane proteins are shuttled between cellular organelles and the plasma membrane through vesicles, which bud from the surface of donor organelle or plasma membranes, then traffic to and fuse with acceptor membranes. Vesicle formation and budding require the formation of a structural protein "coat", which is composed of context-dependent scaffolding proteins (*160*). Trafficking of protein cargo from the TGN, plasma membrane, and endosomes is typically directed through a protein coat made up of a scaffolding coat protein called clathrin, which forms a polyhedral cage around the vesicle membrane (*161*). However, as the clathrin coat has no way of physically interacting with either the vesicle membrane or transmembrane protein cargo, connection between the membrane and coat is reliant upon cargo adaptor proteins. Two of the most widely studied cargo adaptor proteins are adaptor protein complex 1 (AP-1) and adaptor

protein complex 2 (AP-2), which control clathrin-mediated recruitment of vesicles trafficking from the TGN to endosomes or between endosomes (AP1-) or the plasma membrane to endosomes (AP-2). These endocytic adaptors direct the connection of clathrin to the membrane of nascent vesicles, but also directly recruit and package protein cargo into vesicles (*162*).

AP-1 and AP-2 share a similar subunit organization, each composed of two large (100 kDa) subunits (AP-1: β1 and γ, AP-2: β2 and α), one ~50 kDa medium subunit (AP-1: μ1, AP-2: μ2), and a small 18 kDa subunit (AP-1: σ1, AP-2: σ2)(*160*). The β and γ/α subunits contain two separate structured domains, one larger "trunk" domain that associates with the other subunits to form a heterotetrameric core complex, and a smaller "appendage" or "ear" domain that is connected by a hinge region. The ear domains participate in protein-protein interactions that mediate vesicle formation and uncoating, while the hinge domain recruits clathrin through a motif referred to as the clathrin box (*160*). Adaptor proteins tether clathrin to the cell membrane by associating directly with the plasma membrane through engagement of either PI4P for AP-1 (*163*) or PIP2 for AP-2 (*164*). Recruitment of protein cargo is directed by the σ and μ subunits, which recognize sorting signals conserved within the cytoplasmic domains of proteins, including tyrosine (YxxΦ), and di-leucine ([DE]XXXL[LI]) motifs (*165, 166*).

Adaptor protein activity is controlled through "open" and "closed" conformations of the core, the structures of which have been captured through X-ray crystallography and cryo-electron microscopy studies. Alternate conformations have also been observed, including intermediate (*167*) and "hyper-open" forms (*168*). In the closed form of AP-1 and AP-2, binding sites within the core (tyrosine motif binding site, di-leucine binding site, clathrin box, and one of two membrane binding pockets) are either buried or partially blocked. The sole exception is a

membrane-associating pocket within the α subunit, which is surface-exposed within this structure (*160, 169*).

Structures of AP-2 in the "open" conformation have been obtained following co-crystallization with di-leucine and tyrosine motif-containing substrates, conditions under which the structure the binding sites for membrane, cargo, and potentially clathrin are surface-exposed (*170*). However, activation of AP-2 into the open conformation appears to be triggered through membrane association rather than cargo binding, although cargo binding may promote clathrin recruitment (*162*). The structure of the "open" AP-1 core reveals a similar conformation to that of open AP-2. However, AP-1 activation requires interaction with a small GTPase known as ADP ribosylation factor 1 (Arf1). Co-crystallization of AP-1 with Arf1 alone seems to induce the "open" conformation of AP-1, even in the absence of cargo containing signal sorting motifs (*171*).

1.2.4.3 CD4

Cluster of differentiation 4 (CD4) is a ~55 kDa type I integral membrane glycoprotein that serves as a co-receptor for the T Cell Receptor (TCR) and plays an essential role in T lymphocyte development and activation. Expression of CD4 over CD8 during lymphocyte development diverts T cells into a "helper" rather than a cytotoxic lineage, solidifying their immunological role of the cell. CD4 is also is the main receptor for HIV infection, and is bound by the Env gp120 protein to initiate viral recognition and fusion as described above (*172*). CD4 was initially characterized in the late 70s and early 1980s, fortunate timing considering its identification as the HIV receptor in 1984 (*173, 174*).

CD4 is composed of four extracellular immunoglobulin domains (D1-D4), a transmembrane domain, and a short cytoplasmic tail. The extracellular component of CD4 is the

largest, comprising around 370 out of the ~430 total amino acids within human CD4 (*175*). Association of both MHC-II and HIV gp120 are directed through the D1 domain of CD4. CD4 promotes TCR recognition of MHC-II expressed on antigen presenting cells (APC), and plays a role in T cell activation downstream of antigen recognition through the recruitment of Lck to the TCR/CD3 complex (*176*). Interestingly, it has been suggested that this Lck-dependent mechanism is the more relevant activity for enhanced antigen recognition of the TCR, rather than association of CD4 with the MHC-II/TCR complex (*177*).

1.2.4.4 MHC-I

MHC-I molecules (as well as their MHC-II counterparts) play a critical role in adaptive immunity, as they bind and present antigenic peptides for recognition by T cells (*178*). However, unlike MHC-II molecules (which are primarily expressed by antigen-presenting cells) MHC-I is expressed on the surface of virtually all nucleated cells (*127*). MHC-I molecules present peptides from intracellular proteins processed by the proteasome, which are transported to the ER and loaded onto MHC-I molecules for presentation (*127*). While most of these peptides originate from newly synthesized but defective host cell proteins (*179*), virally-infected cells will present antigenic peptides produced from viral proteins, potentially triggering the recognition and clearance of infected cells (*180*). Unsurprisingly, several viruses (HIV-1, influenza, beta and gamma-herpesviruses) have evolved means of downregulating MHC-I, as antigen presentation to circulating cytotoxic T cells represents a major existential threat (*181*). MHC-I is also commonly downregulated within cancer, allowing tumors to similarly escape immune detection (*182*).

Structurally, MHC-I is composed of a single 3-domain heavy chain (~45kDa) non-covalently bound to a beta-2 microglobulin (β2m) light chain (12 kDa)(*183, 184*). Two of the

MHC-I heavy chain domains (α1 and α2) form a binding groove that accommodates antigenic peptides spanning about 8-10 amino acids, and encompass the primary binding interface with the TCR (*180*). The heavy chain of MHC-I also contains a transmembrane helix and a cytoplasmic tail, which anchor MHC-I to the membrane and mediate MHC-I association with intracellular binding partners, respectively(*185*).

In humans, MHC complexes are referred to as Human Leukocyte Antigen (HLA) complexes, which are divided into classical (class IA; HLA-A, HLA-B, and HLA-C) and non-classical (class IB; HLA-E, HLA-F,HLA-G, HLA-H) families (*186*). While both HLA-class IA and HLA-class IB molecules can present intracellular peptides to T cells, class IA molecules are highly polymorphic and widely expressed, compared to the markedly lower polymorphism and expression levels displayed by class IB molecules (*187*). Instead of driving immune recognition of intracellular peptides, HLA-class 1B molecules instead play a critical role in immune regulation, notably the HLA-E and HLA-G directed inhibition of cellular lysis by NK cells (*186, 187*). As discussed in Section 1.2.3.2, Nef selectively downregulates HLA molecules from both class 1A and class 1B to evade immune detection and NK cell mediated killing (*188*).

1.2.5 Critical Nef Motifs and features

1.2.5.1 N-terminal Flexible Arm and Myristoylation Site

Absolutely critical to Nef function is its flexible N-terminal arm, which makes up the first 57-60 amino acids of Nef. The N-terminus of Nef contains a highly conserved recognition sequence (MGxxx[ST]) for the host N-myristoyl transferase protein, which allows Nef to be myristoylated at the second position glycine. This myristoylation site, along with a basic arginine-rich region (Arg17, Arg19, Arg21, Arg22) direct Nef association with the membrane (*189*).

Mutation of either the critical myristoylation sequence glycine (Nef G2A mutant) or disruption of electrostatic interactions between the basic residues and negatively charged polar headgroups in the lipid membrane impair association of Nef with the membrane (*190*). Disruption of myristoylation via the G2A mutation disrupts virtually all Nef functions, demonstrating the essential role for myristoylation and membrane association. Myristoylation-dependent functions of Nef include downregulation of CD4, MHC-I (*189*), antagonism of the SERINC5 restriction factor (*117*), overall HIV-1 pathogenicity (*191*), recruitment of actin and β-COP (*192*, *193*), and Lck retargeting (*194*).

To date, only one structural study of the flexible N-terminal region of Nef in isolation has been conducted, an NMR spectroscopy study of the anchor domain in the presence and absence of myristoylation. That structure confirmed that while the N-terminal region of Nef is primarily unstructured, myristoylation stabilizes at least one helical element within the arm. This helix has an amphipathic nature that helps coordinate membrane association: one side with a basic residues associates with lipid head groups (the aforementioned Arg17, Arg19, Arg21, Arg22) while the opposite side consists of hydrophobic residues which may insert directly into the membrane (Trp5, Trp13, Ile16 and Met20) (*195*).

Two points of membrane contact have suggested a two-step model for Nef association with the lipid bilayer. In the initial "fast phase", the N-terminal myristate group of Nef inserts into the membrane and the basic elements of the amphipathic helix associate with lipid head groups. In the "slow phase", the hydrophobic side of the amphipathic helix inserts into the membrane (*190*).

The possibility has been raised that Nef exists in a compact "closed" conformation prior to membrane insertion, wherein the myristoylated N-terminus and large internal loop are packed against the folded protein core (*196*). Indeed, both NMR and hydrogen-deuterium exchange mass

spectrometry (HDX MS) studies of myristoylated Nef show greater protection from solvent than anticipated for the anchor domain in isolation (*197, 198*). This 'closed' conformation of Nef seems to exist directly outside of the lipid membrane, but following insertion of the N-terminus of Nef, the folded core moves to a distance of 70 Angstroms away from the lipid membrane based on neutron reflectometry (*190*). This extended conformation presumably allows for the exposure of critical binding motifs within Nef, coordinating essential protein-protein interactions and potentially facilitating the dimerization of Nef (*190, 196*). However, a crystal structure of Nef in complex with MHC-I and AP-1 shows that the N-terminal arm is partially packed against the core. Within this structure, Trp13 and Met20 within N-terminal helix 1 associate with the folded core of Nef, while the myristoylation motif is still free to associate with the membrane. The authors propose that interaction between the Nef core and N-terminal helix pulls the complex closer to the plasma membrane (*101*), which suggests that contact between the N-terminal arm of Nef and the folded core may participate in Nef signaling in the context of AP-1 and endocytosis.

1.2.5.2 PxxP Motif: Structural Basis of Kinase Engagement

Directly downstream from the N-terminal anchor domain of HIV-1 Nef is a highly conserved PxxPxR motif. This motif forms a PPII helix that serves as a docking site for recruitment of Src-family kinases and other proteins with SH3 domains. Unsurprisingly, this motif is required for Nef activation of Src family kinases, as SH3 binding by Nef alleviates the auto-inhibitory interaction of the PPII helix within the kinase's linker region as described above. Mutagenesis studies suggest that the Nef PxxP motif also appears to play a role in the recruitment and activation of Tec family kinases and Pak1/2 kinases, although the direct structural basis of this interaction is not known. Disruption of the PxxP motif also impacts Nef downregulation of MHC-I (*199*), Nef promotion of viral replication, and pathogenicity of the virus in murine and primate

models of AIDS (*200, 201*). However, Nef downregulation of CD4 and promotion of infectivity through SERINC5 are largely unimpacted by mutation of the PxxP motif (*117, 199*).

Research over the previous two decades has resulted in a sophisticated understanding of how Nef engages the SH3 domains of Src-family kinases. The conserved Nef motif for SH3 recognition is comprised of Pro72 and Pro75, along with a conserved Arg at residue 77, and a hydrophobic residue (commonly valine) at residue 74 (*202*). The hydrophobic prolines and valine within the Nef core PxxPxR motif engage hydrophobic residues within the SH3 β-sheets, while Arg77 forms an electrostatic contact with a SH3 Asp100 residue (*203*). These core prolines are essential for Nef engagement of SH3, as replacement of prolines 73 and 75 with alanine abolishes SH3 binding (*204*).

Crystal structures of Nef in complex with the SH3 domains of Fyn and Hck have illuminated other points of contact for SH3 engagement (Figure 5). These contacts occur in more variable regions of the SH3 domains and are believed to direct specificity of Nef towards different SH3 domains. For example, Nef has sub-micromolar affinity towards the Hck SH3 domain (K_D as low as ~250 nM by SPR) with much lower affinity towards the Fyn SH3 (K_D > 20 μM). This difference in affinity is dependent upon a single residue within the variable RT loop of the SH3 domain. The Hck SH3 contains an isoleucine residue at position 96 within the RT loop, which engages a hydrophobic pocket in the folded core of Nef. The Fyn SH3 has an arginine at position 96, which is suboptimal for interaction with this Nef pocket. Replacement of Arg96 in the Fyn SH3 with isoleucine restores high affinity binding, illustrating the importance of this Ile residue (*138, 205*).

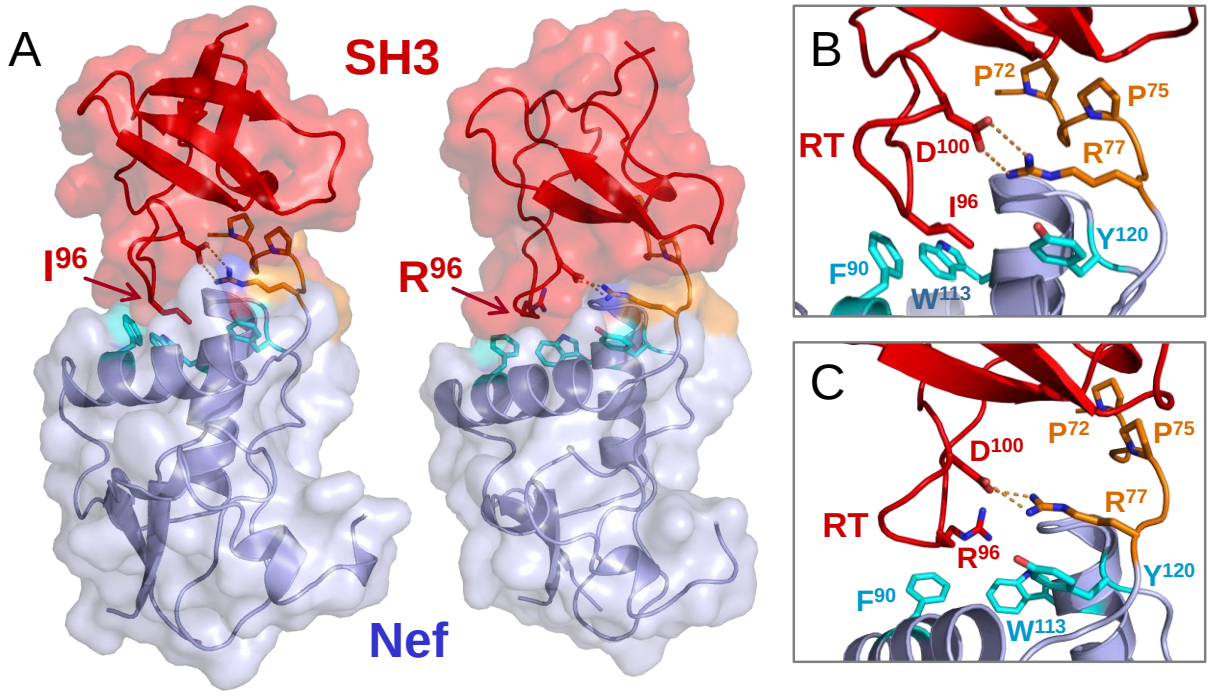

Figure 5: X-ray crystal structures of HIV-1 Nef in complex with the SH3 domain of the Src-family kinase, Fyn

A) Overall structure of the HIV-1 Nef core with the wild-type Fyn SH3 domain (right) and the high-affinity mutant, R96I (left). Both Nef proteins are modeled in blue, with the SH3 domains are shown in red. The conserved PxxPxR motif of Nef is rendered in orange. B) Close-up view of the interface of Nef with the high-affinity SH3 R96I mutant. Nef residues P72 and P75 define a polyproline type II helix that meshes with the hydrophobic grooves of the SH3 surface and is oriented and stabilized by an ionic interaction between Nef R77 and SH3 D100. High affinity interaction requires Ile96 from the SH3 RT loop which accesses a hydrophobic pocket by Nef residues Phe90, Trp113, and Tyr120 (cyan). C) Close-up view of Nef interaction with the wild type Fyn SH3 domain. The interface is the same as in panel B, except the wild type Fyn SH3 has arginine at RT loop position 96 which cannot access the hydrophobic pocket. The Nef cores in both structures form homodimers (not shown). Both models were produced with PyMol using the crystal coordinates of the HIV-1 Nef core in complex with the Fyn R96I mutant SH3 domain (PDB: 1EFN) and the wild-type SH3 domain (PDB: 1AVZ).

The first reported crystal structure of an SH3 domain bound to Nef is based upon this stabilizing Fyn SH3 R96I mutation, which shows that Ile96 contributes to SH3 engagement through a hydrophobic pocket within Nef formed by conserved residues Leu87, Phe90, Trp113, and Tyr120 (*206*). Another structure of Nef in complex with wild-type Fyn SH3 shows that the aliphatic 3-carbon chain of Arg96 engages the hydrophobic Nef pocket in a similar manner as

Ile96. However, while the side-group of Ile96 is fully engaged with this pocket, the basic guanidinium component of the Arg96 side-chain is solvent-exposed in the wild type Fyn SH3-bound structure (*207*). These two crystal structures are compared in Figure 5.

Nef sequence variability can also influence SH3 domain affinity, particularly through the PxxP-adjacent residue 71. This position in Nef is typically occupied by arginine within most subtypes of Nef, but certain strains of HIV-1 (including the common laboratory adapted strains NL4-3 and LAI) contain a threonine at this position. When arginine is present at this position, it contributes an additional point of contact towards the SH3 domain that is absent in the Thr71 version of Nef (*205, 207*). The presence of threonine at this position may be at least partially responsible for the reduced affinity of NL4-3 Nef towards Hck SH3 (*208*), as well as reduced viral replication for the NL4-3 virus (*209-211*).

This established Nef/SH3 binding interface is consistent across other structures of Nef, including a structure of the Nef core in complex with a recombinant protein encompassing both the SH3 and SH2 domains of Hck. As expected, a similar hydrophobic interface forms between the SH3 domain and the PxxP helix (with the contribution of an additional proline), and engagement of the critical RT loop isoleucine by a hydrophobic pocket within Nef is also present. However, within the SH3-SH2-bound structure of Nef (which presents as a 2:2 heterocomplex), a novel inter-complex interaction arises between the RT loop of the Hck SH3 domain and Nef residues from the opposing Nef:Hck SH3-SH2 heterodimer (*212*). Mutation of Hck SH3 residue Glu94, which coordinates a salt bridge with the opposing Nef molecule via Arg105, impairs Nef:Hck association in cells, supporting a functional role for this intermolecular contact in Hck recruitment via Nef (*212*). Other structures of SH3-bound HIV-1 Nef have used an artificially engineered SH3 construct, which replaces residues within the RT loop to maximally optimize

Nef:SH3 affinity. The replacement of Ile96 with five alternative RT loop residues increases Nef/SH3 affinity nearly 40-fold (*208*), and this optimized SH3 domain has been used to stabilize targeting of two different protein inhibitors directed against Nef (*213, 214*), and to crystallize the large internal loop of Nef (*215*).

In addition to kinase activation, the PxxP motif appears to play a critical role in MHC-I downregulation by Nef. Since Nef activation of Hck or Lyn is an essential step for the signaling model of MHC-I downregulation described above, a key contribution of this motif towards MHC-I downregulation is likely through engagement and activation of Src-family kinases (*130*). Among all the Src-family members, only Hck and Lyn have an isoleucine residue at position 96 in the SH3 domain, which is essential for Nef binding as described above. However, a structure of Nef in complex with the cytoplasmic domain of MHC-I and the μ1 subunit of AP-1 suggests an alternate, SH3-independent role for the Nef PxxP motif. Within this structure, the PxxP motif of Nef interacts directly with AP-1 μ1, and helps "clamp" the MHC-I cytoplasmic domain into a binding groove within the heterocomplex (*101*). Thus, the Nef PxxP motif may provide not only a mechanism for Src-family kinase engagement and activation, but also for direct interaction with AP-1.

Tec-family kinases share a similar domain organization to Src-family kinases and are also capable of binding and being activated by Nef. Among the five mammalian Tec-family members, Nef selectively interacts with Itk, Btk, and Bmx (but not Tec or Txk), leading to robust kinase activation at the cell membrane. While there are currently no structures of Nef in complex with either Itk or Btk, binding studies support a similar, SH3-dependent mode of engagement for both kinases. An alignment of the Itk and Btk SH3 domain structures with the Src-family SH3 domain present in the crystal structure with the Nef core (*206*) predicts a similar insertion of the RT loop into a hydrophobic pocket of Nef, led by residue 96. Mutation of residue 96 within Itk and Btk

(Asn96 for Itk, Met96 for Btk) impairs Nef and kinase association in cells, implicating the SH3 RT loop in Nef engagement for both Src and Tec family SH3 domains (*148*). However, mutation of the Nef PxxP motif only partially reduced interaction with Nef in a cell-based interaction assay, suggesting that Tec family kinases may make unique contacts with Nef as well (*148*).

1.2.5.2.1 Dynamics of Kinase Engagement by Nef

While structural studies have provided important snapshots into Nef and Hck engagement, HDX MS studies of both proteins have allowed for a greater understanding of the dynamics controlling this interaction (*216*). HDX MS takes advantage of natural exchange between the backbone amide hydrogens of proteins and water in a solution, the rate of which is dependent upon the solvent-accessibility and hydrogen-bonding of each region of the protein. During HDX MS, recombinant proteins are incubated in buffer made from deuterated water, and exchange between the amide hydrogens and deuterated water proceeds for a pre-determined range of times. Exchange reactions are quenched at various time points (typically seconds to hours) by lowering both the pH and temperature of the solution, and the protein is digested into peptic peptides prior to injection into a mass spectrometer. Each exchange event increases the mass of a given peptide by 1.0 Da, which allows for determination of incorporation of deuterium into specific peptides/regions of the protein over time. Peptides that show significant changes in deuterium uptake can then be related to X-ray or NMR structures, providing meaningful temporal information regarding changes in H-bonding or solvent exposure. Deuterium incorporation will change in the presence of protein-protein interactions and shifts in protein conformation, allowing for a dynamic comparison of protein configuration states (*217*). This technique has provided particularly valuable insight as to

the interaction of Nef with partner kinases and other proteins, as well as the effect of small molecule inhibitors on Nef-mediated conformational changes.

HDX MS studies support the suspected mode of Nef binding and Nef-dependent Hck activation, as co-incubation of Nef with near full-length Hck causes a perturbation in the exchange rate for the SH3 domain and SH2-linker region of Nef. This is consistent with a release of Hck SH3 from its auto-inhibitory association with the SH2-kinase linker, and a small shift in exchange within the SH3 domain that signals a shift in binding from the Hck linker to the PxxP helix of Nef (*218*). Interestingly, exchange within the SH2 domain is undisturbed by the presence or absence of Nef, complementing previous cell-based data suggesting that SH3-dependent activation of Hck via Nef does not require release of the auto-inhibitory tail-SH2 interaction (*218, 219*). This SH3-dependent mode of Hck engagement is also supported via studies examining the dynamics of full-length or truncated core domains of Nef in the presence of Hck by both HDX MS and NMR. The region of Nef which contains the PxxP motif demonstrates a clear chemical shift and significant deuterium exchange protection following the addition of the SH3 domain (*220, 221*).

1.2.5.3 Large Internal Loop: Dileucine and Diacidic motifs

Extending from the folded core of Nef is a large flexible loop about 30 amino acids in length, which in solution is the second most solvent-accessible region of Nef after the N-terminal anchor domain (*100*). The loop contains three motifs that are of functional relevance to Nef signaling and function - a centrally located di-leucine motif ([DE]xxxL[LI]), and two acidic motif comprised of E154/E155, and D174/D175. These two diacidic motifs are about equally spaced at the beginning and end of the loop, and electrostatic repulsion between them may contribute to the unstructured nature of the loop in the unbound form of Nef (*100, 202*). Conservation of the di-

leucine motif is complete across nearly all subtypes of Nef, while there is a lesser degree of conservation for the other two motifs (especially E154/E155) (*202*).

The di-leucine motif is essential for the coordination of AP-2 recruitment and downregulation of CD4 from the surface of infected cells. In the absence of HIV infection, CD4 is downregulated in a controlled manner through AP-2 recognition of a non-canonical dileucine sequence within its cytoplasmic tail (SQIKRLL). As canonical di-leucine sorting motifs contain a negatively charged residue at the start of the motif, the nontraditional motif in CD4 is only recognized by AP-2 following phosphorylation of Ser408, which mimics the necessary charge of an acidic residue at this position (*125*). This mechanism allows for a regulated and phosphorylation-dependent downregulation of CD4 during normal cellular conditions. However, Nef contains the complete dileucine motif necessary for AP-2 recruitment, and is able to drive a robust and phosphorylation-independent downregulation of CD4 during infection through a dually-coordinated recruitment of CD4 and AP-2 (*135*).

Nef binds to both the CD4 cytoplasmic tail and the AP-2 α-σ2 subunit hemi-complex with low μM affinity (*124*, *222*). It is suspected that the affinity for CD4 is even higher for the Nef/AP-2 hemicomplex due to the cooperative nature of binding between these proteins (*222*, *223*). While crystal structures have not been able to capture the cytoplasmic tail of CD4 bound to Nef, genetic and modeling studies have implicated the conserved Nef residues Trp57, Leu58, and Leu110 in CD4 binding (*224*). In contrast, a structure of Nef in complex with the AP-2 α/ σ2 hemicomplex has allowed for a comprehensive view of the binding interface between these proteins (*222*). Over a dozen residues within the large internal loop of Nef interact with the AP-2 hemicomplex in this crystal structure, and while Nef interacts with both the α and σ2 subunits, most contacts in the interface are directed towards σ2 (including the dileucine motif) (*222*). Surprisingly, while the

acidic Asp174/Asp175 motif is also required for productive CD4 downregulation (*225*), it does not directly contribute to AP-2 recruitment. Instead, both acidic residues interact with the Nef core to stabilize the dileucine motif loop for productive AP-2 engagement (*222*). Though this Nef/AP-2 structure failed to capture density for the cytoplasmic CD4 tail, the structure was later aligned with a structure of SIVmac239 Nef bound to an ExxxLM dileucine motif (*226*) and the NMR structure of the CD4 tail (*227*) to create a potential model for the AP-2/Nef/CD4 tail complex. Within this model, a hydrophobic pocket within SIV Nef binds to the non-canonical dileucine sequence of CD4, while simultaneously being bound by AP-2 via its own canonical dileucine motif (*226*).

The dileucine and the downstream acidic loop motifs are also critical for an SIV Nef-specific function- AP-2-dependent downregulation of the host restriction factor tetherin (*228*). Tetherin inhibits viral egress by "tethering" nascent virions to the membrane of infected cells during viral budding (*229*). SIV Nef downregulation of tetherin from the cell surface helps the virus overcome inhibition by simian tetherin. However, this AP-2-dependent mode of antagonism is reserved solely for SIV Nef. Most HIV-1 subtypes either rely on the Vpu accessory protein to antagonize human tetherin, or use an alternative AP-1 mechanism to antagonize tetherin (as is the case for HIV-1 Group O Nef proteins) (*230*). Still, examination of SIV Nef engagement of AP-2 is potentially instructive for understanding the mechanistic basis of the coordinated HIV-1 Nef/AP-2 downregulation of host cell targets. Sequence conservation between the large internal loops of SIV and HIV-1 Nef, particularly across the dileucine and diacidic motifs, further supports the functional relevance of this loop (*231*). With that in mind, a recent crystal structure of sooty mangabey-derived SIV (SIVsmm) Nef in complex with the AP-2 hemicomplex and simian tetherin reveals a critical role for the large internal loop and di-leucine motif not only in AP-2 recruitment,

but in recruiting cargo as well. The SIVsmm di-leucine motif assumes a similar conformation as seen in the AP-2/HIV-1 Nef crystal structure, but the backside of the AP-2- bound di-leucine loop directly engages a critical DIWK motif within tetherin (*231*).

The large internal loop also governs Nef downregulation and/or association with several other host cell proteins, including CD28, CD8, and β-COP. Nef downregulation of CD28 and CD8 appears to be driven through a common AP-2 dependent mechanism (*225, 232*), and mutation of both the di-leucine and D174/D175 acidic motif impairs Nef downregulation of both molecules (*233, 234*). While the di-leucine motif and D174/D175 acidic motif drive most internal loop interactions, some data suggest that the less-conserved E154/E154 acidic motif also participates in Nef function via recruitment of β-COP (*131*). Following internalization of MHC-I and CD4 into the endosomal compartment, Nef uses β-COP to direct the lysosomal degradation of both CD4 and MHC-I (*133*).

The majority of Nef structures obtained in the absence of binding partners for the internal loop yield unresolved density for this region due to its unstructured nature (*135*). However, as discussed in the overview of the N-terminal arm of Nef, the large internal loop is somewhat protected from hydrogen exchange within membrane-bound myristoylated Nef, suggesting that interaction with the core helps shield it from solvent exposure (*198*). Intra-molecular association between the internal loop of Nef and the folded core has been captured in structures of Nef, albeit in the presence of partner protein binding. For example, two helical elements within the internal loop of Nef are packed against the Nef core in the AP-2-bound structure (*222*). In addition, structures of both HIV-1 and SIVmac239 Nef bound to affinity-optimized SH3 domains show interaction between the folded core of one Nef molecule and the internal loop of another (*215,*

226). Taken together, these results point to the internal loop of Nef as an active participant in both intermolecular and intramolecular Nef interactions.

1.2.5.4 Dimerization Interface

Early characterization of recombinant Nef revealed a consistent tendency to dimerize in solution, a behavior that was initially suspected to be driven through a combination of non-covalent interactions and disulfide linkages between Nef monomers (*235, 236*). However, while oligomerization in these early studies was sensitive to reducing conditions in solution, deletion of the solvent-accessible C-terminal cysteine residue of Nef did not eliminate its ability to oligomerize, ruling out the contribution of disulfide contacts in dimer formation (*197*). Importantly, NMR spectroscopy shows that dimerization occurred between well-folded Nef proteins, arguing against the possibility that dimerization is an artifact of denatured protein (*235*). Additional biophysical and biochemical analyses of recombinant Nef point towards a reversible and concentration-dependent equilibrium between monomeric and dimeric Nef in solution (*197, 237*), consistent with early evidence for Nef oligomerization in the cytoplasm and on the surface of infected cells (*238*).

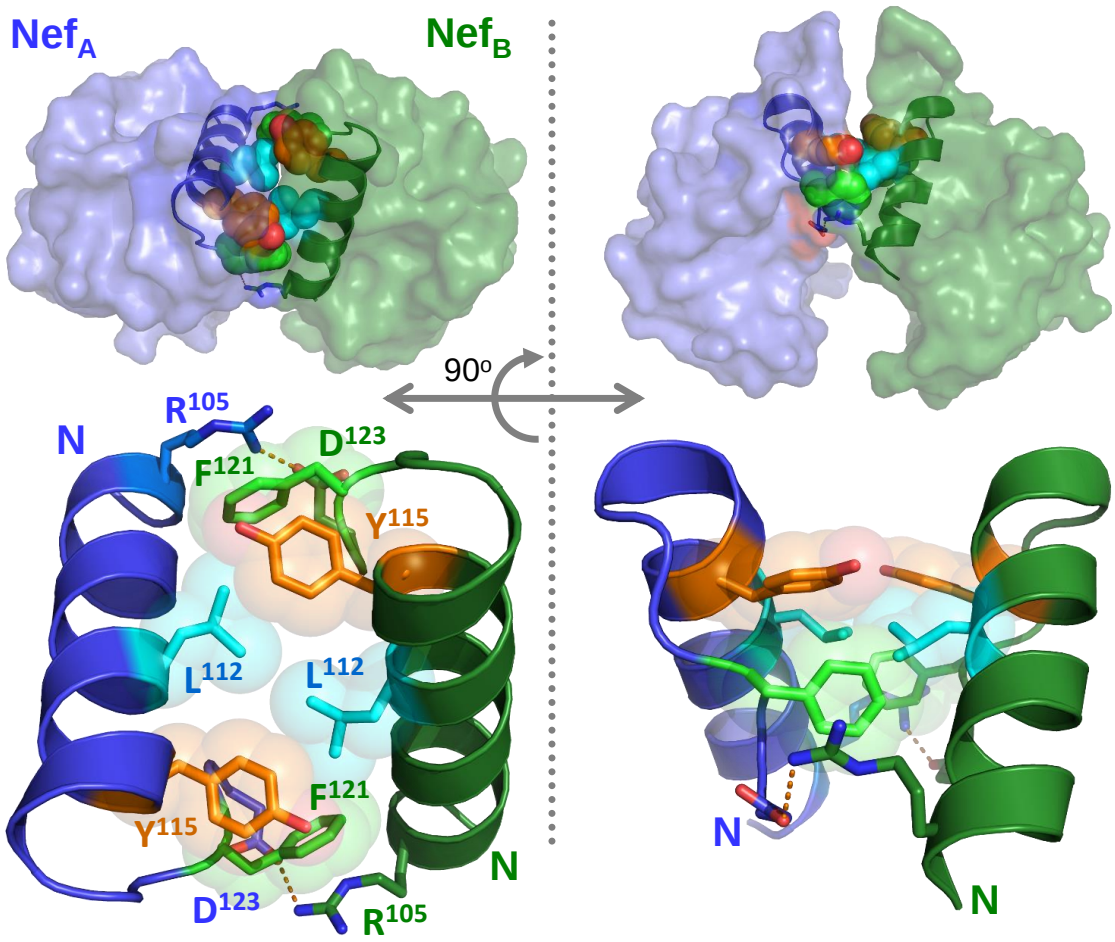

Figure 6: Nef homodimer interface from the X-ray crystal structure in complex with a Src-family kinase SH3 domain.
Overview of the Nef dimer structure is shown on the upper left, with the Nef monomers rendered in blue and green, respectively. The αB helices that form the dimer interface are highlighted (SH3 domains not shown for clarity). The αB helices are enlarged on the lower left, illustrating the side chains of Leu112, Tyr115, and Phe121 from each monomer which form the hydrophobic core of the interface. Also shown are the reciprocal ionic contacts between Arg105 and Asp123. Both models are rotated 90° on the right. These models were produced with PyMol using the crystal coordinates of the HIV-1 Nef core in complex with the Fyn SH3 domain (PDB: 1EFN).

The first crystal structures of HIV-1 Nef (in complex with Src-family kinase SH3 domains) also captured Nef within a dimeric state (*203, 207*), and granted the first glimpse into the structural basis of Nef dimerization. Within both structures, dimerization occurs between the αB helix of each Nef monomer at a hydrophobic interface formed by a cluster of hydrophobic residues

(Ile109, Leu112, Tyr115, His116, Phe121, Pro122; key interface residues are shown in Figure 6). Flanking that interface is a pair of reciprocal electrostatic interactions between Arg105 and Asp123, which appear to stabilize the dimer interface (*206, 207*). All of these residues are highly conserved across subtypes of HIV-1 Nef (*142*), and most are conserved or homologous in Nef expressed by HIV-2 or SIV Nef (*197*). Mutation of hydrophobic interface residues (individually or as a group) has been shown to impair Nef dimerization both in cells and in solution, confirming the apparent contribution towards dimerization in these structures (*149, 239*).

Nef dimerization, including these dimer interface residues, is also implicated in a number of Nef functions, including Src- and Tec-family kinase activation (*149, 240*), CD4 downregulation (*239, 241, 242*), and Nef enhancement of HIV-1 infectivity (this thesis) and replication (*239*). Mutation of Asp123 has also been shown to prevent MHC-I downregulation (*242*). However, another structure implicates Asp123 in the coordinated recruitment of MHC-I and the AP-1 μ1 subunit (*101*), which complicates whether contribution of this residue is through dimerization, complex formation, or dynamic transition involving both roles for Asp123.

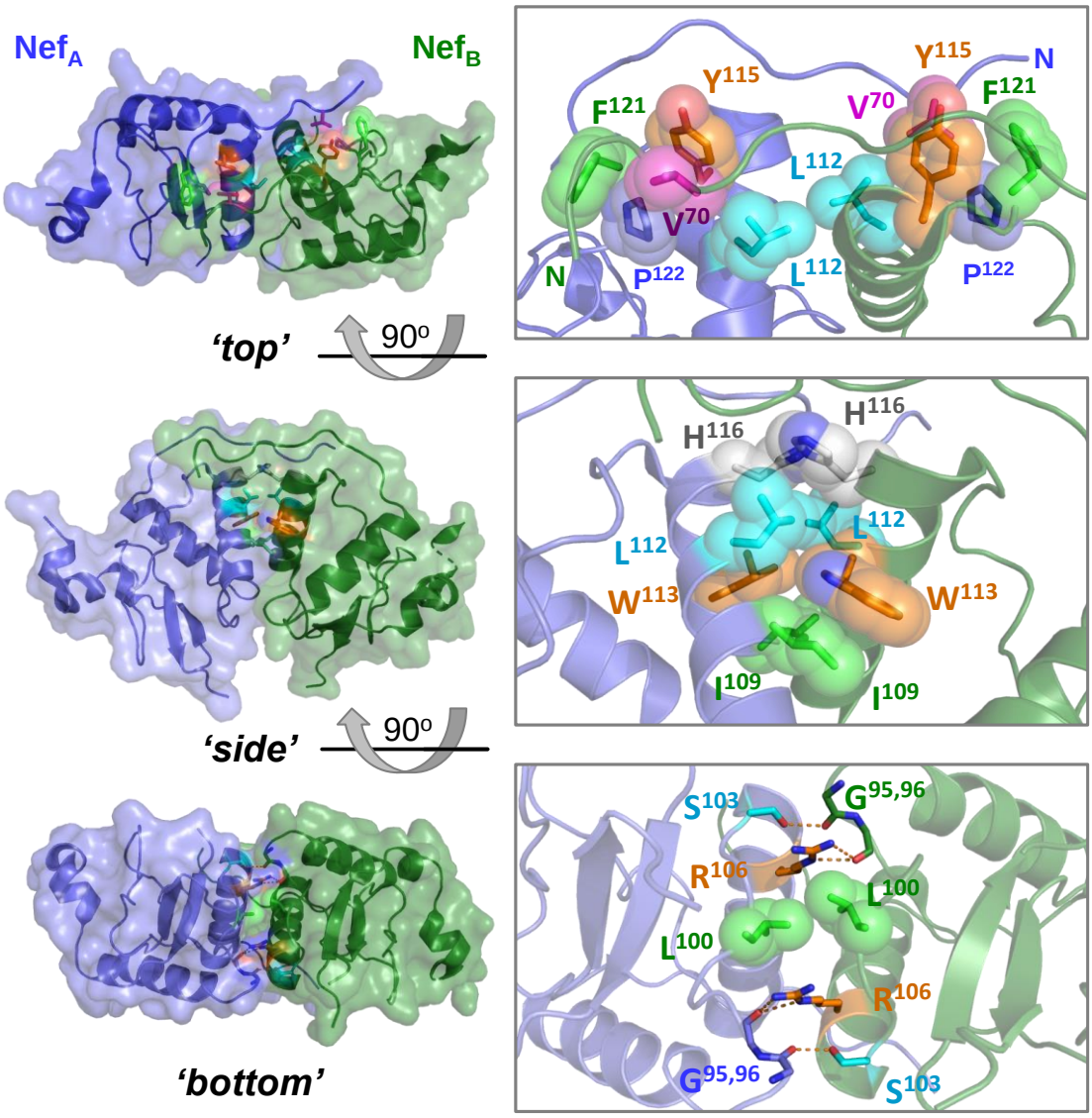

Figure 7: Homodimer interface from the X-ray crystal structure of Nef in complex with Hck SH3-SH2
Three overviews of this Nef homodimer are shown on the left with the Nef monomers rendered in blue and green, respectively (SH3-SH2 proteins not shown for clarity). Three interfaces stabilize this homodimer, which are enlarged on the right. In the 'top' view, the side chains of Leu112, Tyr115, Phe121, and Pro1122 form a hydrophobic cup that interacts with Val70 from the opposing monomer in reciprocal fashion. The 'side' view shows the contributions of Ile109, Leu112, Trp113, and His116 to a hydrophobic interface between the αB helices. The 'bottom' view shows reciprocal polar contacts formed by Ser103 and Arg106 with the main chain carbonyls of Gly95 and Gly96; Leu100 also makes a non-polar contact in this interface. These models were produced with PyMol using the crystal coordinates of the HIV-1 Nef core in complex with the Hck SH3-SH2 region (PDB: 4U5W).

However, a more dynamic, context-dependent dimer interface is also supported by recent crystal structures of the Nef dimer, wherein the conformation of the folded core for each Nef molecule is identical, but the orientation of the dimer interface is quite different relative to that

found in the complex of Nef with SH3 alone (compare Figures 6 and 7) (*212*, *243*). For example, in the presence of the Hck SH3-SH2 regulatory domain, the Nef dimer interface is dramatically rotated, and Asp123 is now solvent exposed and freed from the dimer interface, potentially promoting interaction with MHC-I and AP-1 (*212*). Comparative studies of dimeric Nef in complexes with SH3 vs. SH3-SH2 by HDX MS show that the two distinct dimer interfaces observed in the X-ray crystal structures are also present in solution (*244*). Consistent with these structures and other models of Nef dimerization is the contribution of hydrophobic core residues within and around the αB helix of the Nef core (*245*). The contribution of both Asp123 and hydrophobic interface residues towards varying complexes of Nef will be explored in Chapter 3 of this dissertation, and the role of several of these hydrophobic residues in a newly discovered function for Nef will be explored in Chapter 2.

1.2.6 Nef as a pharmacologic target

The critical role of Nef in HIV pathogenesis and immune escape makes it an attractive target for antiretroviral drug development. To date, only a handful of Nef inhibitors have been reported, with early strategies targeting the binding interface between Nef and the Hck SH3 domain. These efforts have identified small molecules that disrupt SH3 binding by Nef (*246*), a broad small molecule inhibitor of SH3 engagement which inhibits Nef activation of Lyn and c-Src (*139*, *247*), and high affinity recombinant SH3 domains to outcompete kinase binding (*248*). Two recent protein-based inhibitors combine a single chain antibody with high affinity for Nef with an engineered high-affinity SH3 domain to target Nef (*213*, *249*).

Another strategy used to identify small molecule inhibitors of Nef has focused on inhibition of Nef-dependent Hck activation, rather than Hck SH3 displacement. While Nef lacks enzymatic

activity, coupling Nef to Hck activation allowed for high-throughput chemical library screening and identification of Nef inhibitor candidates (*250*). Two classes of small molecule inhibitors were identified through this screening strategy. The first class, characterized by a 4-amino-diphenylfuranopyrimidine (DFP) scaffold, was discovered in a screen of a small library of kinase inhibitor-biased compounds. These compounds showed enhanced inhibition of Hck in the presence of Nef, suggesting that Nef binding may allosterically impact the Hck active site to enhance inhibitor binding. DFP-based Hck inhibitors demonstrated micromolar activity against Nef-mediated enhancement of viral replication, providing additional evidence that the Nef-Src-family kinase signaling pathway is important to viral replication (*251*). In subsequent work, the Nef-Hck assay was used screen a diverse library of more than 220,000 compounds. This screen identified a unique hydroxypyrazole-based inhibitor (designated as B9) that blocks HIV-1 replication at sub-micromolar concentrations in a Nef-dependent manner (*252*). Unlike the DFP compounds, B9 has been shown by SPR to bind directly to recombinant Nef with nanomolar affinity. B9 was also shown to impair Nef dimerization in a cell-based fluorescence complementation assay, suggesting that it may disrupt Nef function by impairing productive dimer formation (*252*). Characterization of both B9 and newer analogs based on their hydroxypyrazole core shows that this class of compounds impairs Nef activation of Tec-family kinases, and reverse Nef downregulation of MHC-I (*253*).

Critically, treatment of latently infected CD4 T cells with B9 and the more-recent hydroxypyrazole inhibitors promoted CD8+ cytotoxic killing of infected cells in co-culture, likely through inhibitor-mediated rescue of MHC-I cell surface expression (*254*). This result highlights the potential utility of hydroxypyrazole Nef inhibitors in shock-and-kill curative strategies. The dual actions of these compounds to restore immune receptor expression and cripple Nef

enhancement of viral replication, may help aid clearance of the latent viral reservoir following reactivation via LRAs. As these compounds have been shown to inhibit Nef enhancement of viral infectivity (*252, 253*), they may also impair the ability of Nef to antagonize a key host restriction factor that inhibits HIV-1 infectivity - the host cell transmembrane protein SERINC5.

1.3 SERINC5

1.3.1 Initial discovery and identification as a retroviral restriction factor

Though the ability of Nef to enhance viral infectivity was first reported in 1995 (*255*), the primary mechanism underlying that enhancement was not determined for nearly two decades. Incremental work over those twenty years showed that Nef expression during viral production within particular cell lines dramatically enhanced viral infectivity, and that this activity was dependent upon Nef motifs associated with CD4 downregulation and recruitment of AP-2 (*106*). This finding was followed by the observation that the murine leukemia virus (MLV) glycoGag protein (a retroviral protein structurally unrelated to Nef) enhanced viral infectivity of both HIV and MLV in the same Nef-responsive producer cell lines (*107*). This led researchers to hypothesize that Nef and glycoGag both targeted an unknown cell-type specific inhibitor of retroviral replication. The search for that inhibitor continued until 2015, when the labs of Dr. Massimo Pizzato and Dr. Heinrich Gottlinger reported that Nef antagonism of two poorly characterized transmembrane proteins, serine incorporator protein 5 (SERINC5) and the related isoform SERINC3, were responsible for cell-type specific enhancement of viral infectivity by Nef (*117, 256*).

Gottlinger and Pizzato took complementary approaches towards identifying the mysterious cellular factor. Pizzato built from the finding that Nef enhances viral infectivity to varying degrees in different HIV-1 producer cell lines, and used RNA-seq to compare the global transcriptome between producer cells that displayed a high degree of Nef-dependent infectivity enhancement with that of cells which saw little Nef-dependent promotion of infectivity. The group reported that RNA expression of SERINC5 within producer cells strongly correlates with the degree of Nef-enhanced viral infectivity (*117*). Looking to answer the same question, Gottlinger's laboratory took a proteomics-based approach, using mass spectrometry to identify membrane proteins that were differentially incorporated into HIV-1 virions in the presence or absence of Nef expression (*256*). Gottlinger found that ΔNef virions display a clear enrichment in SERINC3 compared to wild-type virus, suggesting Nef-dependent exclusion of SERINC3 from the viral membrane (*256*).

Having identified a link between Nef-dependent enhancement of viral infectivity and SERINC expression, the two groups published parallel studies in *Nature* characterizing the antiviral properties of both SERINC3 and SERINC5 and the antagonistic activity of Nef towards each protein. These studies demonstrated that SERINC3 and SERINC5 were incorporated into the lipid envelope during viral budding, and that incorporation of SERINC3/5 inhibited viral infectivity. They also demonstrated that Nef antagonizes SERINC3 and SERINC5 via downregulation through an AP-2 and clathrin-dependent mechanism, and that this antagonism reverses or mitigates SERINC inhibition of viral infectivity (*117*, *256*). A mechanistic model of SERINC5 activity and Nef antagonism can be seen in Figure 8.

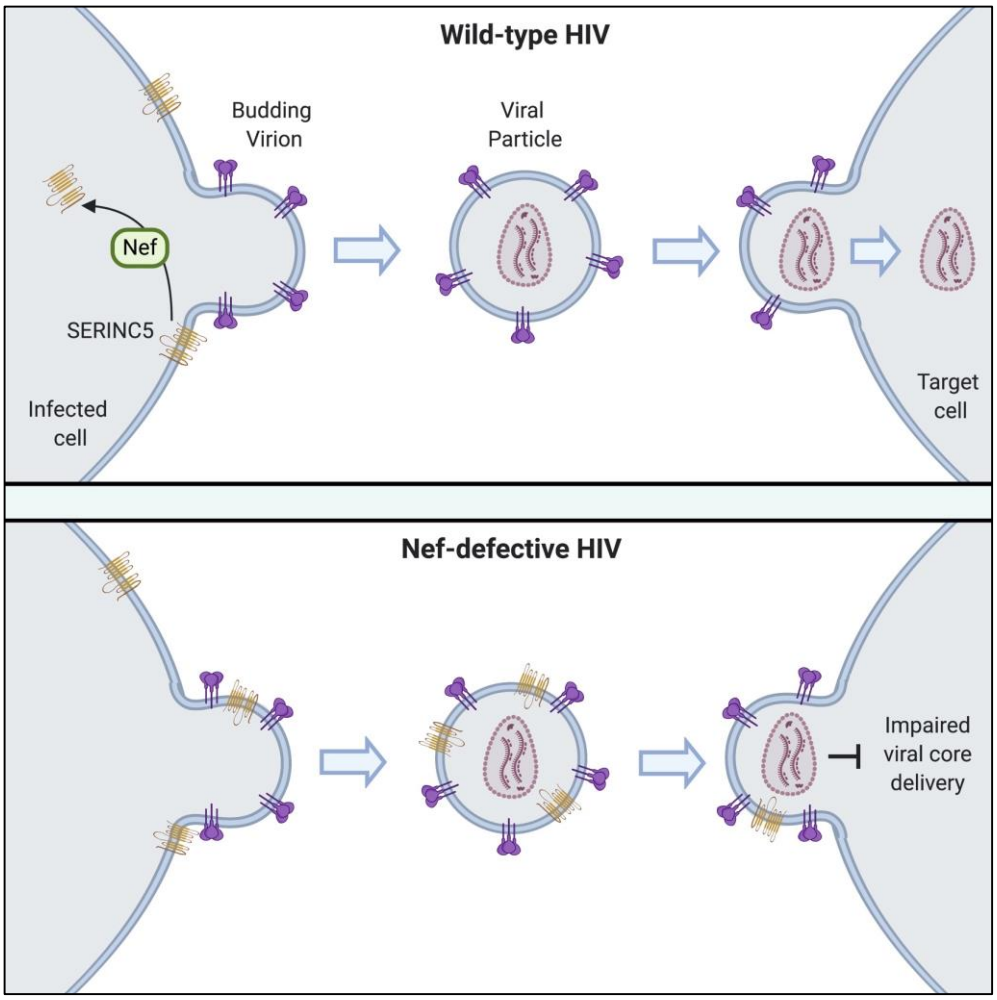

Figure 8: Model of SERINC5 Antagonism via HIV-1 Nef

Overview of Nef antagonism of SERINC5 during viral production. SERINC5 is expressed endogenously on the surface of HIV-infected cells. In the absence of Nef antagonism (lower panel), SERINC5 is incorporated in the viral membrane of newly synthesized virions, and impairs viral infection. In the presence of Nef antagonism (upper panel) SERINC5 is downregulated from the cell surface and excluded from the viral membrane, enhancing infectivity. Model is adapted from Aiken 2015 (*257*), and produced using Biorender.

1.3.2 Structure and critical features of SERINC5

SERINCs are a family of multi-pass transmembrane domain proteins that are evolutionarily conserved across all eukaryotes, but distinct in sequence homology from all other identified protein families. There are five SERINC family members expressed by humans (SERINC1-5), and all SERINCs but SERINC2 inhibit HIV-1 infectivity following incorporation into nascent virions

(*258*). SERINC4 and SERINC5 exhibit the greatest extent of HIV-1 restriction out of all SERINC family members, however, SERINC4 does not appear to be highly expressed within any cells or tissues relevant to HIV-1 infection (*259*). In contrast, SERINC5 (and the less potent antiviral factor SERINC3), are highly expressed within lymphoid and myeloid cells (*256*).

While the ubiquity of SERINC across eukaryotic organisms hints at an ancient endogenous function, the role of SERINCs outside the context of retroviral infection is currently unknown. An early study of SERINC proteins (and the origin of the name SERINC) suggests a potential role in the synthesis of serine and serine-incorporated lipids (*260*), although such a function has not been supported by recent research (*261, 262*). And while SERINCs are highly expressed within some cancer cell lines and enriched within certain neuronal cell types, their function in the context of cancer pathogenesis and neurobiology remain to be determined (*259*).

Recent work has revealed the structure, topology, and features of SERINC5 essential for HIV restriction (*263*). SERINC5 is a 10-transmembrane domain protein with five extracellular loops, four intracellular loops, and cytosolic N- and C-termini (*264*) (Figure 9). Cryo-EM structures of both the *Drosophila* ortholog of SERINC5 and human SERINC5 have confirmed the predicted topology and revealed that the protein assumes a dual subdomain configuration (*263*). Subdomains A and B of SERINC5 are separated by the fourth transmembrane domain, which bridges the second extracellular loop and intracellular loop of SERINC5, and cuts diagonally through the plasma membrane. Subdomain B appears to form a structural groove that can be accommodated both the hydrophilic head group and hydrophobic tail of a number of lipids (*263*).

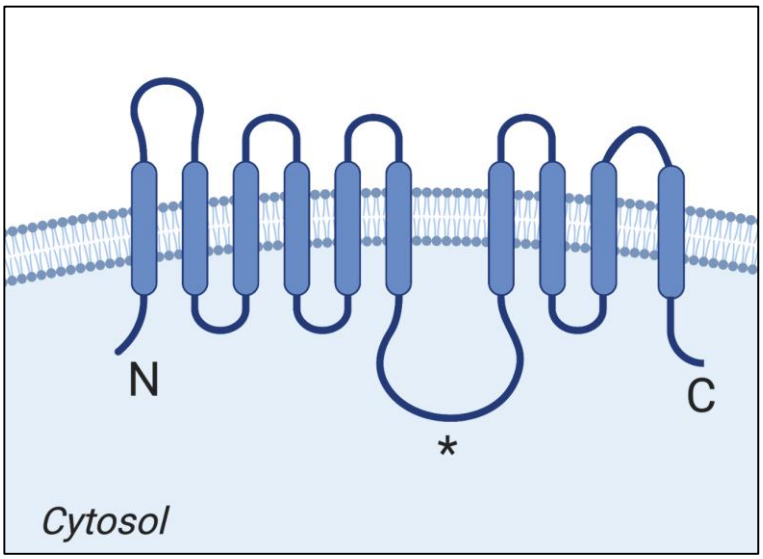

Figure 9: Topology of SERINC5

Model of the SERINC5 structural organization and topology of SERINC5. SERINC5 contains ten transmembrane domains, intracellular N- and C-termini. Asterisk marks the location of the SERINC5 Intracellular Loop 4 (ICL4), the region of SERINC5 which directs sensitivity towards Nef antagonism. Figure produced via Biorender.

There are five alternatively spliced isoforms expressed by the *SER5* gene, however only one isoform (Ser5-001) contains the 10th transmembrane domain that is essential for stable protein expression and antiviral activity (*265*). The majority of expressed SERINC5 is this isoform, as the other four isoforms exhibit poor stability and are expressed at a 10-fold lower level than Ser5-001 (*265*). Stable SERINC5 expression also requires N-glycosylation at residue Asn294 on the fourth extracellular loop, as mutation of this N-glycosylation site decreases steady-state expression of SERINC5 (*266*).

Another critical feature of SERINC5 is intracellular loop 4 (ICL4), both the largest loop within SERINC5 and the primary determinant of SERINC5 sensitivity to Nef antagonism. As Nef antagonism of SERINC5 is not conserved across all orthologs of the protein, replacement of the human SERINC5 ICL4 with the ICL4 loop from Nef-resistant frog (*Xenopus tropicalis*) SERINC5 confers complete resistance to Nef antagonism (*267*). Nef Sensitivity of SERINC5 within the large intracellular loop appears to map specifically to two hydrophobic residues- Leu350 and Ile353,

and mutation of both residues within human SERINC5 impairs downregulation by Nef. While it is tempting to speculate that this loop functions as a binding site for Nef, this remains to be proven experimentally. However, SERINC5 and Nef do appear to associate directly in cells, and it has recently been demonstrated that expression of a fusion construct of Nef/SERINC5-ICL4 promotes complex formation with AP-2 (*268*, *269*).

1.3.3 SERINC5 restriction of viral infectivity

SERINC5 inhibition of viral infectivity is conserved across all orthologs tested, including SERINC5 from rodent, zebrafish, frog, and rabbit (*267*, *270*). The full mechanism controlling SERINC5 inhibition of viral infectivity remains elusive, but it is suspected that SERINC5 incorporated into the viral membrane inhibits viral infectivity by targeting Env function (*271*). This is supported by the observation that virus sensitivity to SERINC5 restriction is entirely dependent upon Env, as HIV-1 pseudotyped with Env from VSV or Ebola is markedly resistant to SERINC5 antagonism (*117, 256*). Env proteins from different subtypes of HIV-1 also display varying sensitivities to SERINC5, suggesting that inhibition of viral infectivity is mediated through Env. SERINC5 appears to directly associate with Env, as shown through via bimolecular fluorescence complementation (BiFC) and immunoprecipitation assays (*271*, *272*). Incorporation of SERINC5 into nascent virions inhibits viral fusion (*273*), and Env conformation (as detected by conformation-dependent neutralizing antibodies) is directly impacted by SERINC5 (*271*, *273*). As Env-Env association is decreased in the presence of SERINC5, it is possible that SERINC5 disrupts formation of the functionally competent Env trimer (*272*), or clustering of the handful of Env spikes (7-14 per virion) on the viral membrane (*259*). Future work will further elucidate the interplay between SERINC5 and Env and how it relates to restriction of HIV-1 infectivity.

Though SERINC5 is one of several antiretroviral restriction factors that targets HIV-1 (tetherin, APOBEC3G and TRIM5α), there are several significant differences between SERINC5 and other restriction factors. For example, while expression of other restriction factors is induced by interferon, SERINC5 is expressed at high levels within HIV-1 target cells in an interferon-independent manner (*256, 274*). Still, while SERINC5 mRNA and protein levels do not increase following interferon stimulation, IFN-α treatment appears to increase cell surface localization of SERINC5 (*275*). Another hallmark of other HIV-1 restriction factors not shared with SERINC5 is a clear signature of positive evolutionary selection. While the evolutionary histories of tetherin, TRIM5α, and APOBEC3G display signs of an evolutionary arms race with HIV, SERINC3 and SERINC5 do not appear to have been shaped by positive selective pressure under the virus (*276, 277*). However, positive selection could simply be confined to a few select regions with SERINC5 rather than the entire ORF (as in seen for other restriction factors) (*276*). Indeed, a cluster of serines within SERINC3 appear to be the result of positive selective pressure (*278*). In any case, the lack of complete positive selection is interesting considering the clear antagonistic relationship between SERINC5 and several distinct retroviruses.

1.3.4 Retroviral antagonism of SERINC5

SERINC5 antagonism via Nef is driven primarily through exclusion of SERINC5 from incorporation into newly synthesized virions, which Nef achieves through downregulation of SERINC5 from the cell surface. Following Nef-directed internalization, SERINC5 is directed into the endosome system, colocalizing with early (Rab5+) and late (Rab7+) endosomes en route to lysosomal degradation (*135, 268*). As a result, Nef decreases both cell-surface and steady-state levels of SERINC5 within viral producer cells, decreasing the quantity of restriction factor that

gets incorporated into the membrane of nascent virions (*268*). While exclusion of SERINC5 from HIV-1 virions appears to be largely responsible for the phenotype of Nef antagonism, Nef seems to be able to additionally antagonize SERINC5 in the presence of high SERINC5 expression and virion incorporation. However, the mechanism behind this observation remains to be determined (*279*).

Nef antagonism of SERINC5 is widely conserved across HIV-1, HIV-2, and SIV (*280*), and Nef proteins expressed by various primate lentiviruses are able to widely antagonize SERINC5 orthologs across primate and murine species (*281*). There is, however, some inherent variation in the degree to which Nef can antagonize SERINC5, and Nef proteins from the HIV-1/SIVcpz lineage are more active against SERINC5 than Nef proteins from the HIV-2/SIVsmm lineage (*281*). Interestingly, the extent to which SIV Nef proteins antagonize SERINC5 directly correlates with how prevalent that SIV strain is within infected primate populations. This suggests that SERINC5 restriction is a barrier to effective lentiviral transmission within primates (*281*).

In addition to SIV and HIV-2, at least two other retroviruses demonstrate the ability to overcome SERINC5 restriction: Murine Leukemia Virus (MLV) via the glycoGag protein, and Equine Infectious Anemia Virus (EIAV) via the S2 auxiliary protein. Like Nef, MLV glycoGag and EIAV S2 retarget SERINC5 into intracellular compartments, promoting exclusion of SERINC5 from newly synthesized virions (*117, 282*). Remarkably, despite their shared function, there is no sequence homology between these three proteins (*259*). Instead, glycoGag, S2, and Nef share two key molecular determinants- the ability to associate with both the plasma membrane and clathrin adaptor binding motifs (*282*). MLV glycoGag associates with the membrane as a Type II single-pass transmembrane protein, while Nef and S2 associate with the membrane following myristoylation. Mutation of the myristoylation site within S2 and Nef, or the clathrin adaptor

protein binding motifs (YxxL for glycoGag, di-leucine motif for S2 and Nef) completely abolishes SERINC5 antagonism by these proteins (*282, 283*).

In addition to their critical contribution to Nef antagonism of SERINC5, the myristylation sequence and di-leucine motif are also essential for Nef downregulation of CD4 as described in an earlier section (*256, 284*). CD4 downregulation and SERINC5 antagonism are also both driven through AP-2 and clathrin-dependent internalization, and are similarly targeted by Nef into the endosome-lysosome pathway (*268*). Though a role for Nef dimerization has been established for Nef downregulation of CD4, it remains to be examined whether dimerization also plays a role in Nef antagonism of SERINC5 (*239*). Based on the existing mechanistic similarities between SERINC5 and CD4 downregulation, the Nef dimer interface could potentially represent a third molecular determinant shared between both Nef functions.

1.4 Hypotheses and Specific Aims

1.4.1 Hypothesis 1: Nef homodimerization is essential for downregulation of SERINC5

Mutation of the Nef homodimerization interface residues Leu112, Tyr115, and Phe121 disrupts Nef self-association in cells and solution, and impacts the ability of Nef to downregulate CD4 from the surface of infected cells. CD4 and SERINC5 downregulation via Nef have been described as mechanistically similar, with both functions dependent upon AP-2 recruitment and clathrin-mediated endocytosis. Furthermore, Nef re-targets both CD4 and SERINC5 into Rab7+ late endosomal compartments, directing them towards lysosomal degradation. Based on the inherent similarity of these two mechanisms, *I hypothesize that Nef homodimerization is essential*

for antagonism of SERINC5, and that disrupting the dimerization interface through L112, Y115, and F121 mutations impacts SERINC5 downregulation and thus reduces viral infectivity. To test this hypothesis, I utilized a series of viral infectivity assays, confocal microscopy studies, flow cytometry, virion isolation assays, and immunoblots to explore the three following experimental aims.

1.4.2 Specific Aims for Hypothesis 1

1.4.2.1 Aim 1: Explore the impact of dimerization-defective Nef mutants on HIV-1 infectivity and virion exclusion of SERINC5.

Using a HeLa-based HIV-1 reporter cell line (TZM-bl), we measured whether Nef enhancement of viral infectivity was decreased in the presence of dimer interface mutations (L112A, L112D, Y115D, F121A). HIV-1 encoding wild-type, mutant, or no Nef (ΔNef) was produced in 293T cells, Jurkat JTAg T cells, or peripheral blood mononuclear cells (PBMCs) in the presence and absence of SERINC5, and the resulting viral supernatants were collected, quantified, and incubated with TZM-bl cells to measure infectivity. We found that the L112D, Y115D, and F121A mutants displayed severely impaired Nef promotion of infectivity, similar to what was observed for the ΔNef viral mutant. In contrast, we found that the L112A mutant had infectivity close to that displayed by the virus expressing wild-type Nef. This observation is consistent with the limited impact of the L112A mutation on Nef dimerization in cells. In order to connect impaired promotion of infectivity to impaired antagonism of SERINC5, we collected wild-type, ΔNef, and Nef dimer mutant virus produced in 293T cells transfected with SERINC5, and used sucrose cushion ultracentrifugation to purify the resulting virions, which were analyzed via immunoblot. We found that ΔNef, L112D, Y115D, and F121A incorporated significantly more

SERINC5 than the wild-type and L112A Nef viruses, suggesting a reduced capability of those mutants to antagonize and exclude SERINC5. This observation suggests that Nef mutants known to display significant impairment of dimerization (L112D, Y115D, F121A) are unable to effectively antagonize SERINC5 or promote infectivity.

1.4.2.2 Aim 2: Examine whether disruption of Nef dimerization impairs Nef downregulation and intracellular retargeting of SERINC5.

Nef downregulates SERINC5 from the cell surface and retargets it into the endosome/lysosome system for degradation. In order to determine whether impaired exclusion of SERINC5 from nascent virions is due to dysfunctional downregulation of SERINC5 from the cell surface, we transfected cells with a SERINC5 construct labeled with an extracellular HA-tag (SERINC5-iHA) and either wild-type or Nef dimer mutants, and quantified Nef downregulation of SERINC5-iHA via flow cytometry. We observed downregulation of cell-surface SERINC5 in the presence of wild type Nef or the L112A mutant, but attenuated downregulation of SERINC5 for the L112D, Y115D, and F121A mutants. As a control, we also compared the ability of these Nef mutants to downregulate endogenous cell surface CD4. As expected, wild-type Nef robustly downregulated CD4, while L112D, Y115D, F121A did not. The Nef-L112A mutant partially downregulated CD4, presenting an intermediate phenotype between wild-type Nef and the other mutants. In order to determine if mutation of the Nef dimer interface impaired intracellular targeting of SERINC5 following downregulation, we used confocal microscopy to study the localization of RFP-labeled SERINC5 in the presence of wild-type or mutant Nef fused to YFP. SERINC5 was primarily localized at the cell surface when expressed alone, but in the presence of wild-type Nef or the L112A mutant, SERINC5 was retargeted into intracellular compartments which colocalized with the Rab7+ late endosomal marker. Co-expression of L112D, Y115D, and

F121A decreased internalization of SERINC5 and colocalization with Rab7. These results show that Nef dimerization is required for both initial downregulation of SERINC5 as well as its intracellular trafficking to late endosomes.

1.4.2.3 Aim 3: Evaluate whether dimerization interface mutations impair Nef association with SERINC5, AP-2, or Nef within cells.

To determine the impact of Nef dimer interface mutations on Nef function and signaling, we used bimolecular fluorescence complementation (BiFC) assays to compare the association of Nef dimer mutants with cellular binding partners. We found that all Nef mutants retained functional association with SERINC5, AP-2α and AP-2σ2 in the BiFC assay, suggesting that disruption of Nef dimerization does not impair recruitment of either the SERINC5 cargo or endocytic machinery. However, Nef dimer mutants displayed reduced capability to homodimerize in cells by BiFC which mirrored their ability to antagonize SERINC5. In summary, our studies support a mechanism in which Nef homodimers serve to bridge SERINC5 with the AP-2 pathway for internalization, thereby excluding incorporation of this restriction factor into newly synthesized virions.

1.4.3 Hypothesis 2

Previous genetic and cellular studies of the Nef dimer interface have been based upon a crystal structure of the Nef:Hck SH3 "dimer of complexes" (*239*) (Figure 6). Hck is a member of the Src-kinase family expressed in monocytes and macrophages, and interaction with Nef leads to kinase activation that enhances replication in host cells of myeloid origin. In this structure, two Hck SH3-bound Nef monomers form a dimer through a hydrophobic interface between their αB

helices (*285*). This dimer interface is further stabilized by reciprocal electrostatic interactions between Arg105 and Asp123 on complementary Nef monomers (*285*). However, more recent structural studies of the Nef dimer bound to a Hck SH3-SH2 dual regulatory domain protein demonstrate a completely different orientation of the dimer interface (Figure 7), in which Nef Asp123 swings out of the dimer interface in the Hck SH3-SH2 bound structure (*212*). Dynamic changes suggested by the two crystal structures were further supported by HDX MS, where a charge reversal mutation of Asp123 disrupted dimerization in the Hck SH3 but not the Hck SH3-SH2-bound structure in solution (*244*). Importantly, only the orientation of the dimer interface is impacted by Nef binding partners, while the overall global fold of the Nef core region is identical across these and other crystal structures of Nef associated with diverse binding partners (*212, 222, 239*). Comparison of the Hck SH3 and SH3-SH2-bound Nef dimer structures reveals multiple Nef residues that contribute to the dimer interface in both structures. Three of these residues have already been characterized in detail in cells – Leu112, Tyr115, and F121 (see Figures 6 and 7). However, the individual contribution of these residues towards the dimer interface across different stages of kinase regulatory domain association remain to be evaluated. In addition, further inspection of these crystal structures suggested important contributions of Ile109 and His116 to these interfaces as well as regulation of homodimer transitions in solution important for function. *Therefore, I hypothesized that Ile109, Leu112, Tyr115, and His116 individually contribute to unique Nef homodimer transitions captured by the crystal structures of Nef in complexes with the Hck SH3 domain alone vs. the complete SH3-SH2 regulatory subunit.* To test this hypothesis, I expressed and purified four recombinant Nef dimerization interface mutants: I109A and His116A along with L112A and Y115A for comparison. All four mutants yielded soluble protein in high

yield, and were subsequently analyzed by surface plasmon resonance, size-exclusion chromatography, and in vitro kinase assays as described in the following Aims:

1.4.4 Specific Aims for Hypothesis 2

1.4.4.1 Aim 1: Determine the binding affinity of Nef dimer mutants towards Hck SH3 and SH3-SH2 regulatory domain proteins

As described in detail in Section 1.2.5.2, interaction of Nef with SH3 domains requires an intact Nef PxxPxR motif and a hydrophobic pocket dependent upon the appropriate 3-dimenional fold of the Nef core. Prior to examining the impact of Nef dimer interface mutations on SH3/SH3-SH2 complex formation in solution, therefore, we first compared the effect of each mutation on the affinity of Nef towards both the Hck SH3 and SH3-SH2 regulatory domain proteins. Using a flow-based surface plasmon resonance (SPR) system, recombinant purified Hck SH3 and SH3-SH2 domains were covalently linked to the surface of a sensor chip within a flow channel, and each recombinant Nef protein was then flowed across the surface of the chip. We observed that the Nef I109A, L112A, and H116A mutants displayed similar affinities as wild-type Nef for the SH3 and SH3-SH2 proteins, suggesting that these dimer interface substitutions had no impact on SH3 binding. However, Nef-Y115A displayed about 5-fold lower affinity towards both regulatory domain proteins, suggesting a potential allosteric effect of this mutation on SH3 engagement.

1.4.4.2 Aim 2: Evaluate whether Nef dimer mutants form 2:2 heterocomplexes with SH3 and SH3-SH2 in solution

In order to evaluate the impact of these substitutions on dimerization and complex formation in solution, we mixed either wild-type or Nef dimer mutant proteins with Hck SH3 and

SH3-SH2 in equimolar ratios, and then injected them onto an analytical size-exclusion chromatography column. We found that wild-type, I109A, L112A, and H116A Nef appear to form similarly sized complexes in the presence of SH3 and SH3-SH2, potentially corresponding to the 2:2 heterodimer complexes observed in previous structures with wild-type Nef. However, complexes of Nef-Y115A with SH3 and SH3-SH2 eluted at later retention times, signaling impaired 2:2 complex formation. These results suggest the Y115 is essential to Hck dimer complex formation, with the other three residues playing a supporting role.

1.4.4.3 Aim 3: Explore whether Nef dimer interface mutants display functional activation of Hck in vitro

In this Aim, we explored the effect of each Nef dimer interface mutant on recombinant, downregulated Hck activity in a solution-based assay. We found that that the Nef I109A, L112A, and H116A mutants all activated Hck to a similar extent as wild-type Nef. While the Y115A mutant was about 2-fold less potent in terms of Hck activation, this mutant was still capable of fully activating Hck. These results suggest that substitution of large hydrophobic residues with alanine produces functionally stable Nef, but that Y115A may impact dimer formation and/or Hck recruitment. Furthermore, the crystal structure of the Nef dimer interface when in complex with the Hck SH3-SH2 region is quite complex, involving three distinct interfaces and at least 13 unique residues. Thus, substitution of a single residue (except for Tyr115) may not be sufficient to disrupt complex formation and Hck activation in solution, a conclusion supported by the SEC studies.

2.0 Nef homodimers couple SERINC5 to AP-2 for Downregulation in HIV-1 Producer Cells

2.1 Chapter 2 summary

SERINC5 is a multi-pass intrinsic membrane protein that suppresses HIV-1 infectivity when incorporated into budding virions. The HIV-1 Nef virulence factor prevents viral incorporation of SERINC5 by triggering its downregulation from the producer cell membrane through an AP-2-dependent endolysosomal pathway. However, the mechanistic basis for SERINC5 downregulation by Nef remains elusive. Here we demonstrate that Nef homodimers are required for SERINC5 downregulation, trafficking to late endosomes, and exclusion from newly synthesized viral particles. Based on previous X-ray crystal structures, we mutated three conserved residues in the Nef dimer interface (L112, Y115, F121) and demonstrated attenuated homodimer formation in a cell-based fluorescence complementation assay. Point mutations at each of these positions reduced the infectivity of HIV-1 produced from transfected 293T cells, Jurkat TAg T cells, and primary human mononuclear cells in a SERINC5-dependent manner. In SERINC5-transfected 293T cells, virion incorporation of SERINC5 was increased by dimerization-defective Nef mutants, while downregulation of SERINC5 from the membrane of transfected Jurkat cells by these mutants was significantly reduced. Nef dimer interface mutants also failed to trigger internalization of SERINC5 and localization to Rab7+ late endosomes in T cells. Importantly, dimerization-defective Nef mutants retained interaction with both SERINC5 and AP-2 by fluorescence complementation assay. These results demonstrate that downregulation of SERINC5 and subsequent enhancement of viral infectivity requires Nef homodimers and support a mechanism by which the Nef dimer bridges SERINC5 to AP-2 for endocytosis. Pharmacological

disruption of Nef homodimers may provide a new approach to control HIV-1 infectivity and viral spread by enhancing incorporation of SERINC5.

2.2 Introduction

The HIV-1 Nef accessory protein is expressed early in the HIV-1 life cycle where it promotes viral replication and AIDS progression (*286*). Expression of Nef within the CD4-positive cell compartment is sufficient to induce an AIDS-like disease in transgenic mice (*287, 288*). Conversely, patients harboring Nef-defective strains of HIV-1 exhibit reduced viral loads and delayed progression to AIDS (*289, 290*). Enhancement of lentiviral pathogenicity by Nef is conserved across species. Disruption of the *nef* open reading frame of simian immunodeficiency virus (SIV) significantly reduces viral replication and prevents the development of AIDS-like disease in SIV-infected macaques (*291*). These are just a few examples of the evidence supporting a central role for Nef in HIV-1 and SIV pathogenicity.

Nef is a small protein (27-34 kDa, depending on the viral subtype) that is associated with host cell membranes by virtue of N-terminal myristylation (*292*). Nef lacks inherent enzymatic activity, functioning instead through multiple protein-protein interactions that alter host cell signaling and protein trafficking networks involving as many as 70 host cell proteins (*109*). Nef selectively binds and activates members of the Src and Tec protein-tyrosine kinase families (*293-296*). Disruption of Nef-dependent kinase activation through genetic or pharmacological means impairs Nef-mediated enhancement of HIV-1 infectivity and replication (*295-299*). In terms of protein trafficking, Nef drives the downregulation of cell surface receptors essential for immune recognition and viral entry, including MHC-I, CXCR4, CCR5, and CD4 (*112, 292, 300*). Receptor

downregulation involves Nef interactions with endosomal trafficking proteins, including the adaptor protein complexes 1 and 2 (AP-1 and AP-2) (*301, 302*). Downregulation of CD4 requires simultaneous engagement of Nef with both the cytoplasmic tail of CD4 and a hemicomplex formed by the α and σ2 subunits of AP-2 (*222*). Nef•CD4•AP-2 complexes form clathrin-coated pits at the cell surface, leading to endocytosis and lysosomal degradation of internalized CD4 (*303*).

Nef-mediated endocytosis of the SERINC5 restriction factor, essential for enhancement of HIV-1 infectivity, is also mediated by the AP-2 trafficking pathway. In the absence of Nef, SERINC5 is present on the surface of HIV-1 infected cells and incorporated into the membrane of newly synthesized virions (*304-306*). Incorporation of SERINC5 disrupts viral fusion with host cells and delivery of the viral core through a cryptic, Env-dependent mechanism. Nef antagonizes SERINC5 in part by promoting AP-2-dependent downregulation of SERINC5 from the plasma membrane of infected cells, thereby preventing incorporation into budding virions (*305*). Following downregulation by Nef, internalized SERINC5 is targeted for degradation via the endolysosomal pathway (*307*).

While Nef uses distinct structural motifs to recognize diverse host cell partners, many Nef functions also require homodimer formation. Mutants of Nef that are defective for homodimerization are unable to induce host cell tyrosine kinase activation, even though they retain interaction with the kinases (*296*). This observation is consistent with the formation of Nef•kinase dimer complexes necessary for kinase activation by trans-autophosphorylation. Dimerization-defective Nef mutants are also unable to downregulate CD4 from the host cell surface, and these mutations reduce HIV-1 infectivity and replication efficiency in cell lines (*241, 308*).

In this study, we investigated the role of Nef homodimerization in HIV-1 infectivity and restriction by SERINC5. Using a series of Nef mutants defective for homodimer formation in cells,

we demonstrated that Nef dimers are required to enhance infectivity of HIV-1 produced from T cell lines and donor PBMCs as well as 293T cells co-transfected with SERINC5. These same Nef mutants were attenuated in their ability to exclude SERINC5 from newly synthesized virions. Impairment of Nef dimerization reduced downregulation of SERINC5 from the cell surface and prevented its intracellular trafficking to Rab7+ late endosomes. Critically, cell-based fluorescence complementation assays revealed that these Nef mutants retained interaction with both SERINC5 and the AP-2 α and σ2 subunits, indicating that the reduced antagonism of SERINC5 was not due to loss of Nef association with either partner protein. Taken together, our data demonstrate that Nef antagonizes the SERINC5 restriction factor as a homodimer, which may serve as a bridge linking SERINC5 with AP-2 for endocytosis and degradation.

2.3 Results

2.3.1 Structural basis of HIV-1 Nef homodimerization

In this study, we explored the role of Nef homodimerization in the downregulation of SERINC5 and promotion of HIV-1 infectivity using a genetic approach involving Nef mutants defective for homodimer formation. X-ray crystallography of Nef in complex with the regulatory SH3 and SH2 domains of Src-family kinases have shown that Nef forms homodimers through a hydrophobic interface involving side chains of residues in the Nef αB helices and adjacent loops (*309*, *310*). An example is provided by the structure of HIV-1 Nef in complex with the SH3-SH2 regulatory region of the Src-family kinase, Hck (a model of the overall homodimer is shown in Figure 10A) (*310*). In this structure, three conserved residues from one Nef subunit (Leu112,

Tyr115, Phe121) converge to create a 'hydrophobic cup' that clasps the side chain of Val70 from the opposing Nef monomer in a reciprocal fashion (Figure 10B). A recent study has shown that recombinant Nef proteins in which Leu112 or Tyr115 is replaced with aspartate or Phe121 is substituted with alanine fail to form dimers in solution, providing direct evidence that these residues are essential for dimer stabilization (*296*). Mutations at these positions attenuate multiple Nef functions, including host cell kinase activation, enhancement of HIV-1 replication, and receptor downregulation including CD4 (see Introduction).

While the role of Nef homodimers in SERINC5 antagonism has not been explored, the mechanistic similarity between Nef-mediated downregulation of CD4 and SERINC5 suggests a key role. Both processes involve clathrin-mediated endocytosis via the tetrameric trafficking adaptor protein AP-2, which interacts directly with Nef through a hemicomplex of its α and σ2 subunits (*222, 264*). Importantly, alignment of this Nef homodimer with the crystal structure of Nef bound to the AP-2 α/σ2 hemicomplex shows that the Nef homodimer interface residues do not contact AP-2 (Figure 10C), suggesting that the dimer interface mutations described above will not affect AP-2 recruitment. These mutants were therefore chosen to explore the requirement for Nef dimers in SERINC5 regulation.

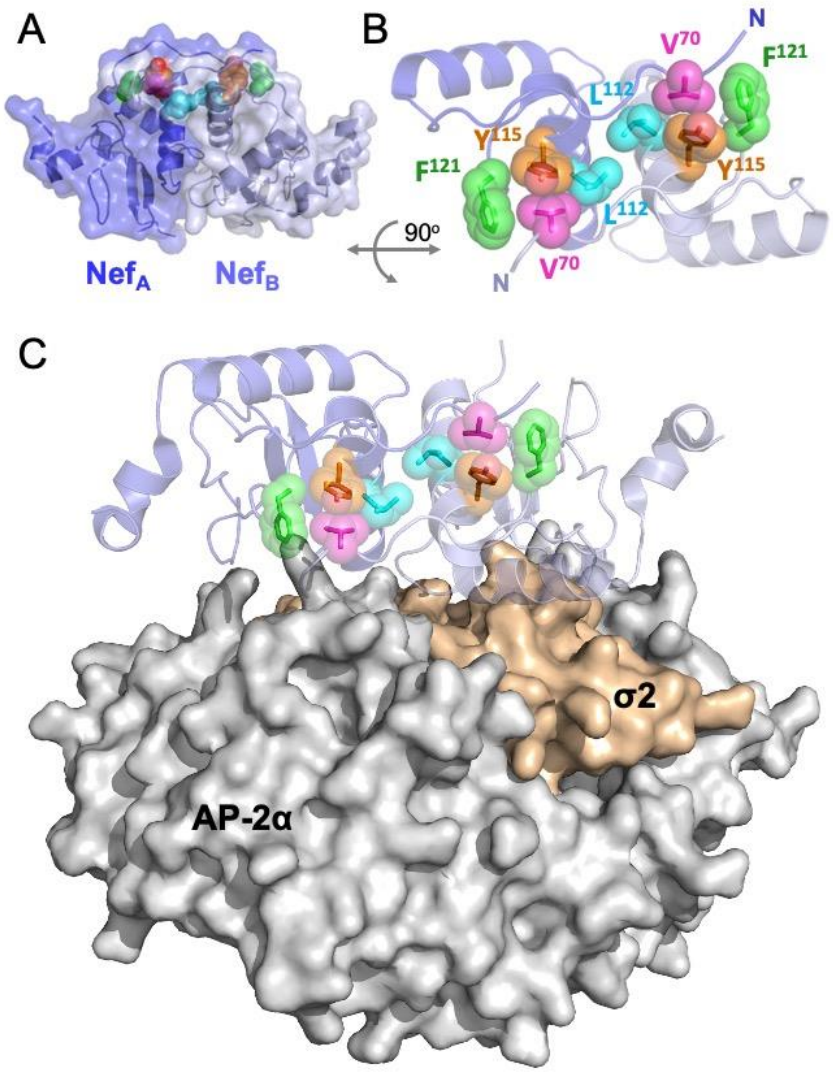

Figure 10: Structural basis of Nef dimerization

A) Overall structure of the HIV-1 Nef homodimer present in the 2:2 heterocomplex with the Hck SH3-SH2 regulatory domain proteins (PDB: 4U5W; the SH3-SH2 proteins are not shown for clarity). The Nef monomers (NefA and NefB) are rendered in dark and light blue, respectively. B) Zoomed and rotated view of the Nef dimerization interface in which conserved residues Leu112, Tyr115, and Phe121 (cyan, orange, and green, respectively) form a hydrophobic cup around Val70(pink) from the opposing monomer. C) One Nef monomer from the homodimer shown in part A was aligned with Nef in complex with the AP-2 α/σ2 hemicomplex (PDB: 4NEE). The AP-2 α and σ2 subunits are shown as surfaces in gray and light orange, respectively. This alignment shows that the Nef homodimer interface is structurally distinct from the point of contact with AP-2, which involves the Nef central internal loop(not shown).

Though Nef is present in HIV-1 virions and expressed early within the viral life cycle (*264*), previous analyses have examined the impact of mutations on Nef self-association 40-48 hours post-transfection (*241, 308*) which corresponds to the end of the HIV-1 life cycle (*311*). We therefore explored the kinetics of wild-type Nef homodimer formation and membrane association at 12-hour intervals using a cell-based bimolecular fluorescence complementation (BiFC) assay (*312*). In this approach, wild-type and mutant Nef coding sequences are fused to an N-terminal fragment of the YFP variant, Venus (Nef-VN), while complementary Nef constructs are fused to a C-terminal Venus fragment (Nef-VC). Co-expression of the Nef-VN and Nef-VC fusion proteins in the same cell results in protein-protein interaction, leading to irreversible complementation of the Venus fluorophore and a bright fluorescent signal (Figure 11).

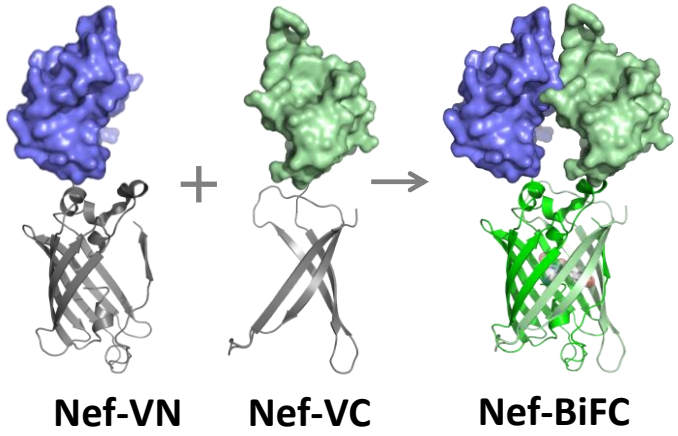

Figure 11: Overview of Bimolecular Fluorescence Complementation (BiFC)

Schematic showing the mechanistic basis of BiFC. The Venus yellow fluorescent protein (YFP) is split into N-terminal and C-terminal halves (VN and VC, respectively). Each half of the split fluorescent reporter is fused to the C-terminus of Nef, and both are expressed within cells. Nef association in cells results in productive reconstitution of the Venus YFP and detectable fluorescence.

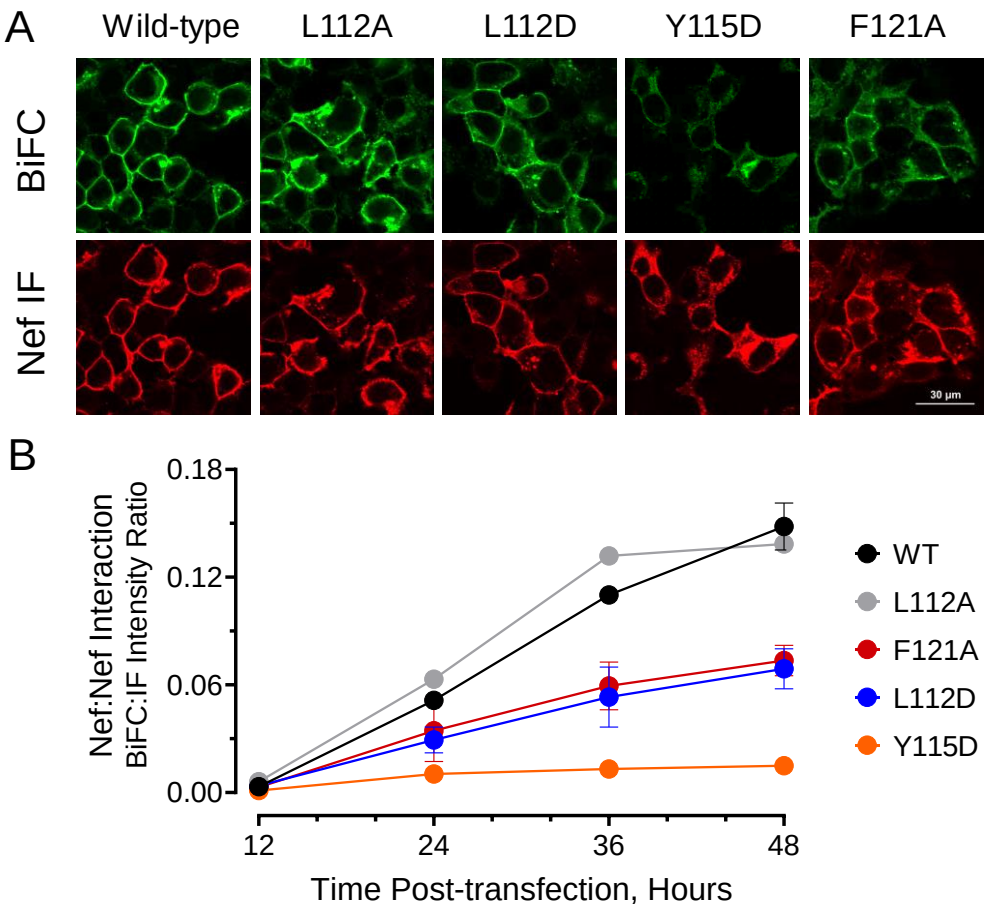

Figure 12: BiFC analysis of self-association kinetics of wild-type Nef and dimerization interface mutants

293T cells were co-transfected with expression plasmids for wild-type and mutant Nef proteins fused to non-fluorescent complementary fragments of the YFP variant, Venus. Cells were fixed 12, 24, 36, and 48 hours post-transfection and immunostained for Nef expression prior to imaging via confocal microscopy. Nef homodimerization results in reconstitution of the Venus fluorophore. A) Representative images comparing self-association of wild-type and mutant Nef proteins(BiFC; green). Nef immunofluorescence is shown in red (Nef IF). B) Time course of Nef dimerization by BiFC assay. The mean fluorescence intensity ratios of the BiFC and Nef immunofluorescence signals were calculated from a minimum of 100 cells across the entire cell for each condition using ImageJ. The entire experiment was repeated in duplicate, and each data point represents the mean ratio ±SD. Complete data for a representative cell population are shown in the Figure 13.

Cultures of 293T cells were transfected with Nef-VN and Nef-VC expression vectors (wild-type or the dimerization interface mutants L112A, L112D, Y115D, F121A) and fixed with paraformaldehyde 12, 24, 36, and 48 hours later. Cells were then immunostained to confirm Nef protein expression, allowing normalization of the resulting BiFC signal to Nef expression levels within each culture. Figure 12A shows representative confocal images of Nef BiFC (homodimer

formation) and immunofluorescence (Nef protein expression) at the 48 hour endpoint of the experiment, while Nef BiFC to immunofluorescence intensity ratios across all four time points are plotted in Figure 12B. Little fluorescence complementation was observed with any of the Nef BiFC pairs at 12 hours, which likely reflects the low levels of Nef expression at this time point. After 24 hours, wild-type Nef self-association was readily observed and increased in a linear fashion over 48 hours. In contrast to wild-type Nef, the L112D, Y115D, and F121A mutants demonstrated statistically significant defects in Nef homodimerization across all time points. The Y115D mutant showed the lowest ratios at each time point, with the L112D and F121A mutants exhibiting an intermediate phenotype. By contrast, the L112A mutation had little to no detectable impact on Nef homodimer formation in the BiFC assay, suggesting that substitution of alanine for leucine does not sufficiently disrupt dimer formation to affect detection in the BiFC assay. Inspection of the BiFC and immunofluorescence images suggests that all four Nef mutants remained associated with the plasma membrane, although the Y115D mutant showed increased expression in the cytoplasm. Box-and-whisker plots of the BiFC-to-immunofluorescence intensity ratios for the wild-type and mutant Nef proteins at each time point, along with statistical comparisons, are shown in Figure 13.

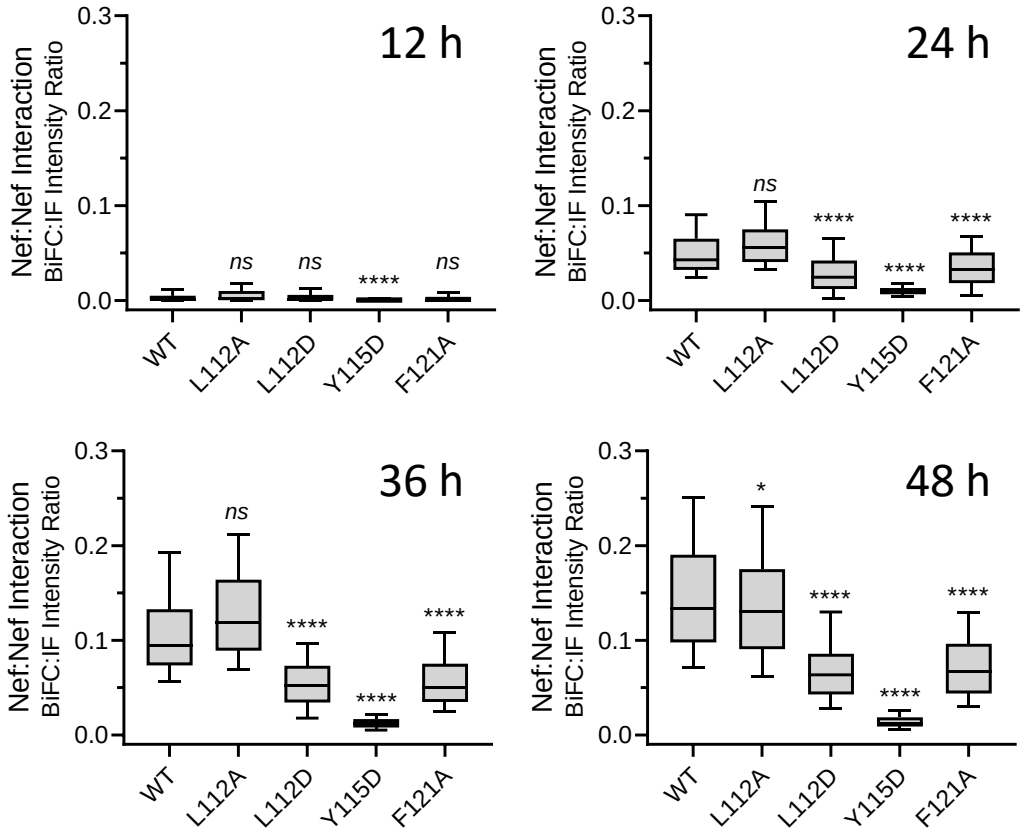

Figure 13: Analysis of BiFC self-association kinetics for wild-type and dimerization interface mutants

293T cells were co-transfected with expression plasmids for wild-type and mutant Nef proteins fused to non-fluorescent complementary fragments of the YFP variant, Venus. Cells were fixed 12, 24, 36, and 48 hours post-transfection and immunostained for Nef expression prior to imaging via confocal microscopy. Nef homodimerization results in reconstitution of the Venus fluorophore. The mean fluorescence intensities of the BiFC and Nef immunofluorescence signals were calculated from a minimum of 100 cells for each condition using ImageJ. The distribution of BiFC:IF ratios for each cell population are plotted as box and whisker plots with the boxes showing the 25thto 75thpercen-tiles and the whiskers showing the 10^{th} to 90^{th} percentiles. Statistical analyses were performed via Dunnett's multiple comparisons test with the wild-type (WT) Nef group as control (****, $p \leq 0.0001$; ns, not significant).The Nef L112A mutant did not show a significant decrease in the ratio, except at the 48h time point (*, $p \leq 0.05$).

2.3.2 Dimerization-defective Nef attenuates HIV-1 infectivity and impairs SERINC5 antagonism

In order to test the role of Nef homodimerization in SERINC5 antagonism, we first validated a 293T producer cell system to assess virion incorporation of SERINC5 and impact on viral infectivity. For these studies, 293T cells were transfected with proviral plasmids encoding wild-type HIV-1 or a mutant that fails to express Nef (ΔNef) in the presence or absence of a SERINC5 expression vector. Newly synthesized virions were concentrated from the culture supernatant two days later and levels of virion-incorporated SERINC5 were analyzed via immunoblot. The infectivity of each viral supernatant was assessed in parallel using the TZM-bl reporter cell line (*313*). Expression of SERINC5 in 293T producer cells inhibited HIV-1 ΔNef infectivity in a dose-dependent manner but had little impact on the infectivity of the wild-type virus, consistent with previous results (Figure 14A) (*304*, *305*). Nef antagonism of SERINC5 within this system is consistent with levels of virion-incorporated SERINC5 observed by immunoblot, with wild-type virions exhibiting decreased levels of SERINC5 compared to the ΔNef virions (Figure 14B). Co-transfection of an expression plasmid encoding Nef along with SERINC5 and the ΔNef proviral plasmid rescued infectivity (Figure 14C) and promoted exclusion of SERINC5 from newly synthesized virions (Figure 14D). These observations validate the use of the 293T producer cell system to explore the role of Nef homodimerization in SERINC5-mediated restriction of HIV-1 infectivity.

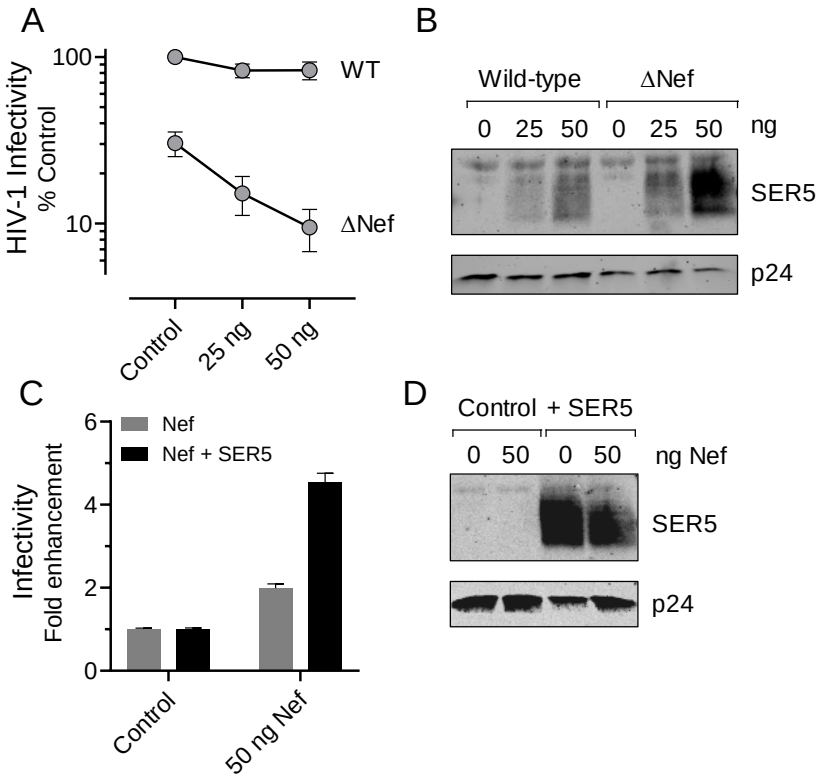

Figure 14: Nef expression antagonizes SERINC5 restriction of viral infectivity at the producer cell level.

A) 293T cells were co-transfected with HIV-1 NL4-3 proviral plasmids competent (wild-type) or defective (ΔNef) for Nef expression along with 0, 25, or 50 ng of a SERINC5expression vector. Newly released virions were harvested after 48h, quantified via p24 AlphaLISA, and used to infect TZM-bl re-porter cells. Luciferase activity was measured 48 h later and normalized to that observed with wild-type virus produced in the absence of SERINC5. Mean values ± SE are shown from three independent experiments. B) Representative western blot depicting incorporation of SERINC5-HA into wild-type and ΔNef virions. Virions were collected in parallel during the infectivity assays and purified via ultracentrifugation through a 20% sucrose cushion, lysed into sample buffer, subjected to SDS-PAGE, and immunoblotted using antibodies to p24 Gag and the HA tag on SERINC5. C) Viral antagonism of SERINC5 is rescued following ectopic expression of Nef within producer cells. The ΔNef virus was expressed in 293Tcells in the presence and absence of SERINC5 and Nef expression plasmids. Data are presented as the fold enhancement of viral infectivity, defined as the ratio of infectivity between Nef-expressing and Nef-deficient producer cells. Results represent normalized mean values ± SE from three independent experiments. D) Representative immunoblots displaying incorporation of SERINC5 into purified ΔNef virions produced in the presence and absence of Nef.

We next transfected 293T cells with HIV-1 proviral DNA bearing the Nef dimerization interface mutations L112A, L112D, Y115D, and F121A in the presence or absence of the SERINC5 expression vector. The infectivity of HIV-1 expressing the L112D, Y115D, and F121A Nef mutants was reduced in the presence of SERINC5 to the levels observed with the ΔNef virus,

while the L112A mutant exhibited a partial loss of function (Figure 15A). This finding is consistent with BiFC results, showing that L112A has little impact on Nef homodimer formation in this system. Immunoblot analysis confirmed that each of the Nef mutants was expressed in transfected 293T cells (Figure 15B).

In a complementary set of experiments, we explored the role of Nef dimerization in SERINC5 antagonism using the Jurkat JTAg producer cell system, which expresses a relatively high level of endogenous SERINC5 like that observed in normal CD4 T cells. An isogenic Jurkat JTag cell population in which both SERINC5 alleles are inactivated by CRISPR/Cas9 was studied in parallel (*304*). Wild-type and SERINC5-knockout Jurkat T cells were transfected with HIV-1 proviral constructs bearing the same Nef dimerization interface mutations, along with wild-type or ΔNef HIV-1. The infectivity of the viruses expressing the L112D, Y115D, and F121A Nef mutants produced in wild-type Jurkat JTAg cells was reduced to that of the ΔNef virus, consistent with the results in 293T producer cells co-expressing SERINC5. The infectivity of these Nef mutant viruses was restored when produced in the SERINC5-knockout cells, providing rigorous evidence of a SERINC5-dependent mechanism in this T cell line (Figure 15C). Wild-type HIV-1 produced from either of the Jurkat producer cell lines displayed similar infectivity, consistent with the ability of wild-type Nef to antagonize SERINC5. Infectivity of the Nef-L112A mutant virus was unaffected by the presence or absence of SERINC5, consistent with the lack of an effect of this mutation on Nef self-association in the BiFC assay. Expression of wild-type and mutant forms of Nef in Jurkat producer cells was verified by immunoblot analysis (Figure 15D).

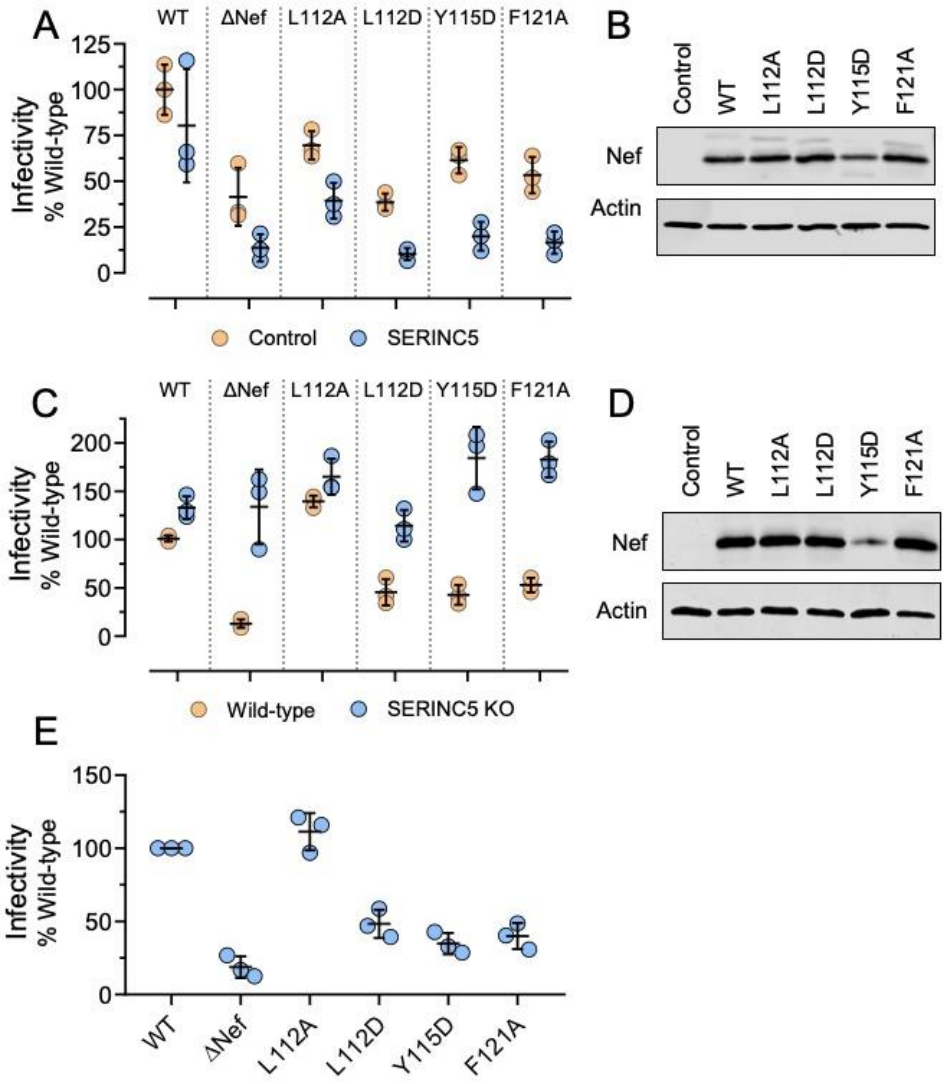

Figure 15: HIV-1 expressing dimerization-defective Nef mutants exhibit reduced infectivity

A) 293T cells were co-transfected with wild-type, ΔNef, and dimerization-defective Nef mutant (L112A, L112D, Y115D, F121A) proviruses in the presence and absence of SERINC5, and infectivity of equivalent p24 inputs was analyzed 48 h later in TZM-bl reporter cells. Results from three independent experiments are shown normalized to the infectivity of wild-type virus produced in the absence of SERINC5 (Control). The horizontal bar represents the mean ±SE.B) Representative immunoblots verifying expression of wild-type and dimerization-defective Nef mutants in lysates of transfected 293T cells. Actin blots are shown as a loading control. C) Wild-type and SERINC5-knockout Jurkat TAg T cells were transfected with wild-type, ΔNef, and dimerization-defective Nef mutant proviruses. Infectivity of equivalent p24 inputs was analyzed 48 h later in TZM-bl reporter cells. Results from three independent experiments are shown normalized to the infectivity of wild-type virus produced in wild-type Jurkat cells. The horizontal bar represents the mean ±SE.D) Representative immunoblots verifying expression of wild-type and dimerization-defective Nef mutants in lysates of transfected Jurkat cells. Actin blots are shown as a loading control. E) PBMCs from uninfected donors were activated with PHA and IL-2 for three days, then infected with 150pgp24/mL of wild-type, ΔNef, and Nef dimerization-defective mutant viruses for four days. Infectivity of equivalent p24 inputs of the resulting viral supernatants were analyzed 48 h later in TZM-bl reporter cells. Results from three independent experiments are shown normalized to the infectivity of wild-type virus. The horizontal bar represents the mean ±SE.

We also addressed whether Nef dimerization is important for infectivity of HIV-1 produced during a spreading infection in primary host cell culture. SERINC5-mediated restriction has been previously observed in donor PBMCs, which also express relatively high levels of endogenous SERINC5 (*304*, *305*). For this experiment, PBMCs were infected with equivalent titers of wild-type, ΔNef, and Nef dimer mutant viruses (initially produced in 293T cells) and allowed to replicate in PBMCs for 4 days followed by infectivity assay in TZM-bl cells. As observed in the other two producer cell systems, viruses expressing the Nef L112D, Y115D, and F121A mutations showed reduced infectivity comparable to that of the ΔNef virus following amplification in PBMCs, with higher infectivity for wild-type and Nef-L112A HIV-1 (Figure 15E).

We next investigated the requirement for Nef homodimers in the exclusion of SERINC5 from newly synthesized virions. For these experiments, 293T cells were co-transfected with HIV-1 wild-type, ΔNef, and Nef dimerization-defective mutant proviral DNA in the presence of the SERINC5 expression plasmids. Newly synthesized virions were isolated and incorporation of SERINC5 was assessed by immunoblotting (Figure 16A). The amount of virus-associated SERINC5 was then normalized to p24 Gag levels from three independent experiments (Figure 16B). SERINC5 incorporation into virions mirrored the infectivity data, with the L112D, Y115D, F121A, and ΔNef virions exhibiting significantly higher levels of SERINC5 than the wild-type and L112A viruses. These findings demonstrate that enhancement of HIV-1 infectivity requires Nef homodimers and involves a mechanism linked to antagonism of SERINC5 incorporation by Nef dimers at the producer cell level.

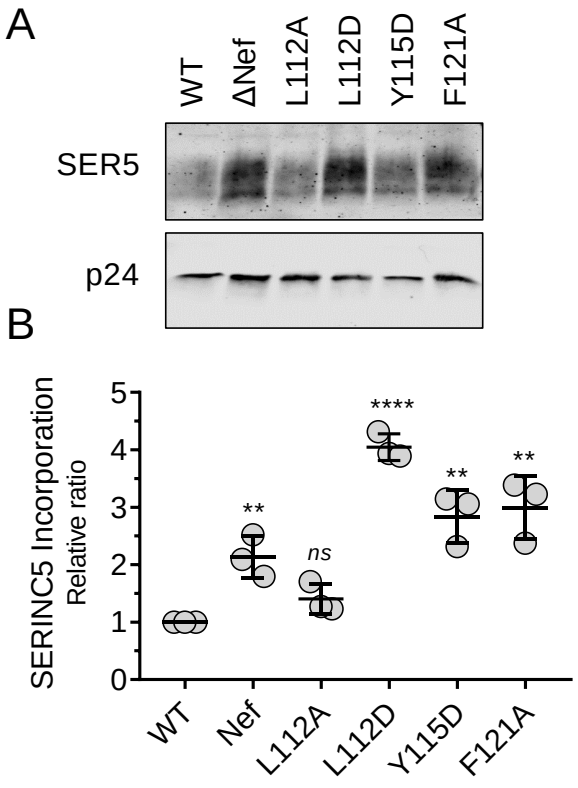

Figure 16: Dimerization-defective Nef mutants display attenuated exclusion of SERINC5 from newly synthesized virions

293T cells were co-transfected with wild-type, ΔNef, and Nef dimerization interface mutant proviruses (L112A, L112D, Y115D, F121A) in the presence of a SERINC5-HA expression vector. Newly synthesized virions were purified by ultracentrifugation through a 20% sucrose cushion, and SERINC5 incorporation was analyzed via immunoblotting along with p24 Gag as a control. A) Representative SERINC5 and p24 immunoblots. B) SERINC5 and p24 protein expression levels were quantified by LI-COR Odyssey image analysis, and each data point represents the SERINC5 to p24 expression ratio for three independent experiments. Mean values in each group are indicated by the horizontal bar ±SE. Statistical significance relative to wild-type (WT) was determined by Student's t-test (**, $p \leq 0.01$; ****, $p \leq 0.0001$; ns, not significant).

2.3.3 Nef homodimerization is required for SERINC5 internalization and endosomal trafficking.

Previous studies have shown that Nef homodimers are required for CD4 downregulation (*241*, *308*), a process that requires the endocytic trafficking adaptor protein, AP-2. Nef-mediated antagonism of SERINC5 is also mediated by AP-2-dependent downregulation of SERINC5 from

the cell membrane, resulting in endocytosis and lysosomal degradation (*305*, *307*). Here we demonstrate a clear increase in virion-associated SERINC5 with HIV-1 expressing dimerization-defective Nef (Figure 16), suggesting that impaired exclusion of SERINC5 from virions expressing these Nef mutants was due to dysfunctional downregulation of SERINC5 from the producer cell surface. To address this issue, the Jurkat SERINC5-knockout cells were transfected with expression vectors for Nef (wild-type or dimerization-defective mutants) which also expresses GFP as a gating marker and for SERINC5 with a hemagglutinin (HA) epitope tag on one of the extracellular loops (*266*). Transfected cells were then immunostained with an anti-HA antibody to detect cell-surface SERINC5 expression in the Nef-transfected (GFP+) cell population via flow cytometry. Expression of wild-type Nef decreased cell-surface SERINC5 expression by nearly 90% relative to the GFP-only control population. In contrast to wild-type Nef, the dimerization-defective mutants L112D, Y1125D, and F121A all showed significantly impaired SERINC5 downregulation, ranging from 65% to 85% relative to the control (Figure 17A and 17B). The Nef-L112A mutant was not affected, consistent with the lack of a dimerization defect observed with this mutant. These results demonstrate that Nef homodimers are required for efficient downregulation of SERINC5 from the cell surface.

Because of the mechanistic similarity between Nef-induced downregulation of SERINC5 and CD4, we also explored the impact of the Nef dimer interface mutations on downregulation of endogenous CD4 in the CEM-SS T cell line (*314*). CEM-SS cells were transfected with the same Nef/GFP dual expression plasmid used for the SERINC5 study, followed by immunostaining for endogenous cell-surface CD4 and flow cytometry. Expression of wild-type Nef reduced cell surface CD4 expression by more than 60%, while the L112D, Y115D, and F121A Nef mutants were completely defective for CD4 downmodulation (Figure 18A and 18B). Cells expressing Nef-

L112A exhibited an intermediate phenotype, with about a 30% reduction in cell-surface CD4 expression. While the L112A mutant does not show a decrease in homodimer formation by BiFC assay, alteration of the dimer interface by this mutation may impact the efficiency of CD4 downregulation. Overall, these results are in agreement with those observed with SERINC5 and are consistent with the shared mechanism of action involving AP-2-dependent endocytosis.

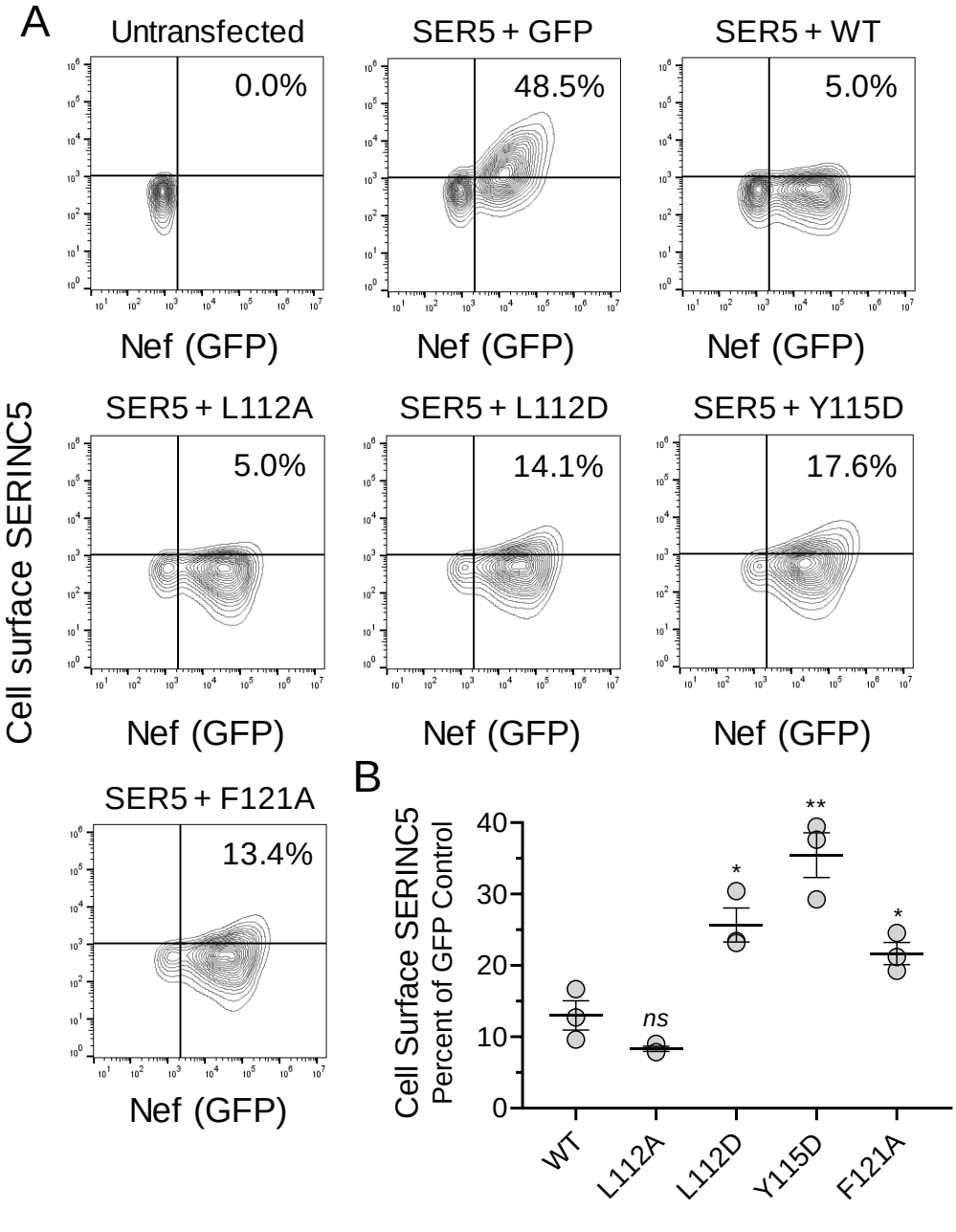

Figure 17: Nef dimerization is required for SERINC5 downregulation

SERINC5-knockout Jurkat T cells were transfected with a dual promoter plasmid expressing wild-type or dimerization-defective Nef mutants as well as GFP as a gating marker. A second plasmid was included for expression of SERINC5 tagged with an extracellular HA epitope (SERINC5-iHA). Forty-eight hours after transfection, cells were immunostained with an HA antibody and cell-surface expression of SERINC5-iHA was quantified via flow cytometry. A) Representative flow cytometry plots showing impaired downregulation of SERINC5 by Nef dimer mutants. Cells were gated on the untransfected cell population, and the percentage of SERINC5-positiveand GFP-positive(marker for Nef expression) cells are indicated. B) Each data point shows percentage of cells expressing surface SERINC5 within the Nef-positive (GFP-positive) cell population relative to the GFP-only control from three independent experiments. Mean values in each group are indicated by the horizontal bar ±SE. Statistical significance relative to wild-type (WT) was determined by Student's t-test (*, $p \leq 0.05$;**, $p \leq 0.01$; ns, not significant).

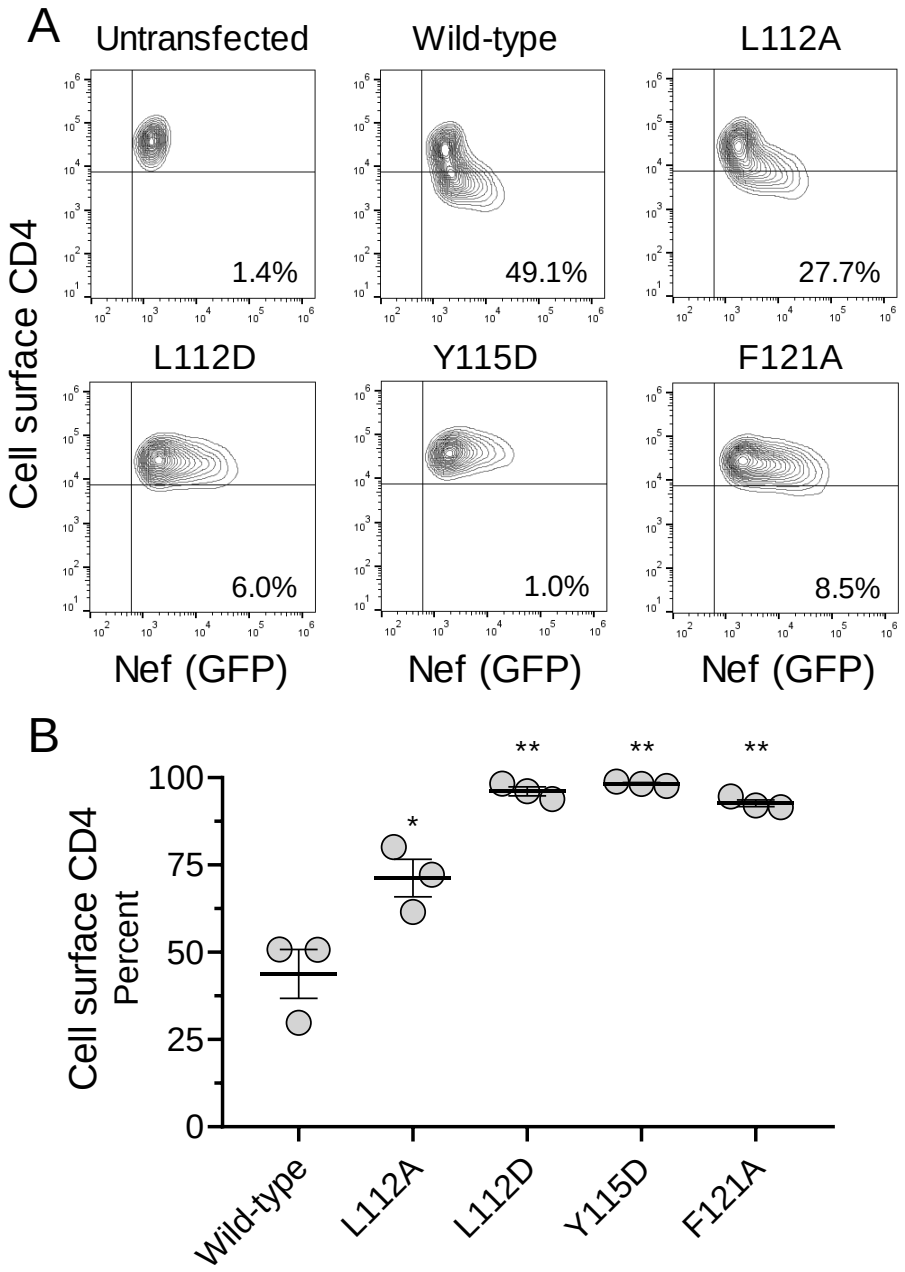

Figure 18: Nef dimerization is required for CD4 downregulation

CEM-SS cells were transfected with a dual promoter plasmid expressing wild-type or dimerization-defective Nef mutants as well as GFP as a gating marker. Forty-eight hours after transfection, cells were immunostained with a CD4 antibody and cell-surface CD4 expression was quantified via flow cytometry. A) Representative flow cytometry plots showing impaired downregulation of CD4 by Nef dimer mutants. Cells were gated on the untransfected CD4-positive cell population, and the percentage of Nef-expressing cells demonstrating downregulation of CD4 from the cell surface(CD4-negativeand GFP-positive) are indicated for each condition. B) Each data point shows CD4 cell surface expression normalized to surface CD4 expression in the absence of Nef (un-transfected) for three independent determinations. Mean values in each group are indicated by the horizontal bar ±SE. Statistical significance relative to wild-type Nef was determined by Student's t-test (*, $p \leq 0.05$; **, $p \leq 0.01$; ns, not significant).

Following Nef-mediated endocytosis, SERINC5 traffics through Rab7+ late endosomes on route to proteolytic destruction following lysosomal fusion (*304, 307*). We therefore investigated whether mutations disrupting Nef dimerization also impact the intracellular trafficking of SERINC5 along this pathway. SERINC5-knockout Jurkat cells were transfected with SERINC5 fused to the mCherry fluorescent protein in combination with wild-type or dimerization-defective forms of Nef fused to YFP. Two days later, transfected cells were immunostained for the late endosomal marker, Rab7. The expression and subcellular localization of SERINC5-mCherry, Nef-YFP, and Rab7 were then analyzed via confocal microscopy. When expressed alone, SERINC5-mCherry localized almost entirely to the plasma membrane with very little co-localization with Rab7 (confocal images of representative cells are shown in Figure 19). Co-expression of wild-type Nef-YFP resulted in a dramatic shift in SERINC5-mCherry localization from the cell surface into the Rab7+ endosomal compartment, observed as the co-localization of SERINC5-mCherry, Nef-YFP, and Rab7 fluorescence within multiple intracellular puncta. In marked contrast, the Nef dimer interface mutants, L112D, Y115D, and F121A all showed reduced intracellular targeting of SERINC5-mCherry, with both proteins retaining co-localization to the plasma membrane. Very few intracellular Rab7+ endosomes were observed with these three Nef mutants, consistent with a defect in endocytosis and intracellular trafficking. On the other hand, the Nef-L112A mutant displayed an intermediate phenotype, co-localizing with SERINC5-mCherry at the plasma membrane and in Rab7+ endosomes.

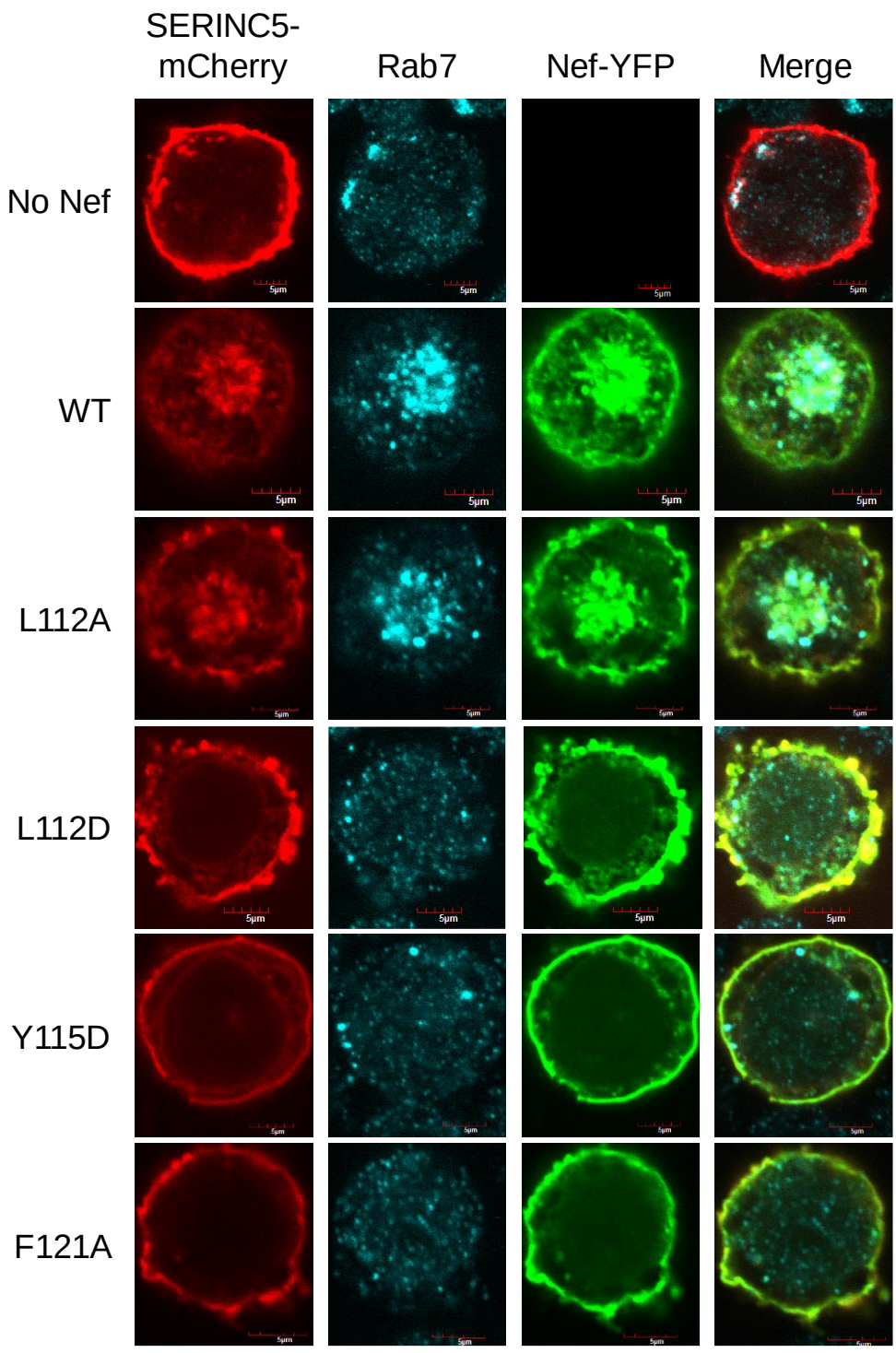

Figure 19: Nef dimerization is required for internalization of SERINC5

SERINC5-knockout Jurkat T cells were co-transfected with expression plasmids for SERINC5-mCherry together with wild-type or dimerization-defective Nef mutants fused to YFP, or with the empty vector as a control. Forty-eight hours later, cells were fixed, permeabilized, and stained with an antibody to the late endosomal marker Rab7. Representative single cell images of SERINC5-mCherry (red), Nef-YFP (green), and Rab7 fluorescence are shown along with a merged image. Scale bar, 5 am.

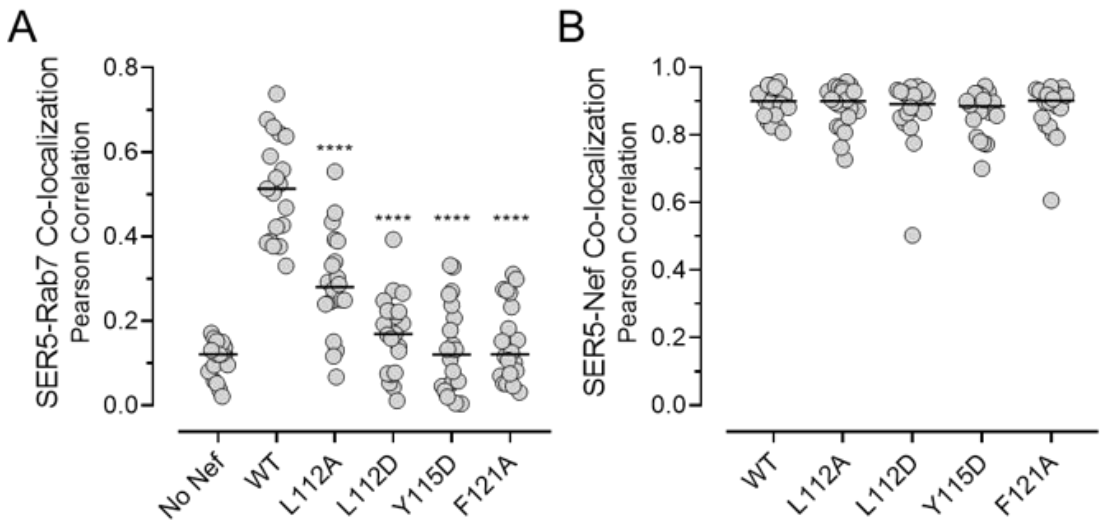

Figure 20: Disruption of Nef dimerization impairs internalization and trafficking of SERINC5-mCherry to Rab7+ endosomes

SERINC5-knockout Jurkat T cells were co-transfected with expression plasmids expressing SERINC5-mCherry together with wild-type or dimerization-defective Nef mutants fused to YFP and immunostained with an antibody to the late endosomal marker Rab7 as described in the legend to Figure 8. A) Single cell confocal images were subjected to Pearson's correlation coefficient analysis to quantify the extent of SERINC5-mCherry colocalization with Rab7. A minimum of 18-20 cells per condition were analyzed across three independent experiments, and the Pearson's correlation coefficient for each cell is shown with the median value indicated by the horizontal bar. Statistical significance among the groups was performed via one-way ANOVA with Dunnett's multiple comparisons test relative to the cell population expressing wild-type (WT) Nef (****, $p \leq 0.0001$). B) Pearson's correlation analysis of SERINC5-mCherry co-localization with Nef-YFP was performed in the same groups of cells, with median correlation coefficients indicated by the horizontal bars. Statistical analysis via ordinary one-way ANOVA did not reveal significant differences between the groups.

To quantify the extent of co-localization, Pearson's correlations were calculated for co-localization of the SERINC5-mCherry and Rab7 fluorescence for a minimum of 18 individual cells (Figure 20A). In the absence of Nef, the average Pearson's correlation coefficient was approximately 0.1, indicating little correlation in terms of subcellular localization and consistent with the lack of SERINC5 internalization in the absence of Nef. Co-expression of Nef resulted in a significant increase in the correlation coefficient (mean $\sigma > 0.5$), consistent with the observed trafficking of SERINC5 to late endosomes. The correlation coefficient was significantly reduced with all four dimerization-defective Nef mutants compared to wild-type Nef, consistent with the

confocal images showing retention of SERINC5-mCherry at the plasma membrane. As a control, we also performed correlation analysis for the co-localization of Nef-YFP and SERINC5-mCherry fluorescence (Figure 20B). Notably, no significant difference was observed in these co-localization correlations (mean $\sigma \approx 0.9$ in each case), hinting that the Nef dimer mutations may not affect interaction of Nef with SERINC5. This possibility was explored directly using BiFC as described in the next section.

2.3.4 Disruption of Nef homodimerization does not impair interaction with SERINC5 or AP-2.

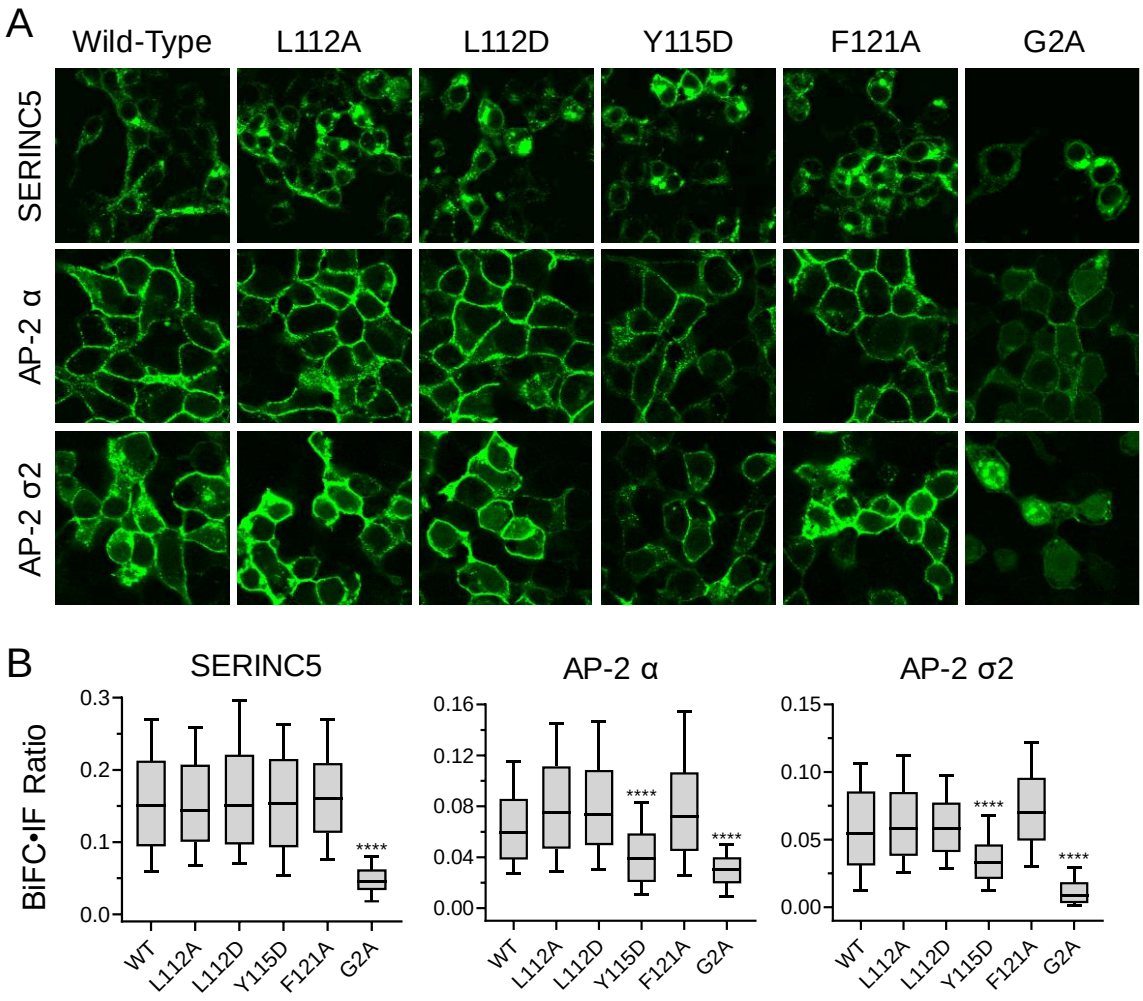

Figure 21: Nef dimerization is not required for interaction with SERINC5 or AP-2

293T cells were co-transfected with expression plasmids for SERINC5, AP-2 α or AP-2 σ2 fused to an N-terminal fragment of Venus along with wild-type Nef, the dimerization-interface mutants (L112A, L112D, Y115D and F121A) or myristylation-defective Nef (G2A) fused to the complementary C-terminal Venus fragment. Cells were fixed, permeabilized, and immunostained 48 hours later for Nef and either SERINC5 or the AP-2 subunits prior to confocal microscopy. A) Representative BiFC images showing interaction of each Nef protein with SERINC5 (upper row), AP-2α (middle), and AP-2 σ2(bottom). B) The mean fluorescence intensities of BiFC and Nef immunofluorescence (IF) were calculated for a minimum of 100 cells within each pair using Image J. The distribution of BiFC:IF ratios for each cell population are plotted as box and whisker plots with the boxes showing the 25th to 75th percentiles and the whiskers showing the 10thto 90thpercentiles. Statistical analysis was performed via one-way ANOVA with Dunnett's multiple comparisons test relative to the cell population expression wild-type (WT) Nef (****, $p \leq 0.0001$; all other cases not significant).

Previous work suggests that Nef and SERINC5 interact directly within cells, with Nef-mediated antagonism of SERINC5 mediated by a large intracellular loop within SERINC5 (*267, 307*). While an X-ray crystal structure of SERINC5 has been elucidated recently (*263*), electron density for this intracellular loop was not observed suggesting that it is unstructured. Furthermore, the specific region of Nef responsible for interaction with SERINC5 is not known. While data presented above support a role for Nef homodimers in SERINC5 downregulation, the possibility remains that the amino acids involved in Nef homodimer formation may also contribute to interaction with SERINC5. To test this possibility, we employed the BiFC assay to visualize and quantify direct interaction of Nef with SERINC5 in cells (*307*).

SERINC5-VN and each of the Nef-VC fusion proteins (wild-type and mutants) were co-expressed in 293T cells followed by immunostaining for Nef and SERINC5 (via the HA tag) to control for protein expression levels. As a negative control, we also included a mutant of Nef that cannot be myristoylated (Nef-G2A) and therefore exhibits impaired membrane localization and SERINC5 interaction (*307*). Co-expression of wild-type Nef-VC with SERINC5-VN resulted in a positive BiFC signal, supporting direct protein-protein interaction in cells (Figure 21A). Immunofluorescence both for Nef and SERINC5 expression was also readily observed in the same cells and colocalizes with the BiFC signal (Figure 22). All four Nef-VC dimer interface mutants also generated a BiFC signal when partnered with SERINC5-VN, while the Nef-G2A mutant resulted in a lower BiFC signal despite a similar level of expression as wild-type Nef based on immunofluorescence. To quantify these results, the fluorescence intensity for the BiFC signal of each Nef interaction with SERINC5 was normalized to Nef expression levels as determined by immunofluorescence, and the resulting fluorescence intensity ratios are plotted for at least 100 cells in Figure 21B. No significant difference in SERINC5 interaction was observed between wild-

type Nef and the dimerization-defective mutants, demonstrating that disruption of the Nef homodimerization interface does not affect interaction with SERINC5. In contrast, the Nef-G2A mutant showed a significant decrease in SERINC5 interaction, consistent with the inability of this mutant to localize to the plasma membrane. These observations suggest that impaired antagonism of SERINC5 by the Nef dimer mutants is not due to a defect in SERINC5 interaction with Nef.

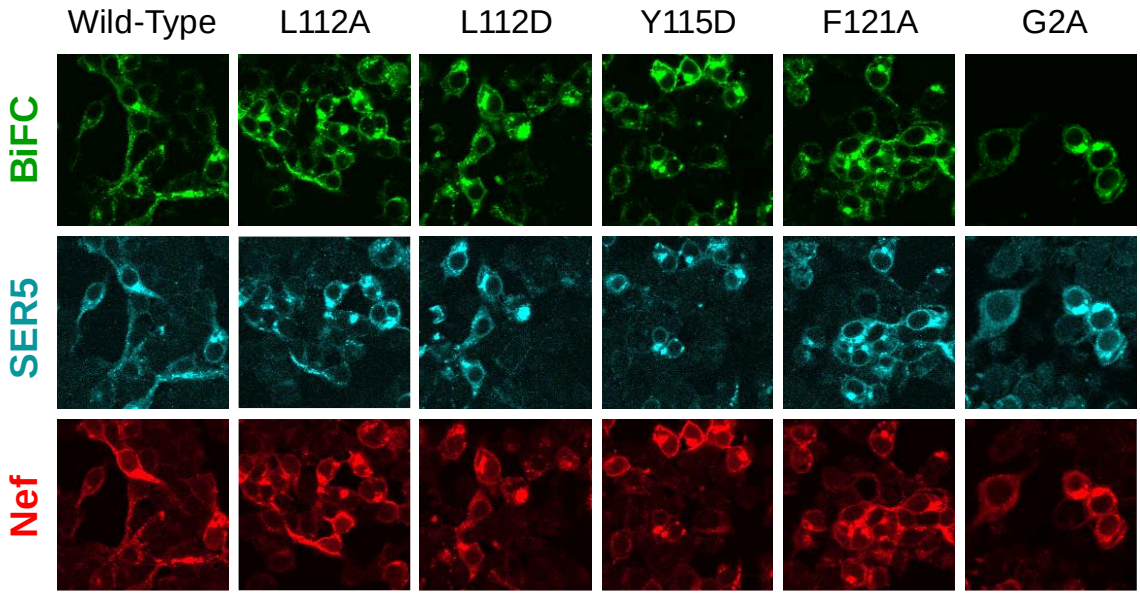

Figure 22: Interaction of dimerization-defective Nef mutants with SERINC5

293T cells were co-transfected with expression plasmids for SERINC5 fused to an N-terminal fragment of Venus along with wild-type Nef, the dimerization-interface mutants (L112A, L112D, Y115D and F121A) or myristylation-defective Nef (G2A) fused to the complementary C-terminal Venus fragment. Cells were fixed, permeabilized, and immunostained 48 hours later for Nef and SERINC5 prior to confocal microscopy. Representative BiFC images show interaction of each Nef protein with SERINC5 (BiFC, top row), SERINC5 immunofluorescence (middle row), and Nef immunofluorescence (bottom row).

Nef-mediated downregulation of SERINC5 also requires interaction with AP-2 through its α and σ2 subunits (*222*), resulting in endocytosis and lysosomal degradation. Structural alignment described above shows that the dimer interface of Nef does not overlap with regions of AP-2 contact, which involve a distinct intracellular loop in the Nef core (see Figure 10B). To determine

whether Nef dimer interface mutations affect AP-2 subunit interaction, we employed a similar BiFC approach in which each Nef protein was fused to the N-terminal fragment of Venus (Nef-VN) while the AP-2 α and σ2 subunits were fused to the C-terminal fragment (α-VC and σ2-VC). The AP-2 fusion proteins also included a V5 tag for immunofluorescence detection as described previously (*241*). Each AP-2-VC construct was co-expressed with the wild-type and mutant forms of Nef-VN in 293T cells, followed by immunofluorescence detection of protein expression and confocal microscopy. Wild-type Nef as well as the dimer interface mutants all exhibited membrane-localized BiFC signals when co-expressed with AP-2 α-VC or σ2-VC (Figure 21A). We then calculated normalized BiFC interaction ratios for Nef with each AP-2 subunit as described above for SERINC5 (Figures 21B). The Nef L112A, L112D and F121A mutants interacted with each AP-2 subunit to the same extent as wild-type Nef, while the Y115D mutant ratio was somewhat reduced despite membrane localization. The Nef-G2A mutant showed a significant loss of interaction with both AP-2 subunits, consistent with its inability to localize to the plasma membrane. Expression of each Nef and AP-2 protein was confirmed by immunofluorescence microscopy, and representative images are presented in the Figures 23 and 24. These experiments show that amino acids present in the Nef dimer interface are not required for interaction with AP-2 at the cell membrane, and support the idea that the defect in SERINC5 antagonism by these mutants is not related to impaired Nef interaction with AP-2.

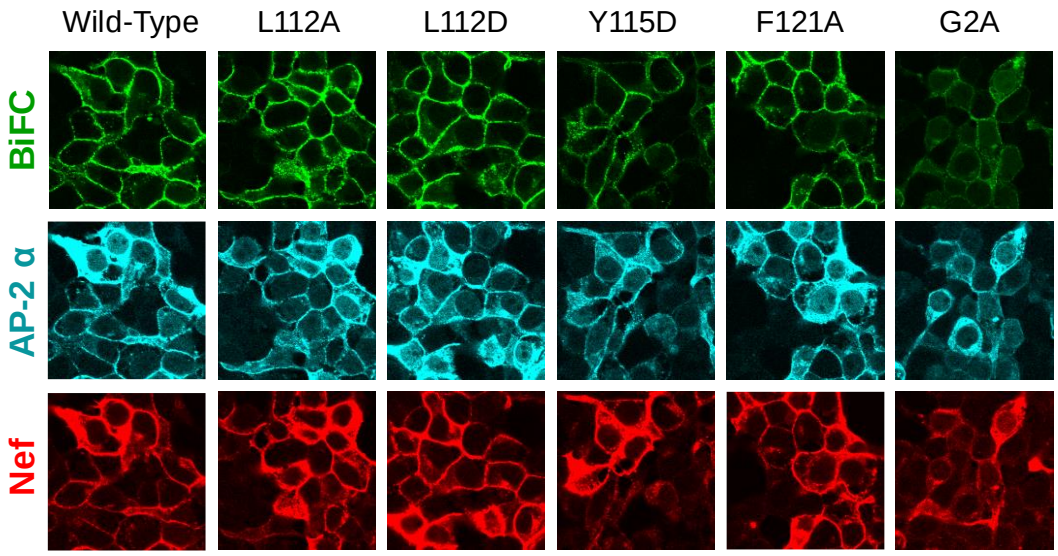

Figure 23: Interaction of dimerization-defective Nef mutants with the AP-2 α subunit

293T cells were co-transfected with expression plasmids for AP-2 α fused to an N-terminal fragment of Venus along with wild-type Nef, the dimerization-interface mutants (L112A, L112D, Y115D and F121A) or myristylation-defective Nef (G2A) fused to the complementary C-terminal Venus fragment. Cells were fixed, permeabilized, and immunostained 48 hours later for Nef and AP-2 α prior to confocal microscopy. Representative BiFC images show interaction of each Nef protein with AP-2 α (BiFC, top row), AP-2 α immunofluorescence (middle row), and Nef immunofluorescence (bottom row).

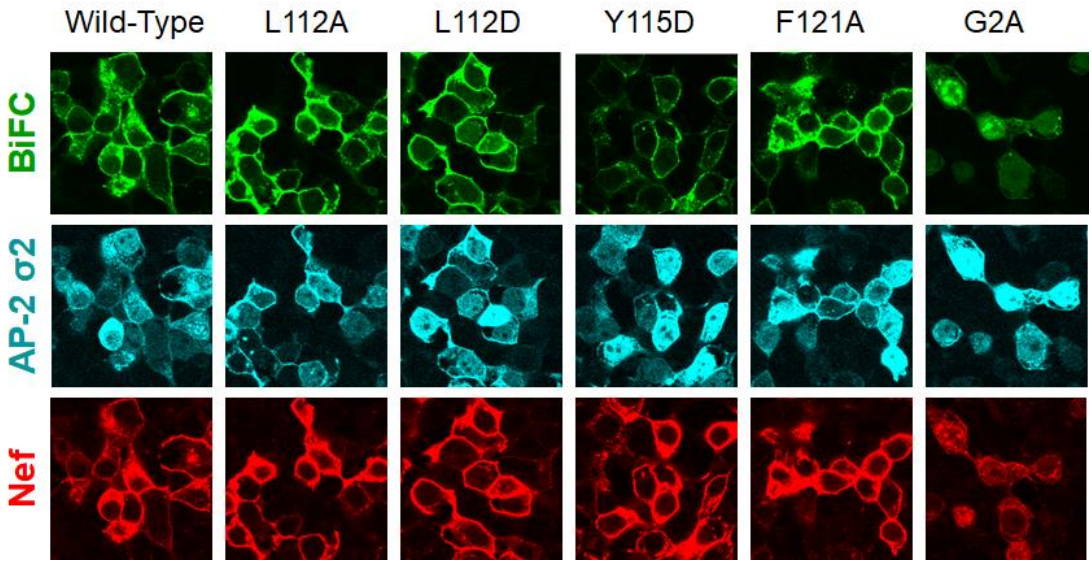

Figure 24: Interaction of dimerization-defective Nef mutants with the AP-2 σ2 subunit

293T cells were co-transfected with expression plasmids for AP-2 σ2 fused to an N-terminal fragment of Venus along with wild-type Nef, the dimerization-interface mutants (L112A, L112D, Y115D and F121A) or myristylation-defective Nef (G2A) fused to the complementary C-terminal Venus fragment. Cells were fixed, permeabilized, and immunostained 48 hours later for Nef and AP-2 σ2 prior to confocal microscopy. Representative BiFC images show interaction of each Nef protein with AP-2 σ2 (BiFC, top row), AP-2 σ2 immunofluorescence (middle row), and Nef immunofluorescence (bottom row).

2.4 Discussion

Antagonism of the host cell restriction factor SERINC5 is a key mechanism by which Nef promotes HIV-1 infectivity. Nef triggers internalization of SERINC5 from the surface of infected cells, thereby preventing incorporation of SERINC5 into budding virions and subsequent impairment of viral entry (*304*, *305*). While the cellular mechanisms of Nef-mediated SERINC5 internalization and degradation have been established, little is known about the structural features of Nef required for SERINC5 engagement and association with AP-2 for downregulation. In this study, we assessed the function of dimerization-defective Nef mutants across all stages of SERINC5 antagonism including viral infectivity, virion incorporation of SERINC5,

downregulation of SERINC5 from the surface of producer cells, and the intracellular fate of SERINC5. We observed consistent impairment of all stages of SERINC5 antagonism with three distinct dimerization-defective Nef mutants, demonstrating that Nef counteracts SERINC5 as a homodimer. Importantly, each of the dimerization-defective Nef mutants retained interaction with both SERINC5 and the AP-2 subunits required for internalization, supporting the idea that the Nef homodimer may act as a bridge to link SERINC5 to the AP-2 pathway, as illustrated in Figure 25.

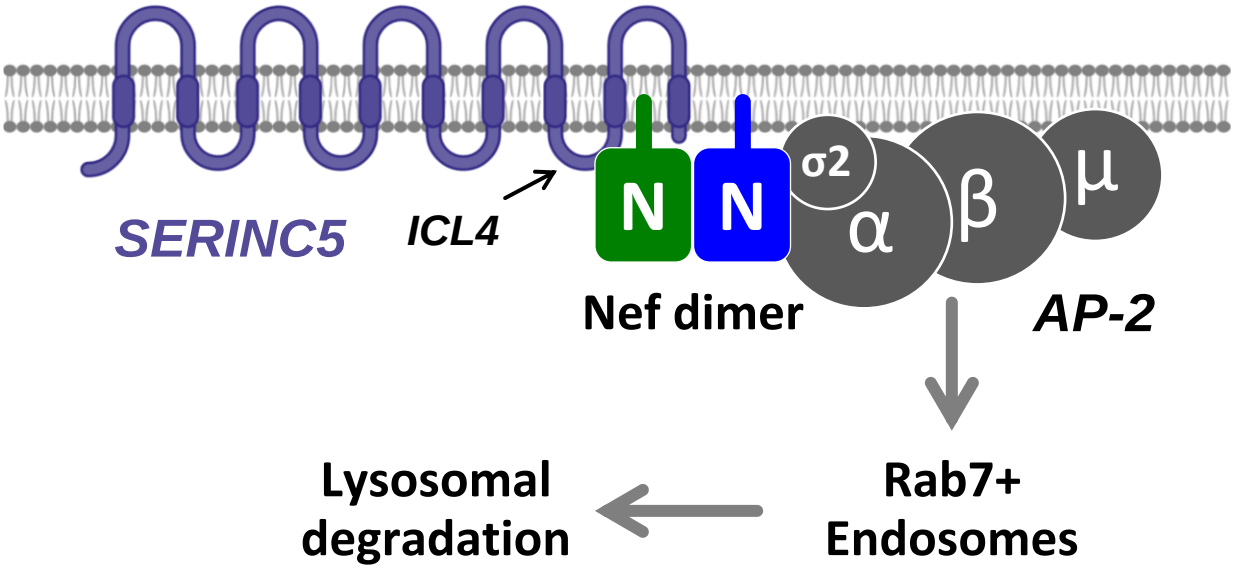

Figure 25: Model of SERINC5 interaction and downregulation by HIV-1 Nef homodimers via AP-2-mediated endocytosis

Myristoylated Nef associates with the host cell membrane and forms homodimers, allowing for simultaneous recruitment of AP-2and SERINC5 through intracellular loop 4 (ICL4). The resulting SERINC5•Nef•AP-2 complex drives downregulation of SERINC5 from the cell membrane, thereby excluding it from budding virions. The complex traffics through Rab7+late endosomes leading to lysosomal degradation.

Our data show that dimerization is required for Nef to promote the infectivity of newly synthesized HIV-1 particles produced by transfected 293T cells as well as a T cell line, in a

SERINC5-dependent manner. These results may provide a mechanistic explanation for previous studies in which similar mutations were shown to influence viral infectivity. For example, substitution of Nef amino acids Leu112 and Phe121 has been shown to negatively impact HIV-1 infectivity and replication (*315*), although the role of SERINC5 was not known at that time. These same residues have also been linked to Nef recruitment of the endocytic GTPase Dynamin-2 as well as the human peroxisomal thioesterase 8 (*315, 316*), suggesting that Nef homodimer formation may affect these interactions as well.

Our study demonstrates that Nef dimerization is required for SERINC5 downregulation from the cell surface, which is mechanistically like Nef-dependent downregulation of CD4. Both SERINC5 and CD4 downregulation are mediated via AP-2 and clathrin-dependent endocytosis. Mutations that disrupt Nef myristoylation and membrane association (G2A) as well as the dileucine motif required for AP-2 recruitment (LL164,165AA) impair downregulation of both proteins (*231, 304, 317*). Nef dimerization-defective mutants impaired for downregulation of SERINC5 were also completely unable to downregulate cell-surface CD4. Expression of wild-type Nef in Jurkat T cells led to the re-localization of SERINC5 from the cell membrane into intracellular Rab7+ compartments (*307*) a fate also shared by CD4 (*318*). Intracellular trafficking and Rab7 co-localization were also significantly disrupted by mutations in the Nef dimerization interface. These findings suggest that Nef homodimers may link both SERINC5 and CD4 to the AP-2 endocytic pathway through separate binding surfaces on each Nef monomer (Figure 25).

Bimolecular fluorescence complementation assays presented here demonstrate direct Nef•SERINC5 interaction at the plasma membrane in cells, consistent with recent work (*269, 307*). Importantly, mutations in residues essential for Nef homodimer formation do not impact interaction of Nef with SERINC5 in the BiFC assay, consistent with a role for the Nef αB helix in

homodimer formation as demonstrated by X-ray crystal structures (*309, 310*) rather than interaction with signaling partners. While the mechanism of SERINC5 engagement by Nef remains enigmatic, recent studies have illuminated the regions of SERINC5 required for viral restriction and susceptibility to Nef antagonism (*263*). SERINC5 is an integral membrane protein with ten trans-membrane helices and four intracellular loops (*263*). Sensitivity of SERINC5 to Nef antagonism appears to map to the fourth intracellular loop, as deletion or replacement of this loop with the Nef-resistant SERINC2 counterpart renders SERINC5 immune to Nef downregulation (*267*). However, whether this loop is sole point of contact in the Nef•SERINC5 complex remains an important open question.

The SERINC5 binding site within Nef also remains elusive. A recent structural study of SIVsmm Nef in complex with AP-2 and tetherin showed that mutation of a critical residue within the tetherin binding site (His196; analogous to HIV-1 Nef His166) also impairs antagonism of SERINC5, suggesting a shared binding site (*231*). This residue is distal to the Nef αB helix required for self-association, consistent with the idea that Nef binds SERINC5 as a dimer. Nevertheless, a direct role for this binding site in HIV-1 Nef SERINC5 association remains to be confirmed, as the proposed binding site may be unique to SIV Nef.

Though the binding site for SERINC5 within Nef remains to be identified, our BiFC data clearly show that conserved residues in the dimer interface are not required for SERINC5 engagement. Nef dimer interface mutants L112A, L112D, and F121A also retained interaction with the AP-2 α and σ2 subunits via BiFC, consistent with the distinct interfaces for homodimerization and AP-2 recruitment illustrated by structural alignment in Figure 10C. However, the Nef Y115D mutant demonstrated statistically lower association with both AP-2 subunits. While the Y115D mutation may impact Nef folding or overall stability, unimpaired

interaction of this mutant with SERINC5 suggests otherwise. Another possibility is that Tyr115 may have an allosteric influence on the binding site for AP-2, given its proximity to the binding site.

In summary, disruption of Nef dimerization attenuates SERINC5 antagonism without impairing recruitment of SERINC5 or AP-2 as required for internalization. While the protein dynamics controlling Nef-dependent SERINC5 downregulation remain a mystery, our data support a mechanism in which Nef homodimers promote Nef•SERINC5•AP-2 complex formation at some point prior to SERINC5 internalization. One Nef monomer within the dimer may contact SERINC5 while the other engages AP-2, with the Nef dimer interface bridging the two proteins to initiate clathrin-mediated endocytosis. Understanding the molecular determinants of SERINC5 antagonism by Nef may help to identify therapeutic strategies that promote SERINC5 virion incorporation and restriction of viral infectivity. Along these lines, docking studies of small molecule inhibitors of Nef-mediated enhancement of viral infectivity have identified potential binding sites within the dimer interface (*297, 319, 320*). Disruption of Nef homodimer formation by these compounds may explain their inhibitory effects on multiple Nef functions, including not only infectivity but also host cell kinase activation, receptor downregulation, and viral replication. Thus, the homodimer interface represents an attractive target for new antiretroviral drug development targeting Nef.

2.5 Materials and Methods

2.5.1 Cell Culture

The human embryonic kidney cell line 293T was purchased from the ATCC. TZM-bl reporter cells were obtained from the AIDS Research and Reference Reagent Program. Both cell lines were grown in Dulbecco's modified Eagle's medium supplemented with 10% fetal bovine serum (FBS; Gemini Bio-Products). Jurkat JTAg T cells (wild-type and SERINC5-knockout) were a kind gift from Dr. Massimo Pizzato, University of Trento, while the CEM-SS T cell line kindly provided by Dr. Mark Brockman, Simon Fraser University. Both T cell lines were cultured in RPMI 1640 medium supplemented with 10% FBS, L-glutamine, and 2 µg/mL puromycin (CEM-SS cells only). Donor PBMCs were obtained from Vitalant Pittsburgh and isolated by Ficoll gradient centrifugation and activated for 3 days with PHA (Sigma, # L1668) and IL-2 (Thermo Fisher, # CB-40043B) as described elsewhere (*319*).

2.5.2 Antibodies

Primary antibodies were obtained from the AIDS Research and Reference Reagent Program (anti-p24, # 4121; anti-Nef polyclonal, # 2949; anti-Nef 6.2, # 153) and purchased from Sigma-Aldrich (anti-HA, # H6908), Millipore (anti-actin, # Mab1501R; anti-V5, # AB3702), BD (anti-CD4-phycoerythrin, # 55534), Biolegend (HA.11-647, # 16B12), and Santa Cruz (anti-Rab7, # B-3). Secondary antibodies were purchased from LICOR (IRDye 680LT Donkey Anti-Mouse, # 926-68022; IRDye 800CW Donkey Anti-Rabbit, # 926-32213), Thermo Fisher (anti-mouse

Alexa Fluor647, # A-21236), Invitrogen (anti-rabbit Pacific Blue, # P-10994), and Southern Biotech (anti-mouse Texas Red, # 1031-07; anti-rabbit Texas Red, # 4050-7).

2.5.3 Plasmids

Construction of the pUC18 HIV-1 NL4-3/SF2Nef proviral plasmid is described elsewhere (*321*). The Nef dimer interface mutations (L112A, L112D, Y115D, F121A) were introduced into the pUC18 NL4-3/SF2Nef and pcDNA3.1 Nef-Venus (*296*) constructs via the Agilent II XL site-directed mutagenesis kit. Expression vectors for SERINC5 (pBJ5-SERINC5-HA and pBJ5-SERINC5-iHA) were the kind gift of Dr. Heinrich Gottlinger, University of Massachusetts Medical School. The pSELECTzeoGFP-based expression plasmids for wild-type and dimer interface mutants of Nef have been previously described (*296*). SERINC5-mCherry was purchased from GeneCopoeia. The pcDNA3.1 SERINC5-VN-HA construct for BiFC was the kind gift of Dr. Yong-Hui Zheng, Michigan State University. Construction of BiFC expression plasmids for AP-2 subunits in pCDNA3.1 (σ2-V5-VC, α-V5-VC) as well as pcDNA3.1 Nef-YFP have been previously reported (*241*).

2.5.4 HIV-1 replication and infectivity assays

Human 293T cells were transfected with proviral expression plasmids using Xtreme Gene 9 (Sigma-Aldrich) for 48 h prior to harvesting the viral supernatant. Jurkat JTAg wild-type and SERINC5-knockout cells were transfected with proviral plasmids using the Amaxa Cell Line Nucleofector Kit V and the resulting viral supernatant was harvested 48 h later. PBMCs were infected with 150 pg/mL of HIV-1 (wild-type, ΔNef, and Nef mutants) for 4 days prior to assay.

HIV-1 titers in clarified supernatants from all producer cells were quantified using the PerkinElmer p24 AlphaLISA Detection kit. Each viral supernatant (5,000 pg/mL p24) was then used to infect TZM-bl cells in 96-well plates (2.5 x 10^4 cells/well). After 48 h, cells were lysed in Promega luciferase buffer, transferred to a white 96-well plate, mixed with luciferase reagent, and measured using a Biotek Cytation 5 plate reader.

2.5.5 SERINC5 incorporation assay

Viral supernatants from 293T cells co-transfected with proviral DNA and the SERINC5-HA expression plasmid pBJ5-SERINC5-HA were clarified by centrifugation and HIV-1 virions were purified through a 20% sucrose cushion at 100,000 x g for 1 h at 4 °C. The supernatant was carefully removed and virions were lysed directly in SDS-PAGE sample buffer (100 mM Tris-HCl, pH 6.8, 5 mM TCEP, 10% glycerol, 4% SDS). The viral lysates were heated to 37 °C for 15 min, resolved on 4-20% SDS-PAGE gradient gels, transferred to nitrocellulose membranes, and incubated overnight at 4 °C with primary antibodies to HIV-1 p24 (mouse monoclonal, NIH 4121, 1:1000) or the HA tag on SERINC5 (rabbit polyclonal, Sigma H6908, 1:500). Blots were washed with Tris-buffered saline with 0.1% Tween-20 (TBST), then incubated for 2 h with Licor IR-Dye secondary antibodies (1:10,000). Blots were imaged using the Licor Odyssey infrared imaging system and the Licor ImageStudio Lite software.

2.5.6 Immunoblotting

Jurkat and 293T producer cells were lysed 48 h post-transfection with RIPA buffer (50 mM Tris-HCl, pH 7.4, 150 mM NaCl, 1 mM EDTA, 1% Triton X-100, 0.1% SDS, 1% sodium

deoxycholate) supplemented with protease inhibitors. Lysate protein concentrations were quantified via Bradford assay (Bio-rad Bradford reagent) and normalized to 50 μg/mL. Aliquots of each lysates were heated in SDS-PAGE sample buffer at 95 °C for 10 min, resolved on 12% SDS-PAGE gels, and transferred to nitrocellulose membranes. Immunoblots were blocked for 1 h with Superblock TBS Blocking Buffer (Thermo Fisher) then probed overnight at 4 °C with antibodies to Nef (anti-Nef polyclonal, # 2949, 1:500) or actin (1:5,000). Following washes in TBST, blots were incubated for 2 h with Licor IR-Dye secondary antibodies (1:10,000) and imaged using the Licor Odyssey system and software.

2.5.7 Flow Cytometry

Jurkat SERINC5-knockout cells and CEM-SS cells were transfected with the pSELECT-GFPzeo expression vector encoding wild-type and mutant forms of Nef, pSELECTGFPzeo alone and/or pBJ-SERINC5-iHA as described above. Forty-eight h later, cells were washed in 1X Phosphate Buffered Saline (PBS) supplemented with 2% fetal bovine serum and stained for 1 h at ambient temperature with APC-conjugated anti-HA.11 (to detect SERINC5-HA) or phycoerythrin-conjugated anti-human CD4 antibody (both antibodies diluted 1:200). After washing, cells were analyzed for GFP (to quantify Nef expression) and either HA (to quantify JTAg cell surface S5-iHA expression) or phycoerythrin (to quantify CEM-SS cell surface CD4 expression) using a BD Accuri Flow Cytometer. Data were analyzed via BD CSampler software and illustrated using the FlowJo software package.

2.5.8 BiFC and confocal microscopy

293T cells were plated onto 35 mm coverslip-bottom dishes (MatTek, # P35G-1.5-14-C) and allowed to attach overnight. Cells were then transfected with pcDNA3.1 expression vectors encoding complementary BiFC partners using Xtreme Gene 9. Forty-eight h later, cells were fixed with 4% paraformaldehyde for 10 min, permeabilized with 0.2% Triton X-100 for 15 min and blocked with 2% BSA in PBS for 1 h. Cells were then stained overnight at 4 °C with primary antibodies directed at the V5 tag, the HA tag, or Nef (#153). Following washing, cells were stained for 1 h with secondary antibodies conjugated to Texas Red (1:1000), Pacific Blue (1:500), or Alexa Fluor 647 (1:1000). Fluorescent images were acquired with an Olympus Fluoview FV1000 confocal microscope using the 40x objective and x-y scan mode. Immunofluorescence and BiFC signal intensities were quantified via Image J and are represented as the ratio of BiFC to Nef immunofluorescence as reported previously (*296*).

To assess co-localization of SERINC5 with Nef and Rab7+ endosomes, Jurkat JTAg SERINC5-knockout cells were transfected with SERINC5-mCherry and/or Nef-YFP (wild-type and dimer mutants) expression vectors as described above. Coverslip-bottom 35 mm dishes (MatTek) were treated with a 0.01% poly-L-Lysine solution (Sigma) for 1 h at 37 °C, and left to air-dry for 30 min. Transfected cells (1.2×10^6 in 200 µL of RPMI) were added to the poly-L-lysine-treated coverslips for 30 min at 37 °C. Cells were then fixed with 4% paraformaldehyde for 10 min, permeabilized with 0.2% Triton X-100 for 15 min, and blocked with 2% BSA in PBS for 1 h at room temperature. Cells were probed with a mouse monoclonal Rab7 antibody (1:1000) overnight at 4 °C, and then stained with an anti-mouse Alexa Fluor 647-conjugated secondary antibody (1:1000). Cells were imaged using an Olympus Fluoview FV1000 confocal microscope

with a 60x oil objective and x-y scan mode. Pearson's correlation coefficients for co-localization were generated using the FV1000 Fluoview software.

3.0 Defining the structural basis of HIV-1 Nef dimerization in functional complexes with host cell effectors

3.1 Chapter 3 Summary

The HIV-1 accessory protein Nef plays a prominent role in viral pathogenesis, particularly through enhancement of viral replication and downregulation of cell surface MHC-I within infected cells. Both functions are reliant upon Nef activation of the Src family kinases Hck and Lyn, which requires Nef engagement of the kinase SH3 regulatory domain. Structures of Nef in the presence of Src family kinase SH3 domains show that Nef engages the SH3 domain via a conserved PxxP motif, and that the SH3-bound form crystallizes as a dimer of Nef:SH3 complexes. According to these structures, Nef homodimerization occurs at a hydrophobic interface between the αB helices of each Nef molecule and is additionally stabilized by a pair of reciprocal electrostatic contacts via Asp123 and Arg105. Validation of this structure via mutagenesis of dimer interface residues (including Asp123) supported that dimerization occurs in cells and is linked to kinase activation and several other Nef functions. However, comparison of this structure with one in which Nef was co-crystallized with the Hck SH3-SH2 regulatory domain protein challenged the idea that a single Nef dimer interface is constant across all stages of Nef-dependent kinase activation, as it revealed a distinct orientation of the dimer interface compared to what was observed for the SH3-bound structure. Comparison of the structures of the two complexes identified dimer interface residues with differential participation in the dimer interface of one but not both structures (e.g. Asp123), as well as dimer interface residues that appeared to contribute towards dimerization in both structures (Ile109, Leu112, Tyr115, His116). Recombinant purified

Nef proteins harboring substitutions at these residues were used to define the dynamics and stoichiometry of complex formation and dimerization in solution-based assays. We found that the mutation of Asp123 disrupted dimerization for a complex corresponding to the SH3 but not the SH3-SH2 bound structure, suggesting that the dimer interface is remodeled through distinct stages of Hck regulatory domain engagement. We also observed that Nef-Y115A mutation disrupted complex formation and Hck activation in vitro, supporting the notion that it may be a consistent contributor to dimerization within both Nef structures, and can be used as a dimerization defective mutant in future studies.

3.2 Introduction

HIV-1 Nef is a small myristoylated accessory protein that plays an important role in primate lentiviral pathogenesis (*286*). Expression of Nef within CD4+ T cells results in the induction of an AIDS-like phenotype within transgenic animal models (*98*), and non-human primates infected with Nef-defective strains of SIV display reduced viral titers and stunted AIDS progression (*289*). Finally, patients infected with Nef-defective HIV-1 often display reduced progression towards full-blown AIDS, further suggesting the importance of Nef in viral pathogenesis (*290*).

Nef lacks any enzymatic activity, functioning instead by interacting with a variety of host cell proteins, hijacking host cell protein trafficking and signaling (*130*). One of the better characterized Nef functions is an inherent ability to activate host cell kinases, including the Src family kinases, Tec family kinases, p21-associated kinase (PAK), and phosphatidylinositol 3-kinase (PI-3K) (*136, 140, 148, 322*). Nef-dependent activation of Src family kinases contributes

to Nef promotion of viral replication and spread in vivo, and pharmacologic inhibition or genetic knockdown of Src family kinases inhibits viral replication (*252*). Activation of Src family kinases via Nef is directed through a conserved polyproline type II (PPII) helix within the folded core of Nef. A PxxPxR motif within the PPII helix serves as a docking site for the SH3 domain of several Src family kinases, including Hck and Lyn (*211*). In the absence of Nef engagement, the SH3 domain of these kinases associates with an internal linker region adjacent to the kinase domain, driving an inactive, auto-regulated conformation of the kinase (*141*). Nef binds and displaces Hck SH3 domain from this auto-inhibitory interaction, resulting in relief of Hck from the regulated conformation and kinase activation (*140*).

Structures of the Nef core region bound to Src family kinase regulatory SH3 domains reveal a 2:2 heterocomplex, with two Nef molecules bound to two SH3 domains and joined by the Nef homodimer into a four molecule complex (*206, 207*). The Nef dimer interface forms between hydrophobic residues within the αB helix, which are flanked on either side by a pair of electrostatic interactions between Asp123 and Arg105 (*206, 207*) (Figure 7). Mutation of Asp123 and several hydrophobic residues impairs self-association of Nef in cells as well as Nef-mediated CD4 downregulation and enhancement of viral replication, suggesting that the Nef dimer is of functional relevance (*239*). In addition, mutation of Asp123 impairs Nef downregulation of MHC-I, a process that is mediated in part through the Src family kinases Hck and Lyn (*101, 323*).

Our group successfully co-crystallized Nef in the presence of a larger, more functionally relevant regulatory domain protein including both the SH3 and SH2 domains of Hck (*212*). This structure also produced a 2:2 heterocomplex, although the orientation of the Nef dimer interface within this structure is unique compared to the Nef/SH3 domain structures (*212*)(Figure 8). While the formation of the dimer interface is still driven through the contribution of hydrophobic residues

within the αB helix, Asp123 and Arg105 do not interact within this structure, and Asp123 is both surface exposed and directed away from the dimer interface. A structure of Nef bound to an AP-1 subunit and MHC-I tail has established a role for Asp123 in the coordinated recruitment of both the MHC-I and AP-1, suggesting that Asp123 must be exposed for Nef-directed downregulation of MHC-I (*101*). As a result, it is possible that kinase-directed remodeling of the Nef dimer from an SH3 domain-specific form to an SH3-SH2 domain form allows for Nef to transition into a conformation amenable to Asp123 presentation for AP-1 recruitment and MHC-I downregulation.

While Asp123 and Arg105 do not appear to interact in either the SH3-bound or SH3-SH2-bound Nef structures, analysis of the dimer interface for both structures reveals several amino acids that are present in both dimer interface structures, including Ile109, Leu112, Tyr115, and His116. While combined mutation of Ile109, Leu112, Tyr115, and F121 to aspartate shows complete ablation of kinase activation (*252*), the individual contribution of these hydrophobic residues towards kinase activation has not been explored. In addition, it has not been confirmed which dimer interface residues consistently participate in the dimer interface of both the SH3-bound and SH3-SH2 bound complexes.

In this chapter, I discuss data from a collaborative study that provides support for transient participation of Asp123 in the dimer interface during kinase-induced remodeling, and discuss data characterizing a series of Nef dimer interface mutants in vitro.

3.3 Results

3.3.1 Kinetics and dynamics of Nef association with Hck regulatory domain proteins

To test the hypothesis that the Nef dimer interface is rearranged in transition through SH3-bound and SH3-SH2 bound states, we produced recombinant full-length and core-length (amino acids 58-205) Nef protein (SF2 subtype), as well as recombinant Hck SH3 and Hck SH3-SH2 protein (wild-type Nef and Hck regulatory proteins purified by John Jeff Alvarado). We also created a recombinant Nef core mutant in which Asp123, which is unique to the SH3-induced Nef dimer interface, is replaced with asparagine (D123N). This mutant allowed us to track the contribution of Asp123 to dimerization across both regulatory domain protein complexes by HDX MS as described below.

Prior to analyzing the dynamics of complex formation and Nef dimerization, we measured the binding affinity of the Nef proteins towards recombinant Hck SH3 and SH3-SH2 domain proteins as a control. As SH3 domain engagement requires proper folding of the 3-dimensional Nef core (see Figure 6), any impairment of Nef folding by the D123N mutation would likely impair binding to either Hck regulatory domain protein. Therefore, we quantified the binding affinity with surface plasmon resonance (SPR), which is an optically based, label-free methodology used to measure the kinetics of molecular interactions in real time.

In SPR, a sensor chip containing a high refractive index prism is inserted into the instrument's flow channel, and a protein ligand is attached (often covalently) to the surface of the chip. Following immobilization of the ligand, a solution containing a putative binding partner (the analyte) is flowed over the sensor chip, and interaction between the analyte and immobilized ligand increases the mass at the surface of the sensor chip. This mass increase changes the refractive index

of polarized light passing through the prism, and that change is detected by an optical detector directed at the prism and transformed into arbitrary binding response units (RUs). Plotting these binding response units as a function of time generates a binding curve detailing association, steady state, and dissociation of two molecules in solution, which can be used to generate binding kinetics and affinity data for a given interaction (*324*).

To measure the affinity of recombinant Nef with Hck SH3 and SH3-SH2, we covalently immobilized the SH3 and SH3-SH2 proteins onto a carboxymethyl dextran SPR chip, and injected increasing concentrations of different Nef proteins (0.04 to 3.3 μM) onto the chip surface. Both wild-type Nef and Nef-D123N bound to Hck SH3 and SH3-SH2 with submicromolar affinity, suggesting that the D123N mutation does not impact Nef global structure or impair recruitment of Hck regulatory domain proteins (Figure 26). Interestingly, there was little appreciable difference in binding affinity between the recombinant Nef core protein and full-length Nef, suggesting that the N-terminal anchor region does not participate in this interaction (at least in solution and in a non-myristoylated form).

Hck Ligand	Nef Analyte	k_{a1}, 1/M · s	k_{d1}, 1/s	k_{a2}, 1/M · s	k_{d2}, 1/s	K_D, M
SH3	Full-length	2.84×10^5	4.97×10^{-2}	N/A	N/A	$1.80 \pm 0.42 \times 10^{-7}$
SH3	wild-type core	2.24×10^5	2.76×10^{-2}	N/A	N/A	$1.28 \pm 0.31 \times 10^{-7}$
SH3	D123N core	2.90×10^5	3.00×10^{-2}	N/A	N/A	$1.19 \pm 0.44 \times 10^{-7}$
SH3-SH2	Full-length	1.33×10^5	5.34×10^{-2}	3.44×10^{-3}	3.29×10^{-3}	$4.29 \pm 1.32 \times 10^{-7}$
SH3-SH2	wild-type core	6.29×10^4	5.65×10^{-2}	1.06×10^{-2}	4.72×10^{-3}	$4.08 \pm 0.45 \times 10^{-7}$
SH3-SH2	D123N core	5.72×10^4	4.93×10^{-2}	9.03×10^{-3}	4.88×10^{-3}	$4.75 \pm 0.99 \times 10^{-7}$

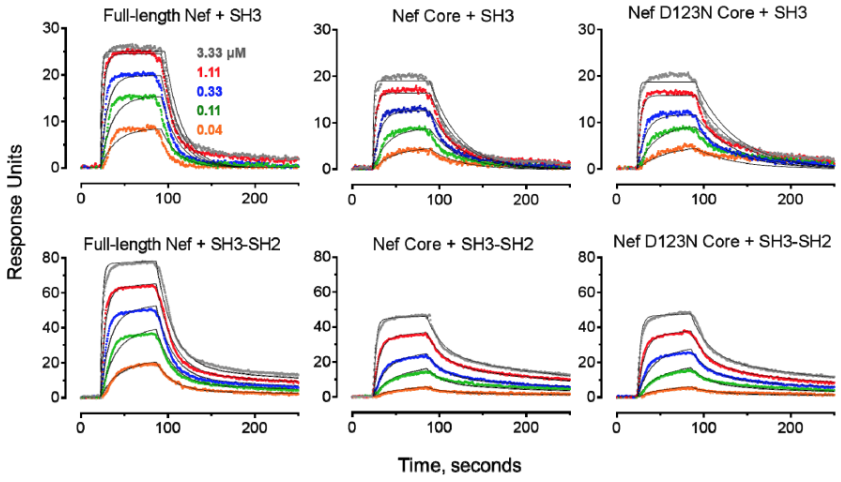

Figure 26: Kinetics of Nef wild-type and D123N protein interactions with Hck SH3 and SH3-SH2 domains

Protein-protein interactions were measured in real time by surface plasmon resonance (SPR). Recombinant Hck SH3 and SH3-SH2 proteins were immobilized covalently as ligand on carboxymethyl dextran SPR chips (Reichert) using standard EDC/NHS amine coupling chemistry. Nef proteins were then injected in triplicate over a range of concentrations (0.04 to 3.3 µM) at a flow rate of 30 µL/min for one min until equilibrium was reached, followed by a 3 min dissociation phase. Kinetic rate constants were calculated from reference-corrected sensorgrams using TraceDrawer software, and were best fit by 1:1 Langmuir (SH3) or two-state (SH3-SH2) binding models. Equilibrium dissociation constants (KD values) calculated from the resulting rate constants are shown, ± S.D. N/A, not applicable. Representative sensorgrams from each experiment are shown below the Table. The SPR responses recorded at each concentration are shown as colored points, with the fitted curves superimposed as black lines.

With the kinetics of Nef association with Hck SH3 and SH3-SH2 established, we next studied the dynamics of complex formation in solution using HDX-MS (see Section 1.2.5.2 for an overview of this method). We compared deuterium exchange between the wild-type Nef core alone

with wild-type Nef core co-purified as a stable complex with the Hck SH3 or SH3-SH2 domain proteins. Co-purification was performed by John Jeff Alvarado (Smithgall laboratory), and HDX MS studies were performed and analyzed by Jamie Moroco and Thomas Wales (laboratory of John Engen, Northeastern University) (*244*). Comparison of deuterium uptake between the Nef core alone vs. the Nef core bound to Hck regulatory domain proteins displayed early protection of the PxxP helix of Nef for both complexes, followed by additional protection within the αB helix at longer time points (Figure 27). This result is consistent with the crystal structures of the SH3- and SH3-SH2-bound Nef complexes (*207*), as it demonstrates PxxP-dependent engagement of the SH3 domain and stabilization of Nef dimerization at the αB helix in the complexes relative to Nef alone.

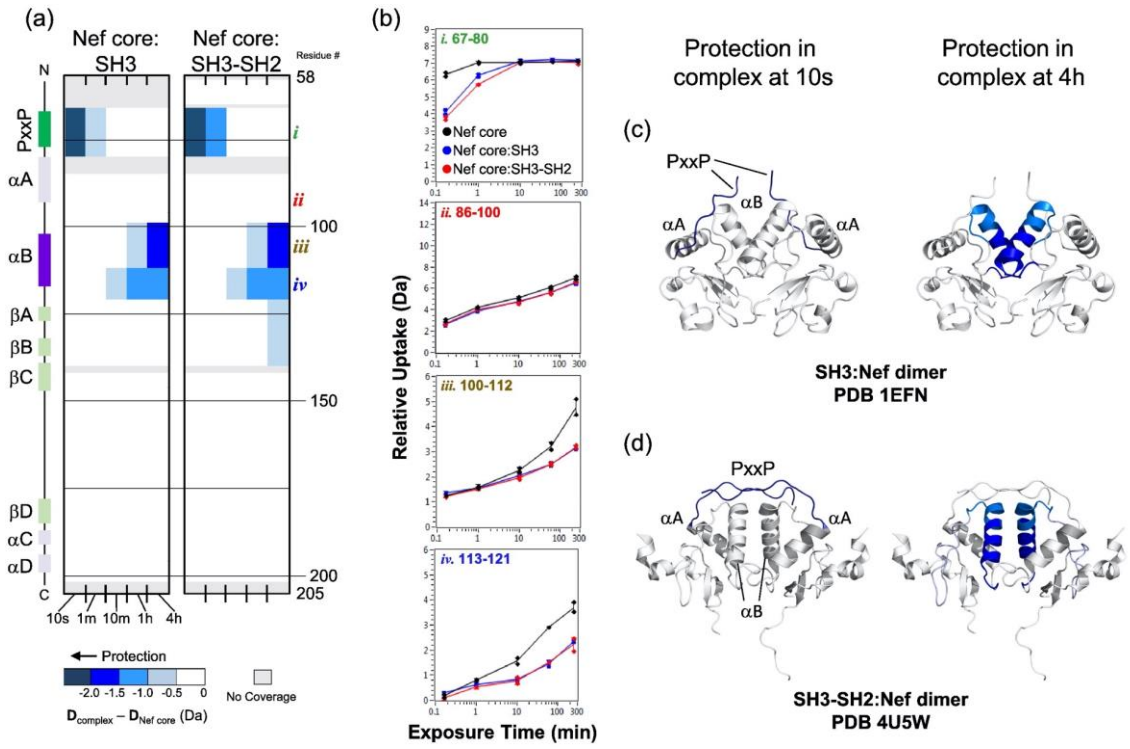

Figure 27: HDX MS analysis demonstrates stabilization of the Nef dimer via kinase regulatory domain engagement

a) Comparison of deuterium uptake by Nef core alone versus the core complex with Hck SH3 (left) or SH3-SH2 (right) is presented in a vertical difference map of the Nef core secondary structure. The deuterium level in each peptide from the Nef core alone was subtracted from those recorded from each complex and the differences are color-coded as indicated in the legend. The differences in non-overlapping peptides, displayed vertically from N- to C-terminus, are indicated for the corresponding exchange times (10 s to 4 h; shown horizontally). Greater protection is represented as a more intense shade of blue. (b) Deuterium incorporation graphs for selected peptides i, ii, iii, iv. Uptake curves from Nef core peptides are shown in black, Nef core:SH3 complex peptides are shown in blue, and Nef core:SH3-SH2 complex peptides are shown in red. (c,d) The protection observed in Nef when bound to Hck SH3 (c) or Hck SH3-SH2 (d) after 10 s (left) or 4 h (right) of deuterium exchange is mapped onto the corresponding crystal structures as indicated.

3.3.2 Conformation of Nef dimer interface is distinct in the presence of Src family kinase SH3 and SH3-SH2 regulatory domain engagement

After determining the kinetics and dynamics of wild-type Nef association with Hck SH3 and SH3-SH2, we next determined whether Nef-D123N impacts the dynamics of complex formation in solution (HDX MS performed by Jamie Moroco and Thomas Wales). Deuterium

exchange kinetics were compared between the D123N Nef core protein alone and in complexes with either Hck SH3 or SH3-SH2. For the SH3-bound complex, the D123N mutation displayed no deuterium uptake protection within the αB helix, in stark contrast to the protection observed within the wild-type Nef complex (Figure 28). In contrast, the Nef-SH3-SH2 domain complex displayed reduced deuterium exchange within peptides derived from the αB helix, similar to the results with wild-type Nef in this complex. Peptides derived from the PxxP interface of the SH3-bound D123N Nef core complex also showed reduced protection when compared to the wild-type complex, a surprising result considering the similar affinity of both Nef proteins observed in Figure 26. Still, the dynamics observed within this study support the crystal structures of the SH3 and SH3-SH2 bound Nef complexes, wherein Asp123 participates within the SH3-bound but not the SH3-SH2 bound dimer interface.

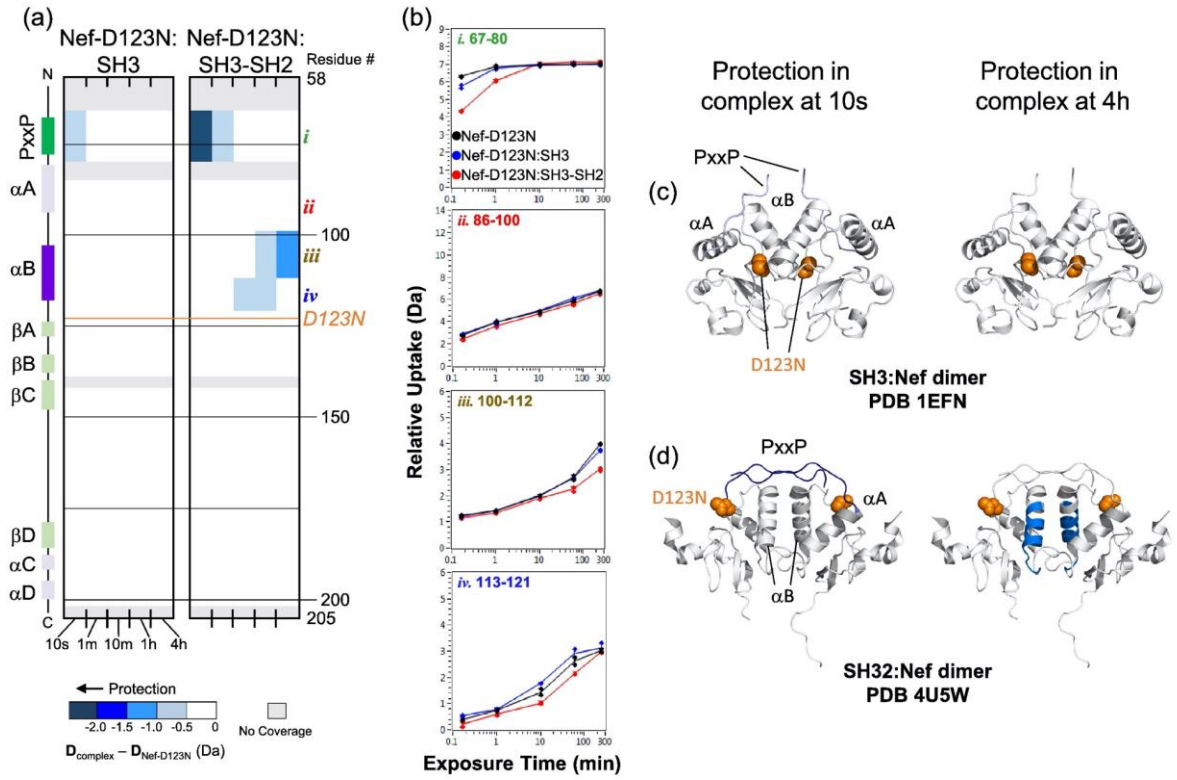

Figure 28: HDX MS reveals that Nef D123N mutation impairs dimer formation for Hck SH3-bound but not Hck SH3-SH2-bound complex

(a) Comparison of deuterium uptake by the Nef-D123N core alone versus Nef-D123N in complex with Hck SH3 (left) or Hck SH3–SH2 (right) is presented in a vertical difference map of the Nef core secondary structure. The deuterium level of each peptide from Nef-D123N alone was subtracted from that in Nef-D123N when part of a complex and the differences are color coded as indicated in the legend. The differences in non-overlapping peptides are displayed vertically from N- to C-terminus for each exchange time point (10 s to 4 h; shown horizontally). Greater protection is represented as a more intense shade of blue. The location of the D123N mutation is indicated in orange on the difference maps and the structures in panel d. (b) Deuterium incorporation graphs for selected peptides i, ii, iii, and iv. Uptake curves from Nef-D123N core peptides are shown in black, Nef-D123N core:SH3 complex peptides are shown in blue, and Nef-D123N core:SH3–SH2 complex peptides are shown in red. (c, d) The protection observed in Nef-D123N when bound to Hck SH3 (c) or Hck SH3–SH2 (d) after 10 s (left) or 4 h (right) of deuterium exchange is plotted onto the corresponding crystal structures as indicated. Protection in the Nef-D123N αB helix is only observed in the complex with Hck SH3–SH2.

The stoichiometry of the Nef/Hck regulatory domain complexes was also analyzed via size-exclusion chromatography (SEC). Wild-type and D123N Nef core proteins were co-purified in the presence of Hck SH3 or Hck SH3-SH2 domain, and then injected onto an analytical size exclusion column (worked performed by John Jeff Alvarado). SEC of the wild-type Nef/SH3-SH2

domain complex resulted in an elution volume consistent with a 2:2 heterocomplex, as confirmed by multi-angle light scattering in a previous study (*212*). The D123N Nef/SH3-SH2 domain complex eluted in a similar volume as the wild-type Nef complex, suggesting that the D123N Nef complex is of a similar size and composition (Figure 29). However, the complex composed of Nef D123N and Hck SH3 domain alone resulted in a doublet in which one peak matched the elution volume of the wild-type Nef/Hck SH3 heterodimeric complex, and another peak matched monomeric Nef. This result supports the dynamics of the D123N Nef seen in Figure 28 and the notion that Asp123 participates in the SH3 domain-bound, but not the SH3-SH2-bound, complex. These findings further suggest that Asp123 may participate in the dimer interface during an initial stage of Hck engagement that involves SH3 domain binding but is then reorganized within the SH3-SH2 domain complex to expose Asp123 for interaction MHC-I/AP-1 or other host cell proteins.

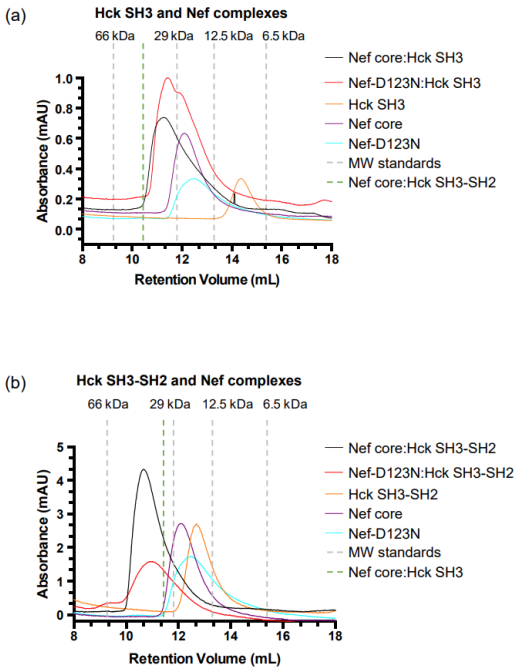

Figure 29: Analytical size-exclusion chromatography of Nef:Hck complexes

Part (a) shows size-exclusion chromatography (SEC) elution profiles of the purified Nef core: Hck SH3 complex, the Nef-D123N:Hck SH3 complex, and individual proteins making up the complexes. Part (b) shows SEC elution profiles of the purified Nef core: Hck SH3-SH2 complex, the Nef-D123N:Hck SH3-SH2 complex, and individual proteins making up the complexes. The positions of the elution peaks for the protein standards bovine serum albumin (66 kDa), carbonic anhydrase (29 kDa), cytochrome C (12.5 kDa) and aprotinin (6.5 kDa) are indicated with grey dotted lines. The positions of the Nef core complexes with SH3 and SH3-SH2 are also indicated on the plots for reference (green dotted lines). Note that the stoichiometry of an identical Nef core complex with the Hck SH3:SH2 protein was previously determined by SEC combined with multi-angle light scattering to be a dimer of complexes

3.3.3 Identification of conserved Nef dimerization interface residues

While the participation of Asp123 in Nef dimerization is unique to the SH3-bound state, a commonality between both structures is the presence of a dimer interface composed of several highly conserved, hydrophobic residues (modeled in Figure 30). The side chains of residues Ile109, Leu112, Tyr115, His116, and Phe121 participate directly in dimerization in both crystal structures, either by projecting directly into the hydrophobic interface or through external dimer-stabilizing interactions (engagement of Val70 in the SH3-SH2 domain dimer). Leu112, Tyr115, and Phe121 have been well characterized as participating in dimerization (Chapter 2), and

mutation of these residues disrupts Nef dimerization and function. Meanwhile, the individual roles of Ile109 and His116 in dimerization (both in solution and in cells) have not yet been examined. However, the dynamics and individual contribution of all five residues towards dimerization during Hck regulatory domain engagement remains an open question.

Therefore, in order to compare the contribution of dimer interface residues on Hck regulatory domain engagement and complex formation in solution, we expressed and purified four recombinant Nef mutants I109A, L1112A, Y115A, and H116A. While substitution of these residues with aspartate or another charged residue was considered, we decided that alanine substitution may allow us to study the individual role of each residue's side chain without gross disruption of the overall dimer interface.

Side chains participating in Nef dimer interfaces

Residue	SH3	SH2-SH3
V70		
G95		
G96		
L100		
S103		
R105		
R106		
I109		
L112		
W113		
Y115		
H116		
F121		
D123		

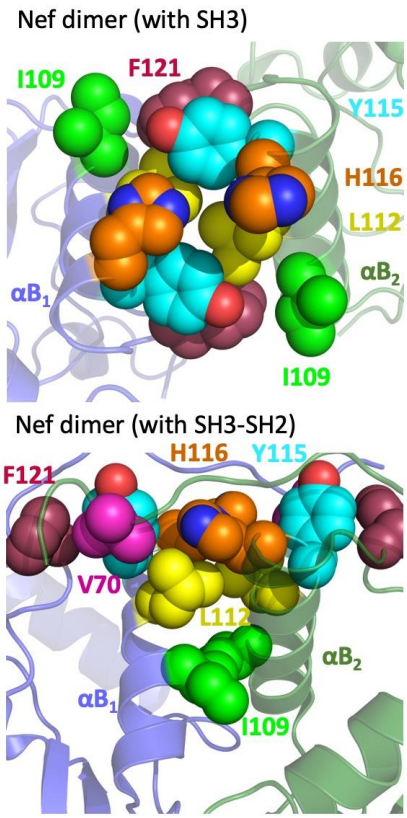

Figure 30: Comparison of the SH3-bound and SH2-SH3-bound Nef dimer interfaces

(A) List of Nef residues which participate in dimerization within two structures of the dimer interface (shown in B,C, PDB 1EFN and 4U5W, respectively). Side chains which participate in one dimer structure are highlighted in green boxes, while side chains that contribute to dimerization are highlighted in blue boxes and red text (Ile109, Leu112, Tyr115, His116, Phe121). (B) View of the Nef dimer interface for the HckSH3-bound structure. Side chains of Ile109, Leu112, Tyr115, His116, Phe121 form a hydrophobic interface between each Nef αB helix (C) View of the Nef dimer interface for the HckSH3-SH2-bound structure. Side chains of Ile109, Leu112, Tyr115, His116, Phe121 contribute towards the hydrophobic interface, or coordinate clasping of Val70 presented by the opposite Nef monomer (Leu112, Tyr115, Phe121). Models were produced in PyMOL (PDB 1EFN and 4U5W).

3.3.4 Affinity of Nef dimer mutants for Hck SH3 and SH3-SH2 regulatory domain proteins

Prior to examining the impact of these dimer interface mutations on Nef dimerization and complex formation in solution, we first wanted to characterize their possible effect on Hck SH3 and SH3-SH2 domain binding. As nearly all of these residues are conserved across subtypes of Nef (>95% for Ile109, Leu112, Tyr115, ~60% for His116) (*325*), there is still a chance that substitution of these residues could impact Nef global structure. In order to confirm productive

folding of these Nef mutants and understand the kinetics of regulatory domain engagement, we immobilized Hck SH3 or SH3-SH2 domain onto SPR sensor chips and flowed Nef wild-type and mutant protein over the immobilized ligands as before. All Nef mutants associated with Hck SH3 and SH3-SH2 domain proteins with micromolar-to-submicromolar affinity (Figure 31), with the affinities of wild-type Nef and several of the mutants in a similar range as previously reported interactions (*244*). The K_D's of the I109A and L112A mutants were similar to wild-type Nef for both the Hck SH3 and SH3-SH2 domains, while Nef H116A affinity was about 2-fold lower than wild-type Nef. Though Nef Y115A still displayed functional association with Hck SH3 and SH3-SH2 domain, the affinity of that mutant was about 5-fold lower than wild-type Nef, suggesting a potential allosteric impact of this mutation on SH3 domain recruitment. These data demonstrate that substitution of individual dimer interface residues with alanine does not markedly impact Nef association with Hck regulatory domain proteins, suggesting a preservation of Nef global structure for these mutant proteins.

A

Nef	HckSH3 Affinity (K_D, M)	HckSH3-SH2 Affinity (K_D, M)
WT	$2.24 \pm 0.09 \times 10^{-7}$	$3.03 \pm 0.07 \times 10^{-7}$
I109A	$3.78 \pm 0.05 \times 10^{-7}$	$4.03 \pm 0.25 \times 10^{-7}$
L112A	$1.71 \pm 0.12 \times 10^{-7}$	$2.14 \pm 0.14 \times 10^{-7}$
Y115A	$10.3 \pm 0.49 \times 10^{-7}$	$17.3 \pm 1.34 \times 10^{-7}$
H116A	$5.04 \pm 0.10 \times 10^{-7}$	$7.07 \pm 0.09 \times 10^{-7}$

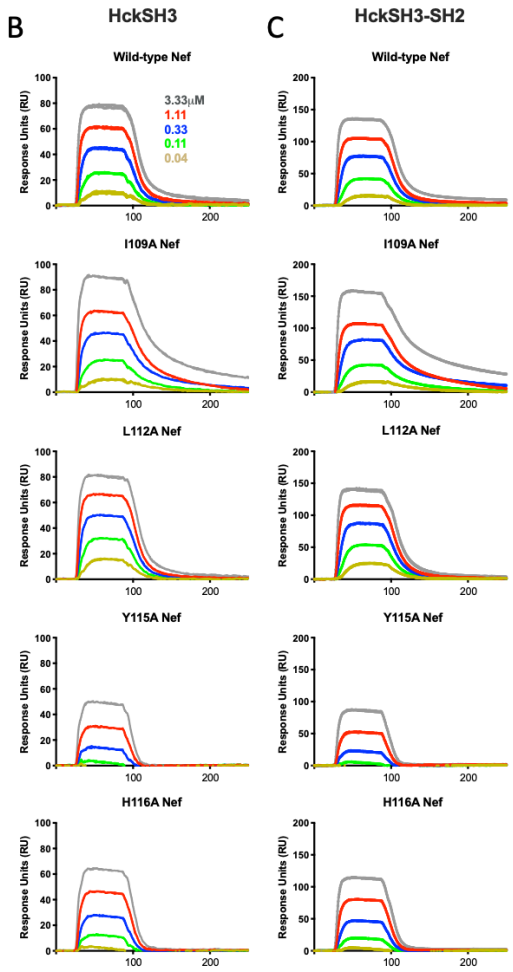

Figure 31: Binding affinity of Nef dimer interface mutants towards Hck regulatory domain proteins

Protein-protein interactions were measured in real time by surface plasmon resonance (SPR). Recombinant Hck SH3 and SH3-SH2 proteins were immobilized covalently as ligand on carboxymethyl dextran SPR chips (Reichert) using standard EDC/NHS amine coupling chemistry. Nef proteins were then injected in triplicate over a range of concentrations (0.04 to 3.3 μM) at a flow rate of 30 μL/min for one min until equilibrium was reached, followed by a 3 min dissociation phase. Steady-state affinities were calculated from reference-corrected sensorgrams using TraceDrawer software, and Equilibrium dissociation constants (KD values) are shown, ± S.D. Representative sensorgrams from each experiment are shown below the Table. The SPR responses recorded at each concentration are shown as colored points.

3.3.5 Impact of Nef dimer mutations on 2:2 heterocomplex formation in solution

Having characterized the affinity of these Nef dimer mutants toward the Hck SH3 and SH3-SH2 domain proteins, we next determined whether mutation of individual dimerization interface side chains was sufficient to disrupt formation of the Nef dimer and 2:2 heterocomplex in solution.

We mixed each recombinant Nef protein with an equimolar ratio of Hck SH3 or SH3-SH2 protein, and injected these complexes onto an analytical size exclusion column. Injection of the wild-type Nef complexed with Hck SH3 and SH3-SH2 domain resulted peak elution volumes of about 10 mL and 10.5 mL (respectively) (Figure 32). The elution volume of these peaks was lower but within a similar range to those observed for complexes of the wild-type Nef core with SH3 and SH3-SH2 proteins (*244*), suggesting the presence of 2:2 heterodimeric complexes in the presence of full-length Nef. The somewhat lower elution volume is likely accounted for by the higher mass of full-length Nef protein.

Analysis of the elution profiles for the I109A, L112A, and H116A Nef proteins revealed complexes which are of a similar size as the wild-type complex, potentially signifying the preservation of Nef dimerization and 2:2 heterocomplex formation in the presence of these mutants (compare the peak positions of the black and blue elution profiles of each complex in Figure 32). However, complexes of Nef-Y115A with both the SH3 and SH3-SH2 domains resulted in a clear rightward shift in the elution volume, consistent with disruption of complex formation. The simplest interpretation of these results is that the Y115A mutation disrupts formation of the dimer complex, with 1:1 Nef-Y115A:SH3 and Nef-Y115A:SH3-SH2 complexes eluting from the column. In either case, no free SH3, SH3-SH2, or Nef is seen, suggesting that Nef remains bound to SH3 under these conditions despite the somewhat lower affinity measured by SPR. Thus, the Nef-Y115A mutant may represent a very useful tool to study the importance of Nef homodimer formation in solution, because it disrupts Nef dimer formation even in complex with SH3-SH2.

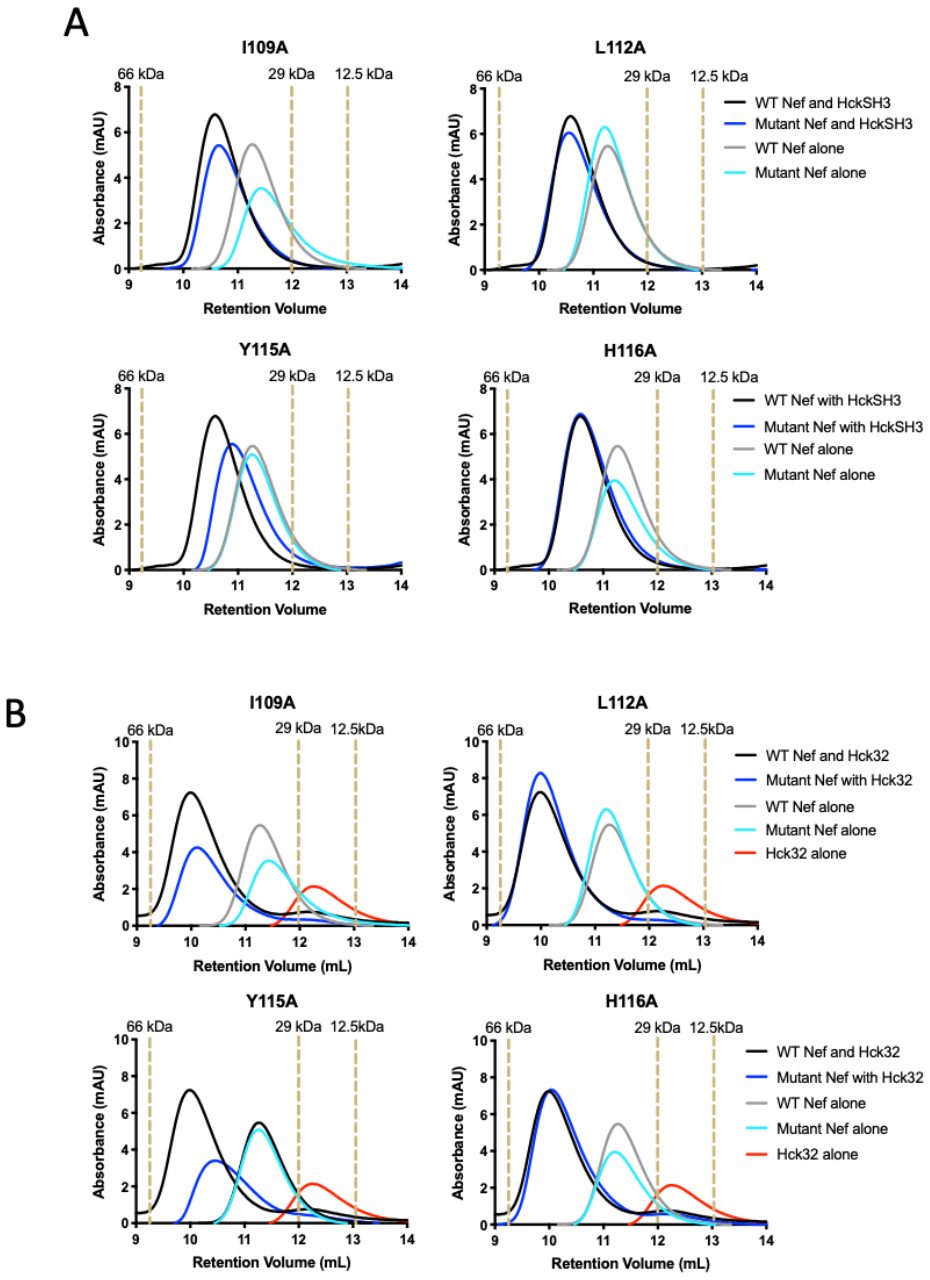

Figure 32: Analytical size-exclusion chromatography of Nef dimer mutants with Hck regulatory domain complexes

Size-exclusion chromatography profiles of Nef proteins mixed with either (A) HckSH3 or (B) HckSH3-SH2. Elution of wild-type Nef complex and wild-type Nef alone are denoted by black and grey curves, respectively. Mutant Nef elution profiles (in complex and in isolation), are indicated by blue and cyan curves, and the identity of each Nef mutant is indicated above each panel. Proteins were injected onto the analytical SEC column at 12.5uM, and complexes were mixed 1:1 at equal molar ratios for 15min prior to injection. Previously determined elution profiles of standards bovine serum albumin (66 kDa), carbonic anhydrase (29 kDa), cytochrome C (12.5 kDa) and aprotinin (6.5 kDa) are indicated with gold dotted lines.

3.3.6 In vitro activation of the Src-family kinase Hck by Nef dimer interface mutants

Nef engagement of Hck results in the release of the kinase from an auto-inhibitory conformation (stabilized by self-association with the SH3 and SH2 domains), and subsequent activation of the kinase (*139*). The presence of the Nef dimer within the Hck SH3- and SH3-SH2-bound crystal structures supports the notion that dimerization may play an important role in kinase activation, which is supported by cellular data implicating Nef dimerization in the activation of both Src and Tec-family kinases (*149, 240*). Analysis of Hck SH3 and SH3-SH2 engagement and complex formation described above allowed for an early glimpse into the role of individual Nef dimer interface residues in Hck recruitment, but we were curious how each Nef mutant would impact Hck activation itself.

Therefore, we used an in vitro kinase assay (Z'-Lyte Kinase Assay) to compare the degree of Hck activation displayed by each Nef mutant. This assay utilizes a FRET-peptide substrate flanked on either side by a donor (coumarin) and acceptor (fluorescein) fluorophore, which are positioned at a distance that allows for productive fluorescence resonance energy transfer (FRET). In the absence of phosphorylation, this substrate is sensitive to digestion by a specific protease, disrupting FRET within the substrate. As a result, kinase activation can be quantified by measuring the preservation of FRET following substrate phosphorylation and protease digestion.

In a cellular context, Hck is self-regulated via SH2 engagement of a pTyr motif within the C-terminal tail, and phosphorylation of this Tyr residue is performed by the host cell tyrosine kinase Csk (*139*). For in vitro kinase assay, we use a form of recombinant Hck in which the C-terminal tail sequence adjacent to the Csk site is modified to pTyr-Glu-Glu-Ile (Hck-YEEI)(*326, 327*). When expressed in insect cells and purified, this form of Hck retains the 'assembled' conformation, with the tyrosine-phosphorylated tail bound to the SH2 domain and the SH3 domain

engaged with the SH2-kinase linker as shown by X-ray crystallography and HDX MS. Previous studies from our group have shown that Hck-YEEI is readily activated by recombinant Nef (*142*) (*252*).

As previously observed, incubation of wild-type Nef with Hck-YEEI promoted activation of the kinase. This is indicated by a leftward shift in the kinase activation titration curve and a decrease in the reported EC_{50} value for the "Hck and WT Nef" condition when compared to "Hck alone" (Figure 33). Compared to wild-type Nef, the I109A, L112A, and H116A Nef mutants activated Hck-YEEI to a similar extent, suggesting these mutations had no clear impact on Nef-dependent kinase activation. However, Nef-Y115A demonstrated a 2-fold reduction in kinase activation compared to wild-type Nef and the other mutants, suggesting a critical contribution of the Tyr115 residue towards kinase activation. The defect in Hck activation by Nef-Y115A may reflect its inability to form dimers, its reduced capacity for SH3 domain engagement, or a combination of both factors.

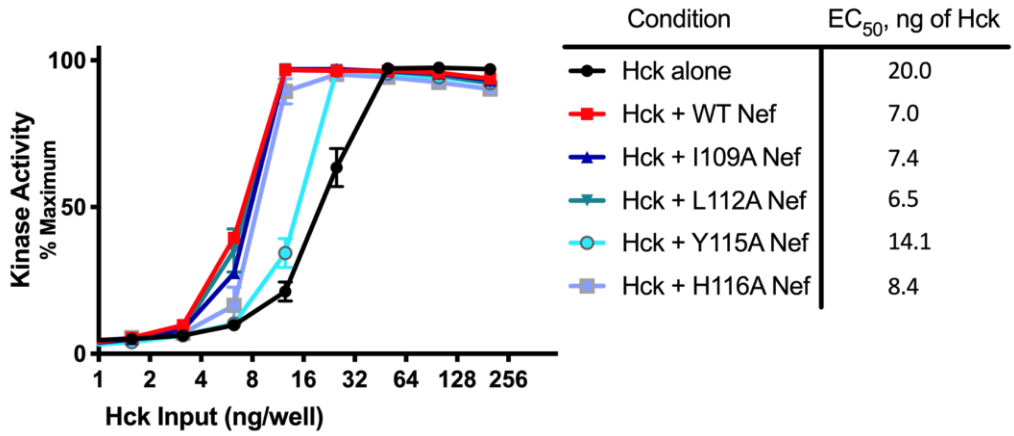

Figure 33: Y115A Nef displays reduced kinase activation in vitro

Hck alone or Nef and HckYEEI at a 10:1 molar ratio were titrated across a series of 2-fold dilutions and incubated with ATP and a FRET-based tyrosine substrate to measure substrate phosphorylation/kinase activation (see methods, Section 3.5.7). Kinase activation was measured in quadruplicate and normalized to unphosphorylated and fully phosphorylated peptide controls. Degree of kinase activity for each Nef/Hck condition across increasing quantities of Hck is presented ± S.D. via protein titration curves (colored curves). Nef activation of Hck is indicated through a leftward shift in the kinase activation curve when compared to Hck alone (black curve). EC_{50} values (per ng of Hck) were calculated by non-linear regression analysis of the "Hck alone" and "Hck + Nef" curves. Assay was repeated in quadruplicate across two independent experiments.

3.4 Discussion

Dimerization is a consistent structural feature of Nef, one that has been observed in cells, in solution, and in structures of Nef co-crystallized with SH3 domains and the Hck SH3-SH2 regulatory region (*149, 206, 212, 239*). However, while the overall fold of the Nef core remains constant in complexes with different effector proteins (Figure 34), the orientation and contribution of individual residues to the dimer interface varies dramatically between the SH3- and SH3-SH2-bound structures of Nef. Indeed, a key electrostatic contact for the SH3-bound Nef dimer (Asp123) becomes surface-exposed in structures of Nef in complex with HckSH3-SH2 or AP-1/MHC-I, suggesting the orientation of the dimer interface is dynamically remodeled during transition from SH3 to SH3-SH2 domain engagement. To test this hypothesis, we tracked the impact of dimer

interface mutations (both Asp123 and hydrophobic interface residues) on complex formation across both the SH3- and SH3-SH2-bound conformations of the Nef dimer.

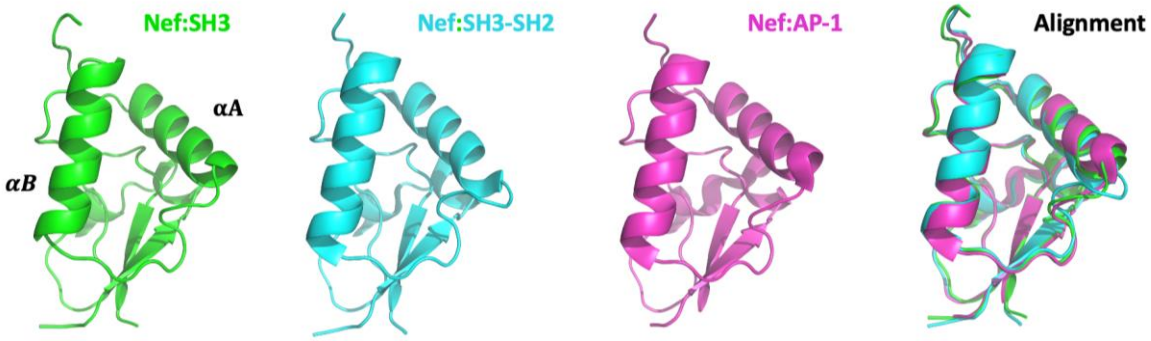

Figure 34: Global fold of the Nef core is conserved across protein partners

Folding of Nef core protein from three separate crystal structures- Nef:SH3 (PDB: 1EFN), Nef:SH3-SH2 (PDB:4U5W), and Nef:AP-1μ1/MHC-I tail (4EMZ). Alignment of the Nef core from each complex (performed via PyMOL) shows preservation of global overall fold of the Nef core structures across distinct structures despite association with different partners.

Our data support the existence of Nef dimers within the Hck SH3- and SH3-SH2-bound structures of Nef. Comparison of solution dynamics between Nef alone vs. Nef in complex with SH3 vs. SH3-SH2 by HDX MS showed increased protection of the αB helix from deuterium uptake for complexed Nef, consistent with promotion of dimerization in solution. Analysis of these complexes via size-exclusion chromatography also supported Nef dimerization, with elution profile consistent with 2:2 heterodimeric complexes. This is consistent with prior validation of SH3 and SH3-SH2 bound structures of Nef, which confirmed the presence of the Nef dimer in solution across several biochemical and/or biophysical methods as described in the Introduction (*197*, *212*).

Distinct orientation of the Nef dimer interface in the presence of SH3 vs. SH3-SH2 domain proteins may represent individual stages of Hck engagement. Primary recruitment of Hck SH3 by Nef may initiate an initial SH3-specific conformation of the dimer, which is reorganized into a

different interface following participation of the SH2 domain within the complex. Analysis of the dynamics for these complexes leaves room for this possibility, as it reveals a temporal order for Hck engagement in solution. Deuterium protection at the Nef PxxP motif (suggesting SH3 engagement) occurs at the earliest labeling times for both complexes, while protection within the αB helix (consistent with Nef dimerization) appears later in the assay. However, the relatively slow rate of deuterium uptake by the helical interface may also reflect hydrogen bonding within the αB helix.

Analysis of the D123N mutant also supports the transition of Nef through two distinct dimer interfaces during Hck SH3 and then SH3-SH2 engagement, and complements the different positions assumed by this residue within each Nef dimer structure. While introduction of the D123N mutation had no impact on the kinetics of SH3 or SH3-SH2 association, protection from deuterium uptake observed at the dimer interface with the wild-type Nef-Hck SH3 complex was eliminated for the Nef-D123N:SH3 complex. Introduction of this mutation also seemed to destabilize complex formation as observed by size-exclusion chromatography. Meanwhile, the Nef D123N/Hck SH3-SH2 complex eluted at the same volume as the wild-type complex, and protection at the αB helix was still evident for the mutant complex. This supports the existence of two structurally separate dimer interfaces, only one of which is dependent upon the Asp123-Arg105 ionic interactions observed by X-ray crystallography.

To track the contribution of hydrophobic dimer interface residues to dimerization within Hck SH3 and Hck SH3-SH2 bound complexes, we developed four recombinant Nef mutants (I109A, L112A, Y115A, H116A). We considered that this mutagenesis strategy which involved the substitution of these bulkier hydrophobic residues with alanine would allow us to study the contribution of these residues without disrupting other dimer interface residues or dramatically

impacting Nef global structure. For three of the Nef mutants (I109A, L112A, H116A), alanine substitutions had little impact on Nef dimerization or complex formation, with each mutant displaying similar affinity for SH3 binding via SPR and Hck activation compared to wild-type Nef. This may not be particularly surprising for the I109A and L112A Nef mutants, as the change in residue size is not as dramatic as what is expected for Nef-His116 or Nef-Tyr115. It is also possible that elimination of bulky hydrophobic side chains from one of these three residues is not enough to weaken the overall dimer interface, especially when Nef is complexed to the Hck SH3-SH2 domain protein (see Figure 8). In this case, alanine substitution of a single residue may not be sufficient to disrupt the entire interface. Creation of Nef mutants with alanine substitutions at least two dimer interface residues may allow for a more complete disruption of the Nef dimer. Also, while this study was performed prior to the experiments detailed in Chapter 2, the very limited impact of the L112A substitution on Nef dimerization and function observed in these experiments is consistent with what was observed for this mutant in cellular studies (Figure 12 and Figure 13).

In contrast, the Nef Y115A mutation appeared to have a noticeable impact on both Hck SH3 and SH3-SH2 complex formation in solution and displayed a functionally impaired ability to activate Hck-YEEI compared to wild-type Nef. While it is tempting to speculate that mutation of Tyr115 disrupts dimerization in complexes with both Hck SH3 and SH3-SH2, (thus impairing Nef-dependent Hck activation), the exact stoichiometry of the resulting Y115A complex is needed to confirm this notion. In addition, this idea is confounded by the apparent impact of this mutation on Hck SH3 and Hck SH3-SH2 domain affinity, which is around 5-fold lower than what is observed for wild-type Nef.

In future work, we plan to use HDX-MS to characterize the dynamics of dimerization within complexes of Nef bound to Hck SH3 and Hck SH3-SH2 for these and similar dimer interface mutations. While a Nef Phe121 mutant was not included within this study, the contribution of this residue to both Nef dimer interface structures suggests it is worth further investigation. We also hope to further understand the full mechanistic basis behind the phenotype demonstrated by Nef-Y115A, starting with confirmation of the stoichiometry of the Y115A complex via size-exclusion chromatography with multi-angle light scattering. As Nef dimerization appears to be a critical component of Nef-dependent Src family kinase activation (and by extension, MHC-I and viral replication), building a complete understanding of the dynamics and structure of Nef dimerization during Nef function could allow for development of antiretroviral agents with broad activity against Nef in the future.

3.5 Methods

3.5.1 Bacterial expression vector construction (adapted from Moroco 2017)

The bacterial expression plasmids encoding the C-terminally His_6-tagged human Hck SH3–SH2 tandem regulatory domains [residues 72–242; numbering based on the crystal structure of human c-Src (PDB 2SRC)] and both the full-length and core domain of HIV-1 Nef [SF2 allele residues 1–205 and 58–205, respectively; numbering based on the crystal structure of Nef NL4-3 (PDB 1EFN)] are described in Alvarado et al (*212*). Plasmids encoding the C-terminally His6-tagged human Hck SH3 (residues 77–140; numbering was based on the structure of human c-Src) were constructed by PCR amplification of the corresponding coding regions. The SH3 and Nef

core PCR products were subcloned via Nde I and Xho I restriction sites into the bacterial expression vectors pET-21a(+) and pET-21b(+) (EMD Millipore), respectively. A fragment of the Nef-SF2 coding region of pET-14b/Nef-D123N was excised with KpnI and EcoRI and subcloned into a pET-30a plasmid encoding the Nef-SF2 core sequence plus the C-terminal His6 affinity tag. Alanine substitutions were introduced into the Nef dimer interface of the pET-21b(+) full-length Nef SF2 (I109A, L112A, Y115A, H116A0 via the Agilant QuikChange II XL Site-Directed Mutagenesis Kit. The coding regions of all final bacterial expression plasmids were confirmed by DNA sequencing.

3.5.2 Protein expression and purification (adapted from Moroco 2017)

Expression and purification conditions for recombinant Nef (full-length, core, D123N mutant) and Hck (SH3 and SH3–SH2) proteins in E. coli are described in detail elsewhere with slight modifications(*212*). For ion-exchange and Ni-IMAC column chromatography steps, the flow rate was increased to 2 mL/min, and buffer exchange after IMAC chromatography involved dialysis against 3 × 1 L of anion-exchange buffer at 4 °C. Purification of the four protein complexes used in this study (wild-type and D123N forms of the Nef core in complex with either Hck SH3 or SH3–SH2) is also based on our previously published methods, in which cell pellets from cultures expressing the individual protein components were combined prior to lysis and column chromatography (*212*)

3.5.3 Surface plasmon resonance (adapted from Moroco 2017)

Recombinant, purified Hck SH3 and SH3–SH2 proteins were exchanged into HBS-EP buffer [10 mM Hepes (pH 7.4), 150 mM NaCl, 3 mM EDTA, 0.05% v/v Surfactant P20], while recombinant Nef proteins were exchanged into HBS-EPD (HBS-EP buffer supplemented with 1 mM DTT) prior to analysis on a two-channel Reichert SR7500DC or a Reichert 4SPR instrument SPR platform. The Hck SH3 and SH3–SH2 proteins were covalently immobilized onto carboxy-methyl dextran SPR chips (Reichert) using standard EDC/NHS amine coupling chemistry. Nef proteins were then injected in triplicate over a range of concentrations (0.041–3.3 μM) at a rate of 30 μL/min for 1 min until equilibrium was reached, followed by dissociation in HBS-EPD for 3 min. Kinetic rate constants were calculated from reference-corrected sensorgrams using TraceDrawer software, and were best fit by 1:1 Langmuir (SH3) or two-state (SH3–SH2) binding models. Steady-state affinities of Nef dimer interface mutants to Hck SH3 and Hck SH3-SH2 were also calculated using TraceDrawer software.

3.5.4 Analytical SEC (adapted from Moroco 2017)

Analytical SEC was conducted using a Superdex 75 10/300 GL column (GE Healthcare Life Sciences) equilibrated with running buffer [20 mM Tris–HCl, 150 mM NaCl, 10% (v/v) glycerol, 2 mM TCEP, pH 8.3]. All SEC runs were conducted at a flow rate of 0.5 mL/min, with each protein sample at a final concentration of 12.5 μM in a volume of 100 μL. SEC protein standards (Sigma-Aldrich) included bovine serum albumin (66 kDa), carbonic anhydrase (29 kDa), cytochrome C (12.5 kDa), and aprotinin (6.5 kDa).

3.5.5 Deuterium labeling (adapted from Moroco 2017)

Stock solutions of individual proteins and complexes were prepared to final concentrations of 65 μM in 20 mM Tris–HCl (pH 8.3), 100 mM NaCl, and 3 mM DTT. Each protein or complex (110 pmol in 1.7 μL) was diluted 15-fold into identical buffer prepared with D_2O. Labeling reactions were quenched after various times (10 s, 1 min, 10 min, 1 h, 4 h) with an equal volume of ice-cold quench buffer (100 mM K_2HPO_4/KH_2PO_4, pH 2.3). Undeuterated controls were prepared in the same way using the H_2O-based buffer and quenched for digestion. One unique protein expression and purification prep was used for all protein samples, with the exceptions of the Nef core: Hck SH3 and Nef core: Hck SH3–SH2 complexes, for which two independent samples were prepared and analyzed. All labeling reactions were performed in duplicate, and a representative experiment is shown for each sample.

3.5.6 Online protein digestion and mass analysis (adapted from Moroco 2017)

After quenching, samples were injected onto a Waters nanoAcquity with HDX technology for online pepsin digestion at 15 °C and UPLC peptide separation at 0 °C. Samples were digested on a 2.1 × 50-mm stainless steel column packed with POROS 20AL resin coupled to porcine pepsin (Sigma). Peptides were trapped and desalted on a VanGuard Pre-Column trap (2.1 × 5 mm, Acquity UPLC BEH C18, 1.7 μm) for 3 min. Peptides were eluted from the trap and separated using an Acquity UPLC HSS T3 1.8 μm 1.0 × 50-mm column with a 5%–35% gradient of acetonitrile over 6 min at a flow rate of 65 μL/min. Mass spectra were acquired using a Waters Synapt G2Si mass spectrometer. Peptides were identified from triplicate undeuterated samples of each protein alone and in complexes using Waters MS^E and Waters Protein Lynx Global Server

(PLGS) 3.0. Peptide maps were generated and deuterium incorporation was analyzed using Waters DynamX 3.0 software.

3.5.7 In vitro kinase assay

Assay was performed in a 384-well format using the Z'-Lyte kinase assay system (ThermoFisher). Near-full-length Hck-YEEI (a downregulated form of the kinase) was used for this assay, and was expressed from SF9 insect cells and purified as previously described (*328*). Hck-YEEI alone (200 ng) or Nef and Hck-YEEI at a 10:1 molar ratio, respectively, were titrated across a series of 2-fold dilutions and transferred in quadruplicate 10 μL volumes to a 384 plate. Kinase activation reactions within each well were initiated through the addition of 100 μM of ATP and 1 μM of a fluorescence resonance energy transfer (FRET)-based tyrosine peptide substrate (Tyr2), and wells were incubated for 45 min prior to the addition of 5 μL of substrate-specific development protease for 60 min. The development protease specifically cleaves unphosphorylated Tyr2 substrate, breaking FRET that occurs between the peptide's donor fluorophore (coumarin) and acceptor fluorophore (fluorescein). Fluorescence of the reporter substrate following kinase activation and protease development was measured via SpectraMax M5 microplate reader at 445 and 520 nm (allowing for measurement of coumarin and fluorescein emission ratios) following excitation at 400 nm. As maintenance of FRET within the peptide (indicated by a low ratio of coumarin:fluorescein emission) is the result of substrate phosphorylation, the degree of kinase activation corresponds directly to the emission ratio between these two fluorophores. Emission ratios for each reaction were normalized to 0% and 100% phosphorylation controls.

4.0 Overall Discussion

4.1 Summary and discussion of major findings

Though both halves of this dissertation work centered around the impact of dimerization on Nef function, each story involved the exploration of this important issue using two very different methodologies. The first half of my thesis, which investigated the role of Nef dimerization in antagonism of the SERINC5 host restriction factor, focused on virology and microscopy techniques, looking at the Nef dimer from the context of viral and cellular membranes. The second half explored changes to the dimer interface across two dynamic and structural stages of Hck regulatory domain association, and involved the use of structural, biochemical, and biophysical methodologies to study the Nef dimer in solution.

4.1.1 Homodimerization is required for Nef antagonism of SERINC5

For the first part of my thesis, I examined the role of Nef dimer interface residues (Leu112, Tyr115, Phe121) in Nef promotion of viral infectivity, a phenotype driven by Nef antagonism of the host restriction factor SERINC5. While the impact of these dimer interface residues has been previously examined in the context of viral replication and CD4 downregulation (*239*), these initial studies predate the discovery of SERINC5 in 2015 (*117*, *256*). Based on the kinetics of dimerization measured by in-cell BiFC across a time scale consistent with single-round virion production (48 h), I identified three dimerization-defective Nef mutants - L112D, Y115D, and

F121A. As a L112A mutant showed functional dimerization, I included this mutant as a control throughout the subsequent assays.

I was able to show that dimerization defective Nef mutants (L112D, Y115D, F121A) demonstrated impaired Nef enhancement of viral particle infectivity, and impairment in infectivity was largely due to reduced antagonism of SERINC5 following disruption of Nef dimerization. Although Asp123 had previously been implicated in this function (*117*), this project represents the first demonstration that hydrophobic dimer interface residues are required for Nef antagonism of SERINC5. Using a single-round infectivity assay, I demonstrated that mutation of dimer interface residues inhibited Nef promotion of viral infectivity in a primarily SERINC5-dependent manner. This finding was confirmed within an artificial 293T producer cell system, as well as a functionally relevant T cell line (Jurkat JTAgs) and donor-derived PBMCs.

Interestingly, some of my data also seem to suggest an impact of dimerization defective mutants on infectivity even in the absence of SERINC5 expression. As only SERINC5 expression was modulated within these experiments, it is possible that Nef antagonism of other endogenous SERINC proteins is similarly impacted by Nef dimerization. However, the HIV-1 Nef subtype used in this study (B-clade SF2) does not antagonize SERINC3, and while mRNA transcripts of SERINC1 are highly expressed in myeloid and lymphoid cells, SERINC1 displays weak inhibition of viral infectivity (*258, 262*). Finally, while the expression of SERINC4 within these cell lines was not examined, a recent analysis of gene-expression data sets was unable to identify any human tissues with detectable SERINC4 expression (*259*).Taken together, it seems unlikely that other SERINC proteins are contributing to Nef promotion of infectivity within this experimental system.

The possibility remains that Nef antagonizes other yet-unknown restriction factors via a dimerization-dependent mechanism. Indeed, a recent study identified a SERINC5-independent

means of Nef enhancement of viral replication, which researchers hypothesized was mediated through an unidentified cellular factor (*329*). In addition, Nef has been shown to antagonize at least two other cellular factors that can restrict HIV-1: TIM-1 and Ezrin (*330*, *331*). While disruption of Asp123 impairs Nef internalization of TIM-1, involvement of the dimerization during Nef antagonism (and the contribution of these proteins to the Nef enhancement of infectivity) remains an open question.

I also demonstrated that dimerization is essential for Nef exclusion of SERINC5 from newly synthesized virions and downregulation of SERINC5 from the cell surface. A limitation of these analyses was a reliance on the detection of transfected SERINC5 via an HA tag, due to the lack of a commercial antibody that can detect endogenous SERINC5 (*275*). However, phenotypic trends observed for the mutants in terms of Nef enhancement of viral infectivity appeared to mirror the degree of SERINC5 incorporation into each corresponding virus. In addition, Nef downregulation of cell-surface CD4 was compared for each mutant as a control, and dimerization-defective mutants that displayed reduced SERINC5 downregulation did not antagonize CD4. These confocal and flow-cytometry-based results enforce the validity and relevance of these data, even though Nef downregulation and exclusion of endogenous SERINC5 could not be explored.

Using confocal microscopy, I found that Nef dimerization is required for the retargeting of SERINC5 into the endosome-lysosome system. Wild-type Nef and SERINC5 were shown to co-localize within the Rab7+ late endosomal compartments, consistent with previous reports (*117*, *268*). Disruption of Nef dimerization impaired trafficking of SERINC5 into late endosomes, which is the first reported evidence that the Nef dimer may be required for Nef sequestration of proteins into the endo-lysosomal pathway. Interestingly, while the L112A mutant had no effect on Nef

downregulation of SERINC5 or its exclusion from the membrane, L112A was less able to redirect SERINC5 into Rab7+ endosomes, compared to wild-type Nef.

Finally, as Nef antagonism of SERINC5 appears to involve coordinated recruitment of both the AP-2 hemicomplex and SERINC5 (*269*), I used BiFC to explore whether mutation of the dimer interface impacted Nef association with SERINC5, AP-2 α, and AP-2 σ2 in cells. As Nef association with AP-2 and SERINC5 is predicted to occur at the cell surface, I used a myristoylation-defective mutant of Nef (Nef-G2A) as a negative control. While Nef-G2A has been previously shown to disrupt association of Nef and SERINC5 in cells (via BiFC) (*268*), this is the first reported use of this control for Nef:AP-2 hemicomplex association in a BiFC system. However, for both sets of interactions, Nef-G2A showed cellular expression but impaired association with SERINC5, AP-2α, and AP-2 σ2, supporting the utility of this mutant as a negative control.

Through BiFC analysis, I observed that genetic disruption of dimerization had no detectable impact on SERINC5 association. The same observation was true for Nef-L112D and Nef-F121A and both the AP-2α and AP-2 σ2 subunits, as no decrease in association was detected for those mutants. However, while Nef-Y115D still bound to AP-2α and AP-2 σ2 at a level above the G2A control, this demonstrated a significant decrease in Nef association compared to wild-type Nef. Since crystal structures of Nef and the AP-2 α/σ2 hemicomplex show no overlap between the AP-2/Nef interface and the dimer interface (*222*), this decrease is likely due to an allosteric impact on the mechanism for AP-2 engagement.

In summary, these data suggest that the Nef homodimer is required for bridging AP-2 and SERINC5 together into a complex that productively drives Nef internalization of SERINC5 from the cell surface. While AP-2 releases from the clathrin-coated vesicle following endocytosis (*332*),

the Nef dimer also appears to coordinate intracellular retargeting of SERINC5 following internalization. However, the mechanistic contribution of the Nef dimer during this stage of Nef antagonism remains underexplored and will hopefully be examined in future studies.

4.1.2 Defining the structural basis of HIV-1 Nef dimerization in functional complexes with host cell effectors

For the second half of this dissertation, we compared the contribution of individual dimer interface residues to dimerization in two stages of Hck regulatory domain engagement. This study began with an observed discrepancy in the participation of Nef Asp123 across two structures of the Nef dimer- one in which Nef is bound to a Src-family kinase SH3 domain, and a second in which Nef is bound to an expanded SH3-SH2 domain. In the SH3 domain-bound structure, Asp123 participates directly in the stabilization of the dimer interface, whereas the second SH3-SH2 bound structure features an Asp123 that is positioned away from the dimer interface and solvent-exposed.

This raised the possibility that the Nef dimer transitions through two stages of Hck regulatory domain engagement, and that transition through these stages involves reorientation of the dimer interface. To test this hypothesis, I developed, expressed, and purified a recombinant Nef mutant where Asp123 was substituted with asparagine (D123N). This mutation eliminated a stabilizing electrostatic interaction present within the Nef:SH3 dimer complex but not the SH3-SH2 domain bound structure of the Nef dimer. To ensure that introduction of this mutation did not impact proper folding of the 3-dimensional Nef core, I used surface plasmon resonance to measure the affinity of binding between the Nef core and the Hck SH3 and SH3-SH2 domain proteins. I observed no difference in SH3 affinity between wild-type and D123N, suggesting that this substitution does not destabilize the Nef core in solution. In addition, there was no apparent impact

of the D123N substitution on solubility of the mutant protein during expression and purification, further supporting that the D123N mutant is properly folded and viable. However, additional examination of the D123N mutant via circular dichroism or thermal stability assays could confirm this further, as well as crystallization of the mutant protein.

We next examined the dynamics of Nef complex formation in solution. Using HDX MS, we were able to compare the dynamics of complex formation between wild-type and D123N Nef in both the SH3- and SH3-SH2-bound complexes. In contrast to the wild-type Nef:SH3 complex, the D123N Nef:SH3 complex displayed a complete lack of deuterium uptake protection within the αB helix, consistent with disruption of dimerization following mutation of Asp123. However, the D123N Nef:SH3-SH2 complex retained significant protection within the same region (as seen in the wild-type complex), consistent with the crystal structure which shows that this residue does not participate in the SH3-SH2 domain-bound Nef dimer structure. We also analyzed the stoichiometry of complex formation in solution and observed that Nef D123N is able to form a stable 2:2 heterodimeric complex with the SH3-SH2 but not the SH3 protein. Both results support the hypothesis that the Nef dimer interface is remodeled during transition from an initial SH3 bound conformation of the 2:2 heterodimer to the SH3-SH2 bound state.

Taking an additional look at the crystal structures of the SH3 and the SH3-SH2 domain bound Nef dimers, I observed several hydrophobic residues that participated to the Nef dimer interface in both Nef dimer structures- Ile109, Leu112, Tyr115, His116, and Phe121. Three of these residues (Ile109, Leu112, Phe121) have already been characterized as driving Nef homodimerization in cells by BiFC, and mutants harboring substitutions at these residues have been validated as bona-fide dimerization defective mutants (Chapter 2, (*149, 239*). Although the contribution of these three residues towards dimerization in this context has not been examined,

their participation in the dimer interface seems consistent across both structures, and they play a clear role in Nef dimerization in cells. In addition, two of the hydrophobic residues in both dimer interface structures (Ile109 and His116) have not been studied to the same extent, and their contribution to the dimer interface in general remains to be further evaluated.

Therefore, I chose to survey the contribution of four hydrophobic residues towards dimerization - two of the well-characterized residues (Leu112 and Tyr115) and two of the poorly characterized dimer residues (Ile109 and His116). I expressed and purified four recombinant Nef mutant proteins- I109A, L112A, Y115A, and H116A. I first performed the same quality control experiment used in the D123N study, using SPR to assess whether introduction of these alanine substitutions impaired proper three-dimensional folding of Nef. I observed that three of the Nef mutants (I109A, L112A, H116A) bound to Hck SH3 and Hck SH3-SH2 with similar affinity as wild-type Nef. Nef-Y115A, also displayed productive association with both regulatory domain proteins, albeit with about 5-fold lower affinity than wild-type Nef.

Curiously, SPR studies of Hck SH3 and SH3-SH2 demonstrated a similar, submicromolar affinities towards wild-type Nef. While binding of both Hck proteins is primarily directed through Nef association with SH3, and the Nef:SH3 interface is largely conserved across both complexes, there are differences between both structures that might be expected to manifest as changes to the affinity (*212*). For example, Arg105 (a residue which coordinates with Asp123 to stabilize the SH3-bound Nef dimer) makes a novel ionic contact with Glu93 in the SH3 domain of the SH3-SH2 dual domain protein, and the SH2 associates with the Nef core via Van der Waals interactions (*212*). However, these novel contacts within the secondary SH3-SH2 bound structure may serve to remodel the dimer interface or induce a conformational change, rather than impact recruitment or affinity of the SH3 domain.

Next, I used analytical size exclusion chromatography to compare the stoichiometry of complex formation between each Nef protein in the presence of the SH3 or SH3-SH2 domain. I observed similar complex formation between wild-type Nef and the I109A, L112A, and H116A mutants, consistent with 2:2 heterocomplex formation. However, the Nef-Y115A/regulatory domain complexes displayed a larger elution volume, consistent with disrupted complex formation, likely through disruption of Nef homodimerization.

Finally, I examined the ability of each Nef mutant to activate Hck in an in vitro kinase assay. Mirroring the results of complex formation in the analytical size exclusion chromatography studies, we observed that I109A, L112A, and H116A mutants displayed kinase activation on par with that of wild-type Nef. However, Nef-Y115A activation of Hck was 2-fold lower than what was observed with wild-type Nef. Reduced kinase activation of this mutant could be due to a defect in dimerization, consistent with the observed disruption to complex formation in solution. Indeed, forced dimerization of the Nef dimer in cells (via a Nef-estrogen receptor fusion construct and 4-hydroxytamoxifen) has been shown to increase Hck activity in cells compared to unfused Nef (*240*), and mutation of the Tyr115 residue also disrupts Nef activation of the similarly organized (i.e. SH3 and SH2 domain containing) Tec family kinases in cells (*149*). And while the reduced affinity of this mutant towards Hck SH3 and SH3-SH2 could also have contributed towards decreased Hck activation, the affinity of these two regulatory domain proteins may not completely reflect the affinity of Nef towards full-length kinase especially when considered in the context of the lipid bilayer where the effective concentrations of each protein is much higher. Taken together, these data suggest a role for Tyr115 in the dimer interface of both SH3 and SH3-SH2 bound dimer structures, and suggest that mutants with multiple alanine substitutions or more aggressive

substitutions may be required to properly examine the contribution of Ile109, Leu112, and His116 towards dimer formation.

In summary, the studies described in this chapter support a 2-step model in which Nef interacts with Hck to trigger kinase activation as well as reorganization of Nef to enable interaction with AP-1 for MHC-I downregulation and immune escape (Figure 35). In the first step, Nef recruits Hck through its SH3 domain, resulting in the formation of a 'loose' dimer structure in which Asp123 is buried in the dimer interface. This Nef: Hck complex then undergoes dynamic reorganization, resulting in a more compact dimer consistent with kinase activation, as well as surface exposure of Asp123 for recruitment of MHC-I and AP-1 as required for downregulation. The crystal structures that support this model offer only snapshots in time of the overall dynamic transitions that occur. However, our HDX MS data support the existence of distinct dimer forms in solution, and potentially in cells.

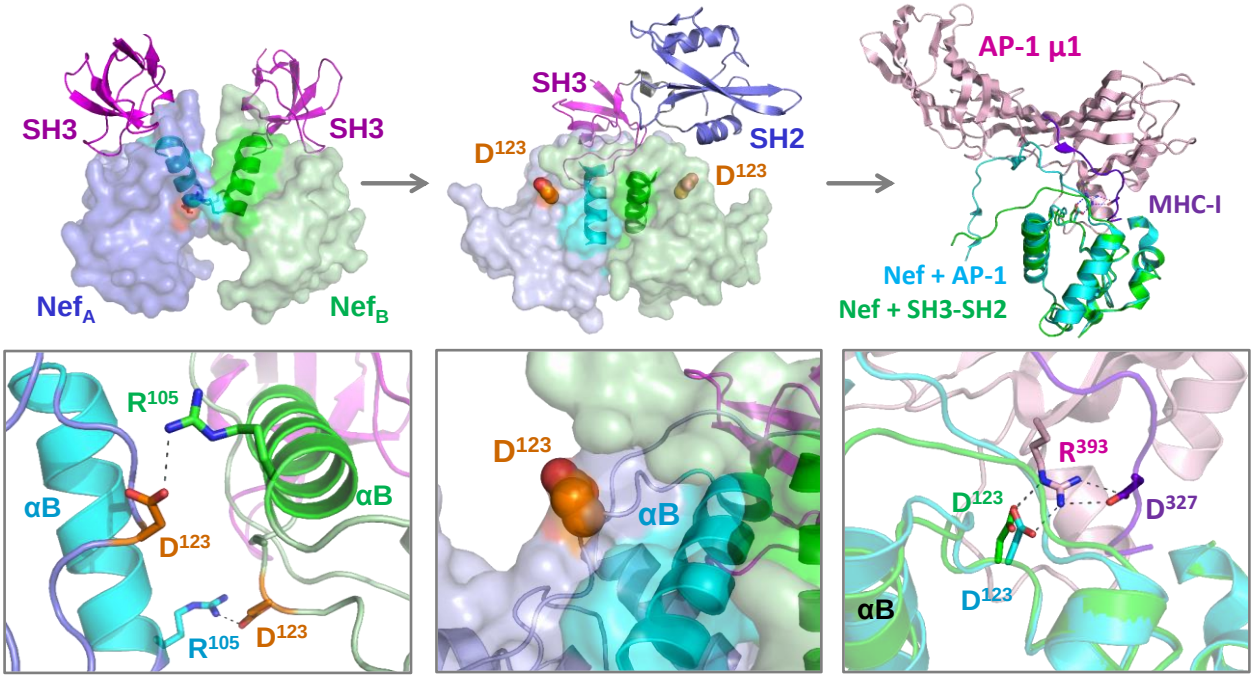

Figure 35: Interaction of HIV-1 Nef with the Src-family kinase Hck may induce conformational changes consistent with MHC-I/AP-1 recruitment

Left: Crystal structure of the HIV-1 Nef core in complex with the SH3 domain of Fyn (high affinity R96I mutant; PDB: 1EFN). Nef forms a dimer of Nef•SH3 complexes in this structure (Nef_A, blue; Nef_B, green). The dimer interface is formed by the Nef αB helices (highlighted; see Figure 4 for details). The SH3 domains shown at the top in red. The helical dimer interface is enlarged in the lower panel and highlights the reciprocal polar contacts between Nef Asp123 and Arg105, which are buried in the core of this structure. *Center*: Top panel shows the crystal structure of the Nef core in complex with the Hck SH3-SH2 region (PDB 4U5W). Color scheme as per the left panel with a single SH3-SH2 unit shown for clarity. Nef also crystallizes as a 2:2 complex Nef•SH3-SH2 dimers in this structure. However, the helical interface is completely re-oriented relative to the Nef•SH3 complex, such that the Nef Asp123 side chain (orange) is now pointed toward the solvent. One of the Asp123 residues is enlarged in lower panel. *Right*: Structural alignment of one of the Nef core proteins in the Nef•SH3-SH2 complex (PDB 4U5W; green ribbon) with the Nef core in complex with the AP-1/µ1 subunit (pink) and MHC-I tail peptide (purple); (PDB 4EN2; Nef core from this complex in cyan). The Nef core proteins from each complex adopt very similar conformations, with nearly identical positioning of Nef Asp123 (enlarged in lower panel). Nef Asp123 forms part of an ionic bond network with Arg393 from AP-1 and Asp327 from MHC-I that is required for Nef-mediated downregulation of MHC-I and immune escape.

4.2 Future directions

4.2.1 Exploring the mode of Nef and SERINC5-ICL4 association

Since the discovery of Nef antagonism of SERINC5 in 2015, one of the larger questions surrounding this function is the mode of binding between the two proteins. Indeed, the ability of Nef to antagonize SERINC5 appears to be mediated through the intracellular loop 4 region (ICL4) of SERINC5. Substitution of this loop with the loop from Nef-resistant orthologs of SERINC5 from other species eliminates Nef antagonism, suggesting a role for this region in Nef recruitment. And while this dissertation and other studies have demonstrated Nef: SERINC5 association via BiFC, a direct interaction between these two proteins remains to be confirmed. However, downregulation of SERINC5 appears to depend upon the formation of a trimeric complex between SERINC5-ICL4, Nef, and AP-2, and a fused Nef-ICL4 construct appears to promote recruitment of AP-2 μ2/σ2/α via GST pull-down (*269*). In order to confirm that Nef and SERINC5-ICL4 interact directly, we can measure the interaction of Nef and a recombinant protein of SERINC5-ICL4, and see if they associate, via SPR, and form a complex in solution, via size exclusion chromatography. If binding requires the presence of the AP-2 hemicomplex, recombinant versions of AP-2 subunits can be developed and introduced into both systems. Additionally, analytical size exclusion chromatography coupled to multi-angle light scattering may provide a more quantitative assessment of the stoichiometry and composition of the complex, potentially implicating the Nef dimer in S5-ICL4 engagement and recruitment.

4.2.2 Track dynamics of Nef dimer formation via fluorescence complementation and live-cell imaging

These data show for the first time that alteration of Nef dimerization in cells appears to impacts intracellular retargeting of SERINC5 into late endosomes. While our proposed mechanism offers an explanation of how the Nef dimer participates in the initial stage of clathrin-mediated endocytosis, the role of the Nef dimer in downstream endosomal trafficking (following release of AP-2) is unknown. One downside of BiFC is the irreversibility of fluorophore formation, which prevents the study of the dynamics of an interaction within a cell. However, the recent development of a fast and reversible fluorogen-based complementation assay, 'Splitfast', may allow us to track Nef dimer assembly and disassembly in real time within live cells (*333*). We could follow Nef dimer formation throughout the entire course of SERINC5 internalization and retargeting and use co-localization and small molecule inhibitors of endosomal trafficking to understand where the Nef dimer is present and which proteins it may be recruiting.

4.2.3 Solution dynamics of Nef dimerization in the membrane-associated state

While this study analyzed the dynamics of dimerization and Hck regulatory domain complex formation in solution, membrane association is a shared feature of both Src family kinases and Nef (*334*). HDX MS has recently been shown to be amenable to the incorporation of a Langmuir monolayer, which allow for the dynamics of membrane-associating proteins to be examined (*198*). Disruption of myristoylation appears to impair both Nef dimer formation and kinase activation in cells, suggesting that the membrane-associated conformation of Nef is the functionally relevant form (*149*). To extend the results from the previous study into a more

physiologically relevant context, we can measure the dynamics of complex formation in the presence of myristoylated Hck regulatory domain proteins and Nef. If stabilization of the dimer interface by regulatory domain proteins is preserved within this system, we can then explore the contribution of individual dimer interface residues toward the dimerization interface in the presence and absence of membrane association.

4.3 Closing remarks

The year 2021 will bring us into a fifth decade of contending with HIV/AIDS as a species. Despite major leaps in antiretroviral therapy, prevention via education and PrEP, and breakthroughs in understanding the intricacies of HIV-1 infection and latency, we are still left without a cure for infection. There is an urgent need to identify novel ways to target the virus, especially in the context of therapeutic strategies that may aid in clearing the latent viral reservoir. The potential of Nef as a novel drug target is exceptionally strong, through both its essential role in viral pathogenesis and its various contributions towards immune escape. Early drug development strategies sought to target single protein-protein interaction interfaces within Nef (e.g. the PxxP motif) (*249, 335*). However, the widespread contribution of Nef dimerization towards Nef function could allow for a nearly comprehensive disruption of Nef function, making it an exceptional drug target. Our lab is working to develop a class of inhibitors that potentially target productive dimer formation, an effort that benefits from having a complete understanding of the dynamics of dimer interface formation during Nef function, and the role of dimerization in essential Nef activities. I hope to have contributed to that understanding in both halves of my dissertation work. First, I was able to implicate the Nef dimer in antagonism of SERINC5,

suggesting that disruption of Nef dimerization could force HIV-1 to succumb to a potent inhibitor of viral infectivity. I also helped to show that the Nef dimer interface can be dynamically remodeled in different stages of binding partner engagement, and worked to identify commonalities between remodeled dimer interfaces. This work helps support a deeper understanding of how the dimer interface can be pharmacologically targeted across different stages of Nef function and regulatory protein engagement. I sincerely hope my previous contributions and future work will help our lab develop an effective therapeutic for HIV-infected individuals.

Bibliography

1. H. W. Jaffe, The early days of the HIV-AIDS epidemic in the USA. *Nat Immunol* **9**, 1201-1203 (2008).

2. *Pneumocystis Pneumonia --- Los Angeles* (1981 https://www.cdc.gov/mmwr/preview/mmwrhtml/june_5.htm).

3. K. A. Sepkowitz, AIDS--the first 20 years. *N Engl J Med* **344**, 1764-1772 (2001).

4. *Current Trends Update on Acquired Immune Deficiency Syndrome (AIDS) --United States* (1982 https://www.cdc.gov/mmwr/preview/mmwrhtml/00001163.htm).

5. F. Barre-Sinoussi *et al.*, Isolation of a T-lymphotropic retrovirus from a patient at risk for acquired immune deficiency syndrome (AIDS). *Science* **220**, 868-871 (1983).

6. R. D. Moore, Epidemiology of HIV infection in the United States: implications for linkage to care. *Clin Infect Dis* **52 Suppl 2**, S208-213 (2011).

7. T. S. Alexander, Human Immunodeficiency Virus Diagnostic Testing: 30 Years of Evolution. *Clin Vaccine Immunol* **23**, 249-253 (2016).

8. H. I. Hall *et al.*, Estimation of HIV incidence in the United States. *JAMA* **300**, 520-529 (2008).

9. *HIV Surveillance Report- Diagnoses of HIV Infection in the United States and Dependent Areas* (2018 http://www.cdc.gov/hiv/library/reports/hiv-surveillance.html.).

10. UNAIDS, "UNAIDS Data 2019," (2019).

11. D. Quammen, *Spillover: Animal Infections And The Next Human Pandemic*. (W.W. Norton & Co., 2012).

12. D. M. Tebit *et al.*, HIV-1 Group O Genotypes and Phenotypes: Relationship to Fitness and Susceptibility to Antiretroviral Drugs. *AIDS Res Hum Retroviruses* **32**, 676-688 (2016).

13. J. Yamaguchi *et al.*, Brief Report: Complete Genome Sequence of CG-0018a-01 Establishes HIV-1 Subtype L. *J Acquir Immune Defic Syndr* **83**, 319-322 (2020).

14. B. S. Taylor, M. E. Sobieszczyk, F. E. McCutchan, S. M. Hammer, The challenge of HIV-1 subtype diversity. *N Engl J Med* **358**, 1590-1602 (2008).

15. U. Timilsina *et al.*, Identification of potent maturation inhibitors against HIV-1 clade C. *Sci Rep* **6**, 27403 (2016).

16. N. R. Faria *et al.*, HIV epidemiology. The early spread and epidemic ignition of HIV-1 in human populations. *Science* **346**, 56-61 (2014).

17. T. Zhu *et al.*, An African HIV-1 sequence from 1959 and implications for the origin of the epidemic. *Nature* **391**, 594-597 (1998).

18. P. M. Sharp, B. H. Hahn, Origins of HIV and the AIDS pandemic. *Cold Spring Harb Perspect Med* **1**, a006841 (2011).

19. J. Hemelaar, The origin and diversity of the HIV-1 pandemic. *Trends Mol Med* **18**, 182-192 (2012).

20. S. Locatelli, M. Peeters, Cross-species transmission of simian retroviruses: how and why they could lead to the emergence of new diseases in the human population. *AIDS* **26**, 659-673 (2012).

21. N. R. Klatt, G. Silvestri, V. Hirsch, Nonpathogenic simian immunodeficiency virus infections. *Cold Spring Harb Perspect Med* **2**, a007153 (2012).

22. B. F. Keele *et al.*, Chimpanzee reservoirs of pandemic and nonpandemic HIV-1. *Science* **313**, 523-526 (2006).

23. F. Van Heuverswyn *et al.*, Human immunodeficiency viruses: SIV infection in wild gorillas. *Nature* **444**, 164 (2006).

24. G. S. Gottlieb, D. N. Raugi, R. A. Smith, 90-90-90 for HIV-2? Ending the HIV-2 epidemic by enhancing care and clinical management of patients infected with HIV-2. *The Lancet HIV* **5**, e390-e399 (2018).

25. B. Visseaux, F. Damond, S. Matheron, D. Descamps, C. Charpentier, Hiv-2 molecular epidemiology. *Infect Genet Evol* **46**, 233-240 (2016).

26. M. Guyader *et al.*, Genome organization and transactivation of the human immunodeficiency virus type 2. *Nature* **326**, 662-669 (1987).

27. F. Clavel *et al.*, Isolation of a new human retrovirus from West African patients with AIDS. *Science* **233**, 343-346 (1986).

28. M. B. Gardner, The history of simian AIDS. *J Med Primatol* **25**, 148-157 (1996).

29. C. Apetrei *et al.*, Molecular epidemiology of simian immunodeficiency virus SIVsm in U.S. primate centers unravels the origin of SIVmac and SIVstm. *J Virol* **79**, 8991-9005 (2005).

30. C. Apetrei *et al.*, Kuru experiments triggered the emergence of pathogenic SIVmac. *AIDS* **20**, 317-321 (2006).

31. A. D. Frankel, J. A. Young, HIV-1: fifteen proteins and an RNA. *Annu Rev Biochem* **67**, 1-25 (1998).

32. K. A. R. a. M. Saifuddin, Regulation of HIV-1 Transcription.

33. R. Craigie, F. D. Bushman, HIV DNA integration. *Cold Spring Harb Perspect Med* **2**, a006890 (2012).

34. S. Mattei *et al.*, High-resolution structures of HIV-1 Gag cleavage mutants determine structural switch for virus maturation. *Proc Natl Acad Sci U S A* **115**, E9401-E9410 (2018).

35. W. S. Hu, S. H. Hughes, HIV-1 reverse transcription. *Cold Spring Harb Perspect Med* **2**, (2012).

36. R. Craigie, The molecular biology of HIV integrase. *Future Virol* **7**, 679-686 (2012).

37. Z. Lv, Y. Chu, Y. Wang, HIV protease inhibitors: a review of molecular selectivity and toxicity. *HIV AIDS (Auckl)* **7**, 95-104 (2015).

38. C. B. Wilen, J. C. Tilton, R. W. Doms, HIV: cell binding and entry. *Cold Spring Harb Perspect Med* **2**, (2012).

39. A. P. Rice, The HIV-1 Tat Protein: Mechanism of Action and Target for HIV-1 Cure Strategies. *Curr Pharm Des* **23**, 4098-4102 (2017).

40. J. R. Williamson, Really exasperating viral protein from HIV. *Elife* **4**, (2015).

41. M. H. Malim, M. Emerman, HIV-1 accessory proteins--ensuring viral survival in a hostile environment. *Cell Host Microbe* **3**, 388-398 (2008).

42. S. Sierra, B. Kupfer, R. Kaiser, Basics of the virology of HIV-1 and its replication. *J Clin Virol* **34**, 233-244 (2005).

43. M. E. Linde *et al.*, The conserved set of host proteins incorporated into HIV-1 virions suggests a common egress pathway in multiple cell types. *J Proteome Res* **12**, 2045-2054 (2013).

44. L. O. Arthur *et al.*, Cellular proteins bound to immunodeficiency viruses: implications for pathogenesis and vaccines. *Science* **258**, 1935-1938 (1992).

45. J. Benjamin, B. K. Ganser-Pornillos, W. F. Tivol, W. I. Sundquist, G. J. Jensen, Three-dimensional structure of HIV-1 virus-like particles by electron cryotomography. *J Mol Biol* **346**, 577-588 (2005).

46. J. A. Briggs *et al.*, The stoichiometry of Gag protein in HIV-1. *Nat Struct Mol Biol* **11**, 672-675 (2004).

47. J. G. Levin, M. Mitra, A. Mascarenhas, K. Musier-Forsyth, Role of HIV-1 nucleocapsid protein in HIV-1 reverse transcription. *RNA Biol* **7**, 754-774 (2010).

48. B. G. Turner, M. F. Summers, Structural biology of HIV. *J Mol Biol* **285**, 1-32 (1999).

49. M. Xie *et al.*, Cell-to-Cell Spreading of HIV-1 in Myeloid Target Cells Escapes SAMHD1 Restriction. *mBio* **10**, (2019).

50. A. Iwamoto, N. Hosoya, A. Kawana-Tachikawa, HIV-1 tropism. *Protein Cell* **1**, 510-513 (2010).

51. Z. Ambrose, C. Aiken, HIV-1 uncoating: connection to nuclear entry and regulation by host proteins. *Virology* **454-455**, 371-379 (2014).

52. B. Bowerman, P. O. Brown, J. M. Bishop, H. E. Varmus, A nucleoprotein complex mediates the integration of retroviral DNA. *Genes Dev* **3**, 469-478 (1989).

53. C. Van Lint, S. Bouchat, A. Marcello, HIV-1 transcription and latency: an update. *Retrovirology* **10**, 67 (2013).

54. J. Karn, C. M. Stoltzfus, Transcriptional and posttranscriptional regulation of HIV-1 gene expression. *Cold Spring Harb Perspect Med* **2**, a006916 (2012).

55. W. I. Sundquist, H. G. Krausslich, HIV-1 assembly, budding, and maturation. *Cold Spring Harb Perspect Med* **2**, a006924 (2012).

56. T. Murakami, Roles of the interactions between Env and Gag proteins in the HIV-1 replication cycle. *Microbiol Immunol* **52**, 287-295 (2008).

57. F. Hladik, M. J. McElrath, Setting the stage: host invasion by HIV. *Nat Rev Immunol* **8**, 447-457 (2008).

58. S. Moir, T. W. Chun, A. S. Fauci, Pathogenic mechanisms of HIV disease. *Annu Rev Pathol* **6**, 223-248 (2011).

59. A. T. Haase, Perils at mucosal front lines for HIV and SIV and their hosts. *Nat Rev Immunol* **5**, 783-792 (2005).

60. A. A. Lackner, M. M. Lederman, B. Rodriguez, HIV pathogenesis: the host. *Cold Spring Harb Perspect Med* **2**, a007005 (2012).

61. V. Simon, D. D. Ho, Q. Abdool Karim, HIV/AIDS epidemiology, pathogenesis, prevention, and treatment. *The Lancet* **368**, 489-504 (2006).

62. J. A. Levy, Pathogenesis of human immunodeficiency virus infection. *Microbiol Rev* **57**, 183-289 (1993).

63. J. J. Mattapallil *et al.*, Massive infection and loss of memory CD4+ T cells in multiple tissues during acute SIV infection. *Nature* **434**, 1093-1097 (2005).

64. J. Coffin, R. Swanstrom, HIV pathogenesis: dynamics and genetics of viral populations and infected cells. *Cold Spring Harb Perspect Med* **3**, a012526 (2013).

65. S. G. Deeks, B. D. Walker, Human immunodeficiency virus controllers: mechanisms of durable virus control in the absence of antiretroviral therapy. *Immunity* **27**, 406-416 (2007).

66. C. Lopez-Galindez, M. Pernas, C. Casado, I. Olivares, R. Lorenzo-Redondo, Elite controllers and lessons learned for HIV-1 cure. *Curr Opin Virol* **38**, 31-36 (2019).

67. K. A. O'Connell, J. R. Bailey, J. N. Blankson, Elucidating the elite: mechanisms of control in HIV-1 infection. *Trends Pharmacol Sci* **30**, 631-637 (2009).

68. K. G. Lassen *et al.*, Elite suppressor-derived HIV-1 envelope glycoproteins exhibit reduced entry efficiency and kinetics. *PLoS Pathog* **5**, e1000377 (2009).

69. A. K. Pau, J. M. George, Antiretroviral therapy: current drugs. *Infect Dis Clin North Am* **28**, 371-402 (2014).

70. S. Broder, The development of antiretroviral therapy and its impact on the HIV-1/AIDS pandemic. *Antiviral Res* **85**, 1-18 (2010).

71. W. Ostertag *et al.*, Induction of endogenous virus and of thymidine kinase by bromodeoxyuridine in cell cultures transformed by Friend virus. *Proc Natl Acad Sci U S A* **71**, 4980-4985 (1974).

72. H. Mitsuya *et al.*, 3'-Azido-3'-deoxythymidine (BW A509U): an antiviral agent that inhibits the infectivity and cytopathic effect of human T-lymphotropic virus type III/lymphadenopathy-associated virus in vitro. *Proc Natl Acad Sci U S A* **82**, 7096-7100 (1985).

73. D. Sarewitz, Better all the time. *Nature* **463**, 607 (2010).

74. C. Marwick, AZT (Zidovudine) Just a Step Away From FDA Approval for AIDS Therapy. *JAMA: The Journal of the American Medical Association* **257**, (1987).

75. F. J. Piacenti, An update and review of antiretroviral therapy. *Pharmacotherapy* **26**, 1111-1133 (2006).

76. M. A. Fischl *et al.*, The efficacy of azidothymidine (AZT) in the treatment of patients with AIDS and AIDS-related complex. A double-blind, placebo-controlled trial. *N Engl J Med* **317**, 185-191 (1987).

77. D. D. Richman *et al.*, The toxicity of azidothymidine (AZT) in the treatment of patients with AIDS and AIDS-related complex. A double-blind, placebo-controlled trial. *N Engl J Med* **317**, 192-197 (1987).

78. S. M. Hammer *et al.*, A trial comparing nucleoside monotherapy with combination therapy in HIV-infected adults with CD4 cell counts from 200 to 500 per cubic millimeter. AIDS Clinical Trials Group Study 175 Study Team. *N Engl J Med* **335**, 1081-1090 (1996).

79. S. Vella, B. Schwartlander, S. P. Sow, S. P. Eholie, R. L. Murphy, The history of antiretroviral therapy and of its implementation in resource-limited areas of the world. *AIDS* **26**, 1231-1241 (2012).

80. D. Warnke, J. Barreto, Z. Temesgen, Antiretroviral drugs. *J Clin Pharmacol* **47**, 1570-1579 (2007).

81. A. M. Wensing, N. M. van Maarseveen, M. Nijhuis, Fifteen years of HIV Protease Inhibitors: raising the barrier to resistance. *Antiviral Res* **85**, 59-74 (2010).

82. F. J. Palella, Jr. *et al.*, Declining morbidity and mortality among patients with advanced human immunodeficiency virus infection. HIV Outpatient Study Investigators. *N Engl J Med* **338**, 853-860 (1998).

83. R. Gulick, Investigational Antiretroviral Drugs: What is Coming Down the Pipeline. (2018).

84. E. J. Arts, D. J. Hazuda, HIV-1 antiretroviral drug therapy. *Cold Spring Harb Perspect Med* **2**, a007161 (2012).

85. T. Ndung'u, J. M. McCune, S. G. Deeks, Why and where an HIV cure is needed and how it might be achieved. *Nature* **576**, 397-405 (2019).

86. D. C. Hsu, R. J. O'Connell, Progress in HIV vaccine development. *Hum Vaccin Immunother* **13**, 1018-1030 (2017).

87. S. Rerks-Ngarm *et al.*, Vaccination with ALVAC and AIDSVAX to prevent HIV-1 infection in Thailand. *N Engl J Med* **361**, 2209-2220 (2009).

88. H. T. Pham, T. Mesplede, The latest evidence for possible HIV-1 curative strategies. *Drugs Context* **7**, 212522 (2018).

89. Y. Kim, J. L. Anderson, S. R. Lewin, Getting the "Kill" into "Shock and Kill": Strategies to Eliminate Latent HIV. *Cell Host Microbe* **23**, 14-26 (2018).

90. T. A. Rasmussen *et al.*, Panobinostat, a histone deacetylase inhibitor, for latent-virus reactivation in HIV-infected patients on suppressive antiretroviral therapy: a phase 1/2, single group, clinical trial. *The Lancet HIV* **1**, e13-e21 (2014).

91. N. M. Archin *et al.*, Administration of vorinostat disrupts HIV-1 latency in patients on antiretroviral therapy. *Nature* **487**, 482-485 (2012).

92. O. S. Sogaard *et al.*, The Depsipeptide Romidepsin Reverses HIV-1 Latency In Vivo. *PLoS Pathog* **11**, e1005142 (2015).

93. E. Abner, A. Jordan, HIV "shock and kill" therapy: In need of revision. *Antiviral Res* **166**, 19-34 (2019).

94. N. Ahmad, S. Venkatesan, Nef protein of HIV-1 is a transcriptional repressor of HIV-1 LTR. *Science* **241**, 1481-1485 (1988).

95. D. I. Rhodes *et al.*, Characterization of three nef-defective human immunodeficiency virus type 1 strains associated with long-term nonprogression. Australian Long-Term Nonprogressor Study Group. *J Virol* **74**, 10581-10588 (2000).

96. F. Kirchhoff, T. C. Greenough, D. B. Brettler, J. L. Sullivan, R. C. Desrosiers, Brief report: absence of intact nef sequences in a long-term survivor with nonprogressive HIV-1 infection. *N Engl J Med* **332**, 228-232 (1995).

97. H. W. Kestler, 3rd *et al.*, Importance of the nef gene for maintenance of high virus loads and for development of AIDS. *Cell* **65**, 651-662 (1991).

98. Z. Hanna *et al.*, Transgenic mice expressing human immunodeficiency virus type 1 in immune cells develop a severe AIDS-like disease. *J Virol* **72**, 121-132 (1998).

99. M. Geyer, C. E. Munte, J. Schorr, R. Kellner, H. R. Kalbitzer, Structure of the anchor-domain of myristoylated and non-myristoylated HIV-1 Nef protein. *J Mol Biol* **289**, 123-138 (1999).

100. M. Geyer, B. M. Peterlin, Domain assembly, surface accessibility and sequence conservation in full length HIV-1 Nef. *FEBS Letters* **496**, 91-95 (2001).

101. X. Jia *et al.*, Structural basis of evasion of cellular adaptive immunity by HIV-1 Nef. *Nat Struct Mol Biol* **19**, 701-706 (2012).

102. J. Vermeire, G. Vanbillemont, W. Witkowski, B. Verhasselt, The Nef-infectivity enigma: mechanisms of enhanced lentiviral infection. *Curr HIV Res* **9**, 474-489 (2011).

103. J. Kimpton, M. Emerman, Detection of replication-competent and pseudotyped human immunodeficiency virus with a sensitive cell line on the basis of activation of an integrated beta-galactosidase gene. *J Virol* **66**, 2232-2239 (1992).

104. X. Wei *et al.*, Emergence of resistant human immunodeficiency virus type 1 in patients receiving fusion inhibitor (T-20) monotherapy. *Antimicrob Agents Chemother* **46**, 1896-1905 (2002).

105. M. Y. Chowers *et al.*, Optimal infectivity in vitro of human immunodeficiency virus type 1 requires an intact nef gene. *J Virol* **68**, 2906-2914 (1994).

106. S. Basmaciogullari, M. Pizzato, The activity of Nef on HIV-1 infectivity. *Front Microbiol* **5**, 232 (2014).

107. M. Pizzato, MLV glycosylated-Gag is an infectivity factor that rescues Nef-deficient HIV-1. *Proc Natl Acad Sci U S A* **107**, 9364-9369 (2010).

108. J. Munch *et al.*, Nef-mediated enhancement of virion infectivity and stimulation of viral replication are fundamental properties of primate lentiviruses. *J Virol* **81**, 13852-13864 (2007).

109. S. Jager *et al.*, Global landscape of HIV-human protein complexes. *Nature* **481**, 365-370 (2011).

110. S. Jager *et al.*, Global landscape of HIV-human protein complexes. *Nature* **481**, 365-370 (2012).

111. R. Chaudhuri, O. W. Lindwasser, W. J. Smith, J. H. Hurley, J. S. Bonifacino, Downregulation of CD4 by human immunodeficiency virus type 1 Nef is dependent on clathrin and involves direct interaction of Nef with the AP2 clathrin adaptor. *J Virol* **81**, 3877-3890 (2007).

112. R. D. Sloan, D. A. Donahue, B. D. Kuhl, T. Bar-Magen, M. A. Wainberg, Expression of Nef from unintegrated HIV-1 DNA downregulates cell surface CXCR4 and CCR5 on T-lymphocytes. *Retrovirology* **7**, 44 (2010).

113. E. N. Pawlak, B. S. Dirk, R. A. Jacob, A. L. Johnson, J. D. Dikeakos, The HIV-1 accessory proteins Nef and Vpu downregulate total and cell surface CD28 in CD4(+) T cells. *Retrovirology* **15**, 6 (2018).

114. P. Stumptner-Cuvelette *et al.*, HIV-1 Nef impairs MHC class II antigen presentation and surface expression. *Proc Natl Acad Sci U S A* **98**, 12144-12149 (2001).

115. E. Shinya *et al.*, Endogenously expressed HIV-1 nef down-regulates antigen-presenting molecules, not only class I MHC but also CD1a, in immature dendritic cells. *Virology* **326**, 79-89 (2004).

116. A. Chaudhry *et al.*, The Nef protein of HIV-1 induces loss of cell surface costimulatory molecules CD80 and CD86 in APCs. *J Immunol* **175**, 4566-4574 (2005).

117. A. Rosa *et al.*, HIV-1 Nef promotes infection by excluding SERINC5 from virion incorporation. *Nature* **526**, 212-217 (2015).

118. J. F. Arias *et al.*, Tetherin Antagonism by HIV-1 Group M Nef Proteins. *J Virol* **90**, 10701-10714 (2016).

119. N. Sol-Foulon *et al.*, HIV-1 Nef-Induced Upregulation of DC-SIGN in Dendritic Cells Promotes Lymphocyte Clustering and Viral Spread. *Immunity* **16**, 145-155 (2002).

120. R. Mariani, J. Skowronski, CD4 down-regulation by nef alleles isolated from human immunodeficiency virus type 1-infected individuals. *Proc Natl Acad Sci U S A* **90**, 5549-5553 (1993).

121. J. Lama, The physiological relevance of CD4 receptor down-modulation during HIV infection. *Curr HIV Res* **1**, 167-184 (2003).

122. T. N. Pham, S. Lukhele, F. Hajjar, J. P. Routy, E. A. Cohen, HIV Nef and Vpu protect HIV-infected CD4+ T cells from antibody-mediated cell lysis through down-modulation of CD4 and BST2. *Retrovirology* **11**, 15 (2014).

123. C. Pitcher, S. Honing, A. Fingerhut, K. Bowers, M. Marsh, Cluster of differentiation antigen 4 (CD4) endocytosis and adaptor complex binding require activation of the CD4 endocytosis signal by serine phosphorylation. *Mol Biol Cell* **10**, 677-691 (1999).

124. A. Preusser, L. Briese, A. S. Baur, D. Willbold, Direct in vitro binding of full-length human immunodeficiency virus type 1 Nef protein to CD4 cytoplasmic domain. *J Virol* **75**, 3960-3964 (2001).

125. J. V. Garcia, A. D. Miller, Serine phosphorylation-independent downregulation of cell-surface CD4 by nef. *Nature* **350**, 508-511 (1991).

126. J. Binette *et al.*, Requirements for the selective degradation of CD4 receptor molecules by the human immunodeficiency virus type 1 Vpu protein in the endoplasmic reticulum. *Retrovirology* **4**, 75 (2007).

127. A. P. Ambagala, J. C. Solheim, S. Srikumaran, Viral interference with MHC class I antigen presentation pathway: the battle continues. *Vet Immunol Immunopathol* **107**, 1-15 (2005).

128. T. H. Hansen, M. Bouvier, MHC class I antigen presentation: learning from viral evasion strategies. *Nat Rev Immunol* **9**, 503-513 (2009).

129. G. B. Cohen *et al.*, The Selective Downregulation of Class I Major Histocompatibility Complex Proteins by HIV-1 Protects HIV-Infected Cells from NK Cells. *Immunity* **10**, 661-671 (1999).

130. E. N. Pawlak, J. D. Dikeakos, HIV-1 Nef: a master manipulator of the membrane trafficking machinery mediating immune evasion. *Biochim Biophys Acta* **1850**, 733-741 (2015).

131. E. A. Pereira, L. L. daSilva, HIV-1 Nef: taking control of protein trafficking. *Traffic*, (2016).

132. Q. T. Shen, X. Ren, R. Zhang, I. H. Lee, J. H. Hurley, HIV-1 Nef hijacks clathrin coats by stabilizing AP-1:Arf1 polygons. *Science* **350**, aac5137 (2015).

133. M. R. Schaefer, E. R. Wonderlich, J. F. Roeth, J. A. Leonard, K. L. Collins, HIV-1 Nef targets MHC-I and CD4 for degradation via a final common beta-COP-dependent pathway in T cells. *PLoS Pathog* **4**, e1000131 (2008).

134. L. J. Costa *et al.*, Interactions between Nef and AIP1 proliferate multivesicular bodies and facilitate egress of HIV-1. *Retrovirology* **3**, 33 (2006).

135. C. Z. Buffalo, Y. Iwamoto, J. H. Hurley, X. Ren, How HIV Nef Proteins Hijack Membrane Traffic To Promote Infection. *J Virol* **93**, (2019).

136. T. Linnemann, Y. H. Zheng, R. Mandic, B. M. Peterlin, Interaction between Nef and phosphatidylinositol-3-kinase leads to activation of p21-activated kinase and increased production of HIV. *Virology* **294**, 246-255 (2002).

137. R. A. Jacob *et al.*, The interaction between HIV-1 Nef and adaptor protein-2 reduces Nef-mediated CD4+ T cell apoptosis. *Virology* **509**, 1-10 (2017).

138. C. H. Lee *et al.*, A single amino acid in the SH3 domain of Hck determines its high affinity and specificity in binding to HIV-1 Nef protein. *EMBO J* **14**, 5006-5015 (1995).

139. R. P. Trible, L. Emert-Sedlak, T. E. Smithgall, HIV-1 Nef selectively activates Src family kinases Hck, Lyn, and c-Src through direct SH3 domain interaction. *J Biol Chem* **281**, 27029-27038 (2006).

140. S. D. Briggs, M. Sharkey, M. Stevenson, T. E. Smithgall, SH3-mediated Hck tyrosine kinase activation and fibroblast transformation by the Nef protein of HIV-1. *J Biol Chem* **272**, 17899-17902 (1997).

141. I. Moarefi *et al.*, Activation of the Src-family tyrosine kinase Hck by SH3 domain displacement. *Nature* **385**, 650-653 (1997).

142. P. S. Narute, T. E. Smithgall, Nef alleles from all major HIV-1 clades activate Src-family kinases and enhance HIV-1 replication in an inhibitor-sensitive manner. *PLoS One* **7**, e32561 (2012).

143. I. Komuro, Y. Yokota, S. Yasuda, A. Iwamoto, K. S. Kagawa, CSF-induced and HIV-1-mediated distinct regulation of Hck and C/EBPbeta represent a heterogeneous susceptibility of monocyte-derived macrophages to M-tropic HIV-1 infection. *J Exp Med* **198**, 443-453 (2003).

144. Y. Collette *et al.*, Physical and functional interaction of Nef with Lck. HIV-1 Nef-induced T-cell signaling defects. *J Biol Chem* **271**, 6333-6341 (1996).

145. S. D. Briggs, E. C. Lerner, T. E. Smithgall, Affinity of Src family kinase SH3 domains for HIV Nef in vitro does not predict kinase activation by Nef in vivo. *Biochemistry* **39**, 489-495 (2000).

146. A. H. Andreotti, P. L. Schwartzberg, R. E. Joseph, L. J. Berg, T-cell signaling regulated by the Tec family kinase, Itk. *Cold Spring Harb Perspect Biol* **2**, a002287 (2010).

147. J. A. Readinger *et al.*, Selective targeting of ITK blocks multiple steps of HIV replication. *Proc Natl Acad Sci U S A* **105**, 6684-6689 (2008).

148. S. Tarafdar, J. A. Poe, T. E. Smithgall, The accessory factor Nef links HIV-1 to Tec/Btk kinases in an Src homology 3 domain-dependent manner. *J Biol Chem* **289**, 15718-15728 (2014).

149. W. F. Li, M. Aryal, S. T. Shu, T. E. Smithgall, HIV-1 Nef dimers short-circuit immune receptor signaling by activating Tec-family kinases at the host cell membrane. *J Biol Chem* **295**, 5163-5174 (2020).

150. S. J. Parsons, J. T. Parsons, Src family kinases, key regulators of signal transduction. *Oncogene* **23**, 7906-7909 (2004).

151. S. M. Thomas, J. S. Brugge, Cellular functions regulated by Src family kinases. *Annu Rev Cell Dev Biol* **13**, 513-609 (1997).

152. K. Saksela, Interactions of the HIV/SIV pathogenicity factor Nef with SH3 domain-containing host cell proteins. *Curr HIV Res* **9**, 531-542 (2011).

153. N. Kurochkina, U. Guha, SH3 domains: modules of protein-protein interactions. *Biophys Rev* **5**, 29-39 (2013).

154. B. J. Mayer, SH3 domains: complexity in moderation. *J Cell Sci* **114**, 1253-1263 (2001).

155. G. Waksman *et al.*, Crystal structure of the phosphotyrosine recognition domain SH2 of v-src complexed with tyrosine-phosphorylated peptides. *Nature* **358**, 646-653 (1992).

156. T. J. Boggon, M. J. Eck, Structure and regulation of Src family kinases. *Oncogene* **23**, 7918-7927 (2004).

157. K. Shen *et al.*, The Src family kinase Fgr is a transforming oncoprotein that functions independently of SH3-SH2 domain regulation. *Sci Signal* **11**, (2018).

158. F. Sicheri, J. Kuriyan, Structures of Src-family tyrosine kinases. *Current Opinion in Structural Biology* **7**, 777-785 (1997).

159. J. A. Cooper, B. Howell, The when and how of Src regulation. *Cell* **73**, 1051-1054 (1993).

160. G. M. Beacham, E. A. Partlow, G. Hollopeter, Conformational regulation of AP1 and AP2 clathrin adaptor complexes. *Traffic* **20**, 741-751 (2019).

161. T. Kirchhausen, D. Owen, S. C. Harrison, Molecular structure, function, and dynamics of clathrin-mediated membrane traffic. *Cold Spring Harb Perspect Biol* **6**, a016725 (2014).

162. J. E. Paczkowski, B. C. Richardson, J. C. Fromme, Cargo adaptors: structures illuminate mechanisms regulating vesicle biogenesis. *Trends Cell Biol* **25**, 408-416 (2015).

163. Y. J. Wang *et al.*, Phosphatidylinositol 4 Phosphate Regulates Targeting of Clathrin Adaptor AP-1 Complexes to the Golgi. *Cell* **114**, 299-310 (2003).

164. D. Padron, Y. J. Wang, M. Yamamoto, H. Yin, M. G. Roth, Phosphatidylinositol phosphate 5-kinase Ibeta recruits AP-2 to the plasma membrane and regulates rates of constitutive endocytosis. *J Cell Biol* **162**, 693-701 (2003).

165. J. S. Bonifacino, L. M. Traub, Signals for sorting of transmembrane proteins to endosomes and lysosomes. *Annu Rev Biochem* **72**, 395-447 (2003).

166. F. Nakatsu, K. Hase, H. Ohno, The Role of the Clathrin Adaptor AP-1: Polarized Sorting and Beyond. *Membranes (Basel)* **4**, 747-763 (2014).

167. B. T. Kelly *et al.*, A structural explanation for the binding of endocytic dileucine motifs by the AP2 complex. *Nature* **456**, 976-979 (2008).

168. X. Jia *et al.*, Structural basis of HIV-1 Vpu-mediated BST2 antagonism via hijacking of the clathrin adaptor protein complex 1. *Elife* **3**, e02362 (2014).

169. B. M. Collins, A. J. McCoy, H. M. Kent, P. R. Evans, D. J. Owen, Molecular Architecture and Functional Model of the Endocytic AP2 Complex. *Cell* **109**, 523-535 (2002).

170. L. P. Jackson *et al.*, A large-scale conformational change couples membrane recruitment to cargo binding in the AP2 clathrin adaptor complex. *Cell* **141**, 1220-1229 (2010).

171. X. Ren, G. G. Farias, B. J. Canagarajah, J. S. Bonifacino, J. H. Hurley, Structural basis for recruitment and activation of the AP-1 clathrin adaptor complex by Arf1. *Cell* **152**, 755-767 (2013).

172. R. W. Sweet, A. Truneh, W. A. Hendrickson, CD4: Its structure, role in immune function and AIDS pathogenesis, and potential as a pharmacological target. *Current Opinion in Biotechnology* **2**, 622-633 (1991).

173. E. L. P. C. K. Reinherz, P.C.; Goldstein, G. ;Schlossman, S.F., Further Characterization of the Human Inducer T Cell Subset Defined by Monoclonal Antibody. *Journal of Immunology* **123**, 2894-2896 (1979).

174. D. Klatzmann *et al.*, T-lymphocyte T4 molecule behaves as the receptor for human retrovirus LAV. *Nature* **312**, 767-768 (1984).

175. K. Bowers, C. Pitcher, M. Marsh, CD4: A co-receptor in the immune response and HIV infection. *The International Journal of Biochemistry & Cell Biology* **29**, 871-875 (1997).

176. D. Glatzova, M. Cebecauer, Dual Role of CD4 in Peripheral T Lymphocytes. *Front Immunol* **10**, 618 (2019).

177. Q. J. Li *et al.*, CD4 enhances T cell sensitivity to antigen by coordinating Lck accumulation at the immunological synapse. *Nat Immunol* **5**, 791-799 (2004).

178. M. Wieczorek *et al.*, Major Histocompatibility Complex (MHC) Class I and MHC Class II Proteins: Conformational Plasticity in Antigen Presentation. *Front Immunol* **8**, 292 (2017).

179. E. A. Reits, J. C. Vos, M. Gromme, J. Neefjes, The major substrates for TAP in vivo are derived from newly synthesized proteins. *Nature* **404**, 774-778 (2000).

180. E. W. Hewitt, The MHC class I antigen presentation pathway: strategies for viral immune evasion. *Immunology* **110**, 163-169 (2003).

181. J. L. Petersen, C. R. Morris, J. C. Solheim, Virus evasion of MHC class I molecule presentation. *J Immunol* **171**, 4473-4478 (2003).

182. F. Garrido, N. Aptsiauri, E. M. Doorduijn, A. M. Garcia Lora, T. van Hall, The urgent need to recover MHC class I in cancers for effective immunotherapy. *Curr Opin Immunol* **39**, 44-51 (2016).

183. E. Y. Jones, MHC class I and class II structures. *Current Opinion in Immunology* **9**, 75-79 (1997).

184. M. T. Ferm, A. Gronberg, Human MHC class I antigens are associated with a 90-kDa cell surface protein. *Scand J Immunol* **34**, 221-227 (1991).

185. A. Halenius, C. Gerke, H. Hengel, Classical and non-classical MHC I molecule manipulation by human cytomegalovirus: so many targets-but how many arrows in the quiver? *Cell Mol Immunol* **12**, 139-153 (2015).

186. C. A. O'Callaghan, J. I. Bell, Structure and function of the human MHC class Ib molecules HLA-E, HLA-F and HLA-G. *Immunol Rev* **163**, 129-138 (1998).

187. F. Morandi, E. Fainardi, R. Rizzo, N. Rouas-Freiss, The role of HLA-class Ib molecules in immune-related diseases, tumors, and infections. *J Immunol Res* **2014**, 231618 (2014).

188. T. van Stigt Thans *et al.*, Primary HIV-1 Strains Use Nef To Downmodulate HLA-E Surface Expression. *J Virol* **93**, (2019).

189. M. Bentham, S. Mazaleyrat, M. Harris, Role of myristoylation and N-terminal basic residues in membrane association of the human immunodeficiency virus type 1 Nef protein. *J Gen Virol* **87**, 563-571 (2006).

190. B. Akgun *et al.*, Conformational transition of membrane-associated terminally acylated HIV-1 Nef. *Structure* **21**, 1822-1833 (2013).

191. G. M. Aldrovandi, L. Gao, G. Bristol, J. A. Zack, Regions of human immunodeficiency virus type 1 nef required for function in vivo. *J Virol* **72**, 7032-7039 (1998).

192. O. T. Fackler *et al.*, Association of human immunodeficiency virus Nef protein with actin is myristoylation dependent and influences its subcellular localization. *Eur J Biochem* **247**, 843-851 (1997).

193. M. Harris, The role of myristoylation in the interactions between human immunodeficiency virus type I Nef and cellular proteins. *Biochem Soc Trans* **23**, 557-561 (1995).

194. A. J. Chase, R. Wombacher, O. T. Fackler, Intrinsic properties and plasma membrane trafficking route of Src family kinase SH4 domains sensitive to retargeting by HIV-1 Nef. *J Biol Chem* **293**, 7824-7840 (2018).

195. H. Gerlach *et al.*, HIV-1 Nef membrane association depends on charge, curvature, composition and sequence. *Nat Chem Biol* **6**, 46-53 (2010).

196. S. T. Arold, A. S. Bauer, Dynamic Nef and Nef dynamics: how structure could explain the complex activities of this small HIV protein. *Trends in Biochemical Sciences* **26**, 356-363 (2001).

197. S. Arold *et al.*, Characterization and molecular basis of the oligomeric structure of HIV-1 nef protein. *Protein Sci* **9**, 1137-1148 (2000).

198. G. F. Pirrone *et al.*, Membrane-Associated Conformation of HIV-1 Nef Investigated with Hydrogen Exchange Mass Spectrometry at a Langmuir Monolayer. *Anal Chem* **87**, 7030-7035 (2015).

199. A. Mangasarian, V. Piguet, J. K. Wang, Y. L. Chen, D. Trono, Nef-induced CD4 and major histocompatibility complex class I (MHC-I) down-regulation are governed by distinct determinants: N-terminal alpha helix and proline repeat of Nef selectively regulate MHC-I trafficking. *J Virol* **73**, 1964-1973 (1999).

200. Z. Hanna *et al.*, The pathogenicity of human immunodeficiency virus (HIV) type 1 Nef in CD4C/HIV transgenic mice is abolished by mutation of its SH3-binding domain, and disease development is delayed in the absence of Hck. *J Virol* **75**, 9378-9392 (2001).

201. I. H. Khan *et al.*, Role of the SH3-ligand domain of simian immunodeficiency virus Nef in interaction with Nef-associated kinase and simian AIDS in rhesus macaques. *J Virol* **72**, 5820-5830 (1998).

202. M. Geyer, O. T. Fackler, B. M. Peterlin, Structure--function relationships in HIV-1 Nef. *EMBO Rep* **2**, 580-585 (2001).

203. C.-H. Lee, K. Saksela, U. A. Mirza, B. T. Chait, J. Kuriyan, Crystal Structure of the Conserved Core of HIV-1 Nef Complexed with a Src Family SH3 Domain. *Cell* **85**, 931-942 (1996).

204. J. L. Foster, S. J. Denial, B. R. Temple, J. V. Garcia, Mechanisms of HIV-1 Nef function and intracellular signaling. *J Neuroimmune Pharmacol* **6**, 230-246 (2011).

205. S. Arold *et al.*, RT loop flexibility enhances the specificity of Src family SH3 domains for HIV-1 Nef. *Biochemistry* **37**, 14683-14691 (1998).

206. S. K. Lee CH, Mirza UA, Chait BT, Kuriyan J., Crystal Structure of the Conserved Core of HIV-1 Nef Complexed with a Src Family SH3 Domain. *Cell* **85**, 931-942 (1996).

207. S. Arold *et al.*, The crystal structure of HIV-1 Nef protein bound to the Fyn kinase SH3 domain suggests a role for this complex in altered T cell receptor signaling. *Structure* **5**, 1361-1372 (1997).

208. M. Hiipakka, K. Poikonen, K. Saksela, SH3 domains with high affinity and engineered ligand specificities targeted to HIV-1 Nef. *J Mol Biol* **293**, 1097-1106 (1999).

209. O. T. Fackler *et al.*, A natural variability in the proline-rich motif of Nef modulates HIV-1 replication in primary T cells. *Current Biology* **11**, 1294-1299 (2001).

210. E. Priceputu *et al.*, Primary human immunodeficiency virus type 1 nef alleles show major differences in pathogenicity in transgenic mice. *J Virol* **81**, 4677-4693 (2007).

211. K. C. Saksela, G.; Baltimore, D., Proline-rich (PxxP) motifs in HIV-1 Nef bind to SH3 domains of a subset of Src kinases and are required for the enhanced growth of Nef+ viruses but not for down-regulation of CD4. *EMBO J* **14**, 484-491 (1995).

212. J. J. Alvarado, S. Tarafdar, J. I. Yeh, T. E. Smithgall, Interaction with the Src homology (SH3-SH2) region of the Src-family kinase Hck structures the HIV-1 Nef dimer for kinase activation and effector recruitment. *J Biol Chem* **289**, 28539-28553 (2014).

213. S. Breuer *et al.*, Molecular design, functional characterization and structural basis of a protein inhibitor against the HIV-1 pathogenicity factor Nef. *PLoS One* **6**, e20033 (2011).

214. S. Lulf *et al.*, Structural basis for the inhibition of HIV-1 Nef by a high-affinity binding single-domain antibody. *Retrovirology* **11**, 24 (2014).

215. F. A. Horenkamp *et al.*, Conformation of the dileucine-based sorting motif in HIV-1 Nef revealed by intermolecular domain assembly. *Traffic* **12**, 867-877 (2011).

216. J. R. Engen *et al.*, Structure and dynamic regulation of Src-family kinases. *Cell Mol Life Sci* **65**, 3058-3073 (2008).

217. S. R. Marcsisin, J. R. Engen, Hydrogen exchange mass spectrometry: what is it and what can it tell us? *Anal Bioanal Chem* **397**, 967-972 (2010).

218. T. E. Wales *et al.*, Subtle Dynamic Changes Accompany Hck Activation by HIV-1 Nef and are Reversed by an Antiretroviral Kinase Inhibitor. *Biochemistry* **54**, 6382-6391 (2015).

219. E. C. Lerner, T. E. Smithgall, SH3-dependent stimulation of Src-family kinase autophosphorylation without tail release from the SH2 domain in vivo. *Nat Struct Biol* **9**, 365-369 (2002).

220. J. Jung, I. J. Byeon, J. Ahn, A. M. Gronenborn, Structure, dynamics, and Hck interaction of full-length HIV-1 Nef. *Proteins* **79**, 1609-1622 (2011).

221. T. E. Wales *et al.*, Hydrogen Exchange Mass Spectrometry of Related Proteins with Divergent Sequences: A Comparative Study of HIV-1 Nef Allelic Variants. *J Am Soc Mass Spectrom* **27**, 1048-1061 (2016).

222. X. Ren, S. Y. Park, J. S. Bonifacino, J. H. Hurley, How HIV-1 Nef hijacks the AP-2 clathrin adaptor to downregulate CD4. *Elife* **3**, e01754 (2014).

223. R. Chaudhuri, R. Mattera, O. W. Lindwasser, M. S. Robinson, J. S. Bonifacino, A basic patch on alpha-adaptin is required for binding of human immunodeficiency virus type 1 Nef and cooperative assembly of a CD4-Nef-AP-2 complex. *J Virol* **83**, 2518-2530 (2009).

224. S. Grzesiek, S. J. Stahl, P. T. Wingfield, A. Bax, The CD4 determinant for downregulation by HIV-1 Nef directly binds to Nef. Mapping of the Nef binding surface by NMR. *Biochemistry* **35**, 10256-10261 (1996).

225. O. W. Lindwasser *et al.*, A diacidic motif in human immunodeficiency virus type 1 Nef is a novel determinant of binding to AP-2. *J Virol* **82**, 1166-1174 (2008).

226. S. Manrique *et al.*, Endocytic sorting motif interactions involved in Nef-mediated downmodulation of CD4 and CD3. *Nat Commun* **8**, 442 (2017).

227. M. Wittlich, P. Thiagarajan, B. W. Koenig, R. Hartmann, D. Willbold, NMR structure of the transmembrane and cytoplasmic domains of human CD4 in micelles. *Biochim Biophys Acta* **1798**, 122-127 (2010).

228. R. Serra-Moreno, K. Zimmermann, L. J. Stern, D. T. Evans, Tetherin/BST-2 antagonism by Nef depends on a direct physical interaction between Nef and tetherin, and on clathrin-mediated endocytosis. *PLoS Pathog* **9**, e1003487 (2013).

229. S. Venkatesh, P. D. Bieniasz, Mechanism of HIV-1 virion entrapment by tetherin. *PLoS Pathog* **9**, e1003483 (2013).

230. S. F. Kluge *et al.*, Nef proteins of epidemic HIV-1 group O strains antagonize human tetherin. *Cell Host Microbe* **16**, 639-650 (2014).

231. C. Z. Buffalo *et al.*, Structural Basis for Tetherin Antagonism as a Barrier to Zoonotic Lentiviral Transmission. *Cell Host Microbe* **26**, 359-368 e358 (2019).

232. T. Swigut, N. Shohdy, J. Skowronski, Mechanism for down-regulation of CD28 by Nef. *EMBO J* **20**, 1593-1604 (2001).

233. V. Stove *et al.*, Human immunodeficiency virus Nef induces rapid internalization of the T-cell coreceptor CD8alphabeta. *J Virol* **79**, 11422-11433 (2005).

234. A. Heigele *et al.*, Down-modulation of CD8alphabeta is a fundamental activity of primate lentiviral Nef proteins. *J Virol* **86**, 36-48 (2012).

235. N. Kienzle, J. Freund, H. R. Kalbitzer, N. Mueller-Lantzsch, Oligomerization of the Nef protein from human immunodeficiency virus (HIV) type 1. *Eur J Biochem* **214**, 451-457 (1993).

236. A. A. Azad *et al.*, Large-scale production and characterization of recombinant human immunodeficiency virus type 1 Nef. *J Gen Virol* **75 (Pt 3)**, 651-655 (1994).

237. S. Grzesiek *et al.*, The solution structure of HIV-1 Nef reveals an unexpected fold and permits delineation of the binding surface for the SH3 domain of Hck tyrosine protein kinase. *Nat Struct Biol* **3**, 340-345 (1996).

238. Y. Fujii *et al.*, Clustered localization of oligomeric Nef protein of human immunodeficiency virus type 1 on the cell surface. *FEBS Letters* **395**, 257-261 (1996).

239. J. A. Poe, T. E. Smithgall, HIV-1 Nef dimerization is required for Nef-mediated receptor downregulation and viral replication. *J Mol Biol* **394**, 329-342 (2009).

240. H. H. Ye, H. J. Choi, J. Poe, T. E. Smithgall, Oligomerization is required for HIV-1 nef-induced activation of the Src family protein-tyrosine kinase, Hck. *Biochemistry* **43**, 15775-15784 (2004).

241. S. T. Shu, L. A. Emert-Sedlak, T. E. Smithgall, Cell-based Fluorescence Complementation Reveals a Role for HIV-1 Nef Protein Dimerization in AP-2 Adaptor Recruitment and CD4 Co-receptor Down-regulation. *J Biol Chem* **292**, 2670-2678 (2017).

242. L. X. Liu *et al.*, Mutation of a conserved residue (D123) required for oligomerization of human immunodeficiency virus type 1 Nef protein abolishes interaction with human thioesterase and results in impairment of Nef biological functions. *J Virol* **74**, 5310-5319 (2000).

243. M. Wu, J. J. Alvarado, C. E. Augelli-Szafran, R. G. Ptak, T. E. Smithgall, A single beta-octyl glucoside molecule induces HIV-1 Nef dimer formation in the absence of partner protein binding. *PLoS One* **13**, e0192512 (2018).

244. J. A. Moroco *et al.*, Remodeling of HIV-1 Nef Structure by Src-Family Kinase Binding. *J Mol Biol* **430**, 310-321 (2018).

245. Y. T. Kwak *et al.*, Self-association of the Lentivirus protein, Nef. *Retrovirology* **7**, 77 (2010).

246. S. Betzi *et al.*, Protein protein interaction inhibition (2P2I) combining high throughput and virtual screening: Application to the HIV-1 Nef protein. *Proc Natl Acad Sci U S A* **104**, 19256-19261 (2007).

247. C. Oneyama, H. Nakano, S. V. Sharma, UCS15A, a novel small molecule, SH3 domain-mediated protein-protein interaction blocking drug. *Oncogene* **21**, 2037-2050 (2002).

248. M. Hiipakka, P. Huotari, A. Manninen, G. H. Renkema, K. Saksela, Inhibition of cellular functions of HIV-1 Nef by artificial SH3 domains. *Virology* **286**, 152-159 (2001).

249. J. Bouchet *et al.*, Single-domain antibody-SH3 fusions for efficient neutralization of HIV-1 Nef functions. *J Virol* **86**, 4856-4867 (2012).

250. T. E. Smithgall, G. Thomas, Small molecule inhibitors of the HIV-1 virulence factor, Nef. *Drug Discov Today Technol* **10**, e523-529 (2013).

251. L. Emert-Sedlak *et al.*, Chemical library screens targeting an HIV-1 accessory factor/host cell kinase complex identify novel antiretroviral compounds. *ACS Chem Biol* **4**, 939-947 (2009).

252. L. A. Emert-Sedlak *et al.*, Effector kinase coupling enables high-throughput screens for direct HIV-1 Nef antagonists with antiretroviral activity. *Chem Biol* **20**, 82-91 (2013).

253. H. Shi *et al.*, Tight-Binding Hydroxypyrazole HIV-1 Nef Inhibitors Suppress Viral Replication in Donor Mononuclear Cells and Reverse Nef-Mediated MHC-I Downregulation. *ACS Infect Dis* **6**, 302-312 (2020).

254. S. Mujib *et al.*, Pharmacologic HIV-1 Nef blockade promotes CD8 T cell-mediated elimination of latently HIV-1-infected cells in vitro. *JCI Insight* **2**, (2017).

255. C. Aiken, D. Trono, Nef stimulates human immunodeficiency virus type 1 proviral DNA synthesis. *J Virol* **69**, 5048-5056 (1995).

256. Y. Usami, Y. Wu, H. G. Gottlinger, SERINC3 and SERINC5 restrict HIV-1 infectivity and are counteracted by Nef. *Nature* **526**, 218-223 (2015).

257. C. Aiken, HIV: Antiviral action countered by Nef. *Nature* **526**, 202-203 (2015).

258. B. Schulte *et al.*, Localization to detergent-resistant membranes and HIV-1 core entry inhibition correlate with HIV-1 restriction by SERINC5. *Virology* **515**, 52-65 (2018).

259. C. Firrito, C. Bertelli, T. Vanzo, A. Chande, M. Pizzato, SERINC5 as a New Restriction Factor for Human Immunodeficiency Virus and Murine Leukemia Virus. *Annu Rev Virol* **5**, 323-340 (2018).

260. M. Inuzuka, M. Hayakawa, T. Ingi, Serinc, an activity-regulated protein family, incorporates serine into membrane lipid synthesis. *J Biol Chem* **280**, 35776-35783 (2005).

261. B. Trautz *et al.*, The host-cell restriction factor SERINC5 restricts HIV-1 infectivity without altering the lipid composition and organization of viral particles. *J Biol Chem* **292**, 13702-13713 (2017).

262. E. P. Chu *et al.*, Disruption of Serinc1, which facilitates serine-derived lipid synthesis, fails to alter macrophage function, lymphocyte proliferation or autoimmune disease susceptibility. *Mol Immunol* **82**, 19-33 (2017).

263. V. E. Pye *et al.*, A bipartite structural organization defines the SERINC family of HIV-1 restriction factors. *Nat Struct Mol Biol* **27**, 78-83 (2020).

264. P. W. Ramirez *et al.*, Plasma Membrane-Associated Restriction Factors and Their Counteraction by HIV-1 Accessory Proteins. *Cells* **8**, (2019).

265. X. Zhang *et al.*, Identification of SERINC5-001 as the Predominant Spliced Isoform for HIV-1 Restriction. *J Virol*, (2017).

266. S. Sharma, M. K. Lewinski, J. Guatelli, An N-Glycosylated Form of SERINC5 Is Specifically Incorporated into HIV-1 Virions. *J Virol* **92**, (2018).

267. W. Dai, Y. Usami, Y. Wu, H. Gottlinger, A Long Cytoplasmic Loop Governs the Sensitivity of the Anti-viral Host Protein SERINC5 to HIV-1 Nef. *Cell Rep* **22**, 869-875 (2018).

268. J. Shi *et al.*, HIV-1 Nef Antagonizes SERINC5 Restriction by Downregulation of SERINC5 via the Endosome/Lysosome System. *J Virol* **92**, (2018).

269. C. A. Stoneham *et al.*, A Conserved Acidic-Cluster Motif in SERINC5 Confers Partial Resistance to Antagonism by HIV-1 Nef. *J Virol* **94**, (2020).

270. P. de Sousa-Pereira *et al.*, The antiviral activity of rodent and lagomorph SERINC3 and SERINC5 is counteracted by known viral antagonists. *J Gen Virol* **100**, 278-288 (2019).

271. S. Beitari, S. Ding, Q. Pan, A. Finzi, C. Liang, Effect of HIV-1 Env on SERINC5 Antagonism. *J Virol* **91**, (2017).

272. X. Zhang *et al.*, CD4 Expression and Env Conformation Are Critical for HIV-1 Restriction by SERINC5. *J Virol* **93**, (2019).

273. C. Sood, M. Marin, A. Chande, M. Pizzato, G. B. Melikyan, SERINC5 Inhibits HIV-1 Fusion Pore Formation by Promoting Functional Inactivation of Envelope Glycoproteins. *J Biol Chem*, (2017).

274. S. Neil, P. Bieniasz, Human immunodeficiency virus, restriction factors, and interferon. *J Interferon Cytokine Res* **29**, 569-580 (2009).

275. V. Passos *et al.*, Characterization of Endogenous SERINC5 Protein as Anti-HIV-1 Factor. *J Virol* **93**, (2019).

276. B. Murrell, T. Vollbrecht, J. Guatelli, J. O. Wertheim, The Evolutionary Histories of Antiretroviral Proteins SERINC3 and SERINC5 Do Not Support an Evolutionary Arms Race in Primates. *J Virol* **90**, 8085-8089 (2016).

277. M. D. Daugherty, H. S. Malik, Rules of engagement: molecular insights from host-virus arms races. *Annu Rev Genet* **46**, 677-700 (2012).

278. R. Singh *et al.*, Phosphoserine acidic cluster motifs bind distinct basic regions on the mu subunits of clathrin adaptor protein complexes. *J Biol Chem* **293**, 15678-15690 (2018).

279. B. Trautz *et al.*, The Antagonism of HIV-1 Nef to SERINC5 Particle Infectivity Restriction Involves the Counteraction of Virion-Associated Pools of the Restriction Factor. *J Virol* **90**, 10915-10927 (2016).

280. G. V. Gonzalez-Enriquez, M. Escoto-Delgadillo, E. Vazquez-Valls, B. M. Torres-Mendoza, SERINC as a Restriction Factor to Inhibit Viral Infectivity and the Interaction with HIV. *J Immunol Res* **2017**, 1548905 (2017).

281. A. Heigele *et al.*, The Potency of Nef-Mediated SERINC5 Antagonism Correlates with the Prevalence of Primate Lentiviruses in the Wild. *Cell Host Microbe* **20**, 381-391 (2016).

282. A. Chande *et al.*, S2 from equine infectious anemia virus is an infectivity factor which counteracts the retroviral inhibitors SERINC5 and SERINC3. *Proc Natl Acad Sci U S A* **113**, 13197-13202 (2016).

283. S. Li *et al.*, Murine Leukemia Virus Glycosylated Gag Reduces Murine SERINC5 Protein Expression at Steady-State Levels via the Endosome/Lysosome Pathway to Counteract SERINC5 Antiretroviral Activity. *J Virol* **93**, (2019).

284. O. W. Lindwasser, R. Chaudhuri, J. S. Bonifacino, Mechanisms of CD4 downregulation by the Nef and Vpu proteins of primate immunodeficiency viruses. *Curr Mol Med* **7**, 171-184 (2007).

285. J. A. Poe, L. Vollmer, A. Vogt, T. E. Smithgall, Development and validation of a high-content bimolecular fluorescence complementation assay for small-molecule inhibitors of HIV-1 Nef dimerization. *J Biomol Screen* **19**, 556-565 (2014).

286. N. Laguette, C. Bregnard, S. Benichou, S. Basmaciogullari, Human immunodeficiency virus (HIV) type-1, HIV-2 and simian immunodeficiency virus Nef proteins. *Mol Aspects Med* **31**, 418-433 (2010).

287. J. H. Hanna, K. Saha, R. Jaenisch, Pluripotency and cellular reprogramming: facts, hypotheses, unresolved issues. *Cell* **143**, 508-525 (2010).

288. Z. Hanna *et al.*, Nef Harbors a Major Determinant of Pathogenicity for an AIDS-like Disease Induced by HIV-1 in Transgenic Mice. *Cell* **95**, 163-175 (1998).

289. N. J. Deacon *et al.*, Genomic structure of an attenuated quasi species of HIV-1 from a blood transfusion donor and recipients. *Science* **270**, 988-991 (1995).

290. F. Kirchhoff, T. C. Greenough, D. B. Brettler, J. L. Sullivan, R. C. Desrosiers, Absence of intact nef sequences in a long-term survivor with nonprogressive HIV-1 infection. *N. Engl. J. Med* **332**, 228-232 (1995).

291. H. Kestler *et al.*, Importance of the nef gene for maintenance of high viral loads and for development of AIDS. *Cell* **65**, 651-662 (1991).

292. C. Aiken, J. Konner, N. R. Landau, M. E. Lenburg, D. Trono, Nef induces CD4 endocytosis: requirement for a critical dileucine motif in the membrane-proximal CD4 cytoplasmic domain. *Cell* **76**, 853-864 (1994).

293. S. D. Briggs, M. Sharkey, M. Stevenson, T. E. Smithgall, SH3-mediated Hck tyrosine kinase activation and fibroblast transformation by the Nef protein of HIV-1. *J. Biol. Chem* **272**, 17899-17902 (1997).

294. R. P. Trible, L. Emert-Sedlak, T. E. Smithgall, HIV-1 Nef selectively activates SRC family kinases HCK, LYN, and c-SRC through direct SH3 domain interaction. *J. Biol. Chem* **281**, 27029-27038 (2006).

295. S. Tarafdar, J. A. Poe, T. E. Smithgall, The Accessory Factor Nef Links HIV-1 to Tec/Btk Kinases in an Src Homology 3 Domain-dependent Manner. *J Biol Chem* **289**, 15718-15728 (2014).

296. W. F. Li, M. Aryal, S. T. Shu, T. E. Smithgall, HIV-1 Nef dimers short-circuit immune receptor signaling by activating Tec-family kinases at the host cell membrane. *J Biol Chem*, (2020).

297. L. A. Emert-Sedlak *et al.*, Effector Kinase Coupling Enables High-Throughput Screens for Direct HIV-1 Nef Antagonists with Antiretroviral Activity. *Chem. Biol* **20**, 82-91 (2013).

298. L. Emert-Sedlak *et al.*, Chemical library screens targeting an HIV-1 accessory factor/host cell kinase complex identify novel antiretroviral compounds. *ACS Chem. Biol* **4**, 939-947 (2009).

299. J. A. Readinger *et al.*, Selective targeting of ITK blocks multiple steps of HIV replication. *Proc. Natl. Acad. Sci. U. S. A* **105**, 6684-6689 (2008).

300. O. Schwartz, V. Marechal, G. S. Le, F. Lemonnier, J. M. Heard, Endocytosis of major histocompatibility complex class I molecules is induced by the HIV-1 Nef protein. *Nat. Med* **2**, 338-342 (1996).

301. E. A. Pereira, L. L. daSilva, HIV-1 Nef: Taking Control of Protein Trafficking. *Traffic* **17**, 976-996 (2016).

302. K. Janvier *et al.*, HIV-1 Nef stabilizes the association of adaptor protein complexes with membranes. *J Biol Chem* **278**, 8725-8732 (2003).

303. M. V. Gondim *et al.*, AP-2 Is the Crucial Clathrin Adaptor Protein for CD4 Downmodulation by HIV-1 Nef in Infected Primary CD4+ T Cells. *J Virol* **89**, 12518-12524 (2015).

304. A. Rosa *et al.*, HIV-1 Nef promotes infection by excluding SERINC5 from virion incorporation. *Nature* **526**, 212-217 (2015).

305. Y. Usami, Y. Wu, H. G. Gottlinger, SERINC3 and SERINC5 restrict HIV-1 infectivity and are counteracted by Nef. *Nature* **526**, 218-223 (2015).

306. C. Sood, M. Marin, A. Chande, M. Pizzato, G. B. Melikyan, SERINC5 protein inhibits HIV-1 fusion pore formation by promoting functional inactivation of envelope glycoproteins. *J. Biol. Chem* **292**, 6014-6026 (2017).

307. J. Shi *et al.*, HIV-1 Nef Antagonizes SERINC5 Restriction by Downregulation of SERINC5 via the Endosome/Lysosome System. *J. Virol* **92**, (2018).

308. J. A. Poe, T. E. Smithgall, HIV-1 Nef dimerization is required for Nef-mediated receptor downregulation and viral replication. *J. Mol. Biol* **394**, 329-342 (2009).

309. C.-H. Lee, K. Saksela, U. A. Mirza, B. T. Chait, J. Kuriyan, Crystal structure of the conserved core of HIV-1 Nef complexed with a Src family SH3 domain. *Cell* **85**, 931-942 (1996).

310. J. J. Alvarado, S. Tarafdar, J. I. Yeh, T. E. Smithgall, Interaction with the Src homology (SH3-SH2) region of the Src-family kinase Hck structures the HIV-1 Nef dimer for kinase activation and effector recruitment. *J Biol Chem* **289**, 28539-28553 (2014).

311. M. Holmes, F. Zhang, P. D. Bieniasz, Single-Cell and Single-Cycle Analysis of HIV-1 Replication. *PLoS Pathog* **11**, e1004961 (2015).

312. T. K. Kerppola, Bimolecular fluorescence complementation (BiFC) analysis as a probe of protein interactions in living cells. *Annu. Rev. Biophys* **37**, 465-487 (2008).

313. A. Gervaix *et al.*, A new reporter cell line to monitor HIV infection and drug susceptibility in vitro. *Proc. Natl. Acad. Sci. U. S. A* **94**, 4653-4658 (1997).

314. G. Anmole *et al.*, A robust and scalable TCR-based reporter cell assay to measure HIV-1 Nef-mediated T cell immune evasion. *J Immunol. Methods* **426**, 104-113 (2015).

315. M. Pizzato *et al.*, Dynamin 2 is required for the enhancement of HIV-1 infectivity by Nef. *Proc. Natl. Acad. Sci. U. S. A* **104**, 6812-6817 (2007).

316. G. B. Cohen, V. S. Rangan, B. K. Chen, S. Smith, D. Baltimore, The human thioesterase II protein binds to a site on HIV-1 Nef critical for CD4 down-regulation. *J Biol Chem* **275**, 23097-23105 (2000).

317. S. M. Sugden, M. G. Bego, T. N. Pham, E. A. Cohen, Remodeling of the Host Cell Plasma Membrane by HIV-1 Nef and Vpu: A Strategy to Ensure Viral Fitness and Persistence. *Viruses* **8**, 67 (2016).

318. M. Schaeffer *et al.*, Signaling through a novel domain of gp130 mediates cell proliferation and activation of Hck and Erk kinases. *Mol. Cell Biol* **21**, 8068-8081 (2001).

319. H. Shi *et al.*, Tight-Binding Hydroxypyrazole HIV-1 Nef Inhibitors Suppress Viral Replication in Donor Mononuclear Cells and Reverse Nef-Mediated MHC-I Downregulation. *ACS Infect. Dis* **6**, 10 (2020).

320. L. A. Emert-Sedlak *et al.*, Synthesis and evaluation of orally active small molecule HIV-1 Nef antagonists. *Bioorg. Med. Chem. Lett* **26**, 1480-1484 (2016).

321. P. S. Narute, T. E. Smithgall, Nef alleles from all major HIV-1 clades activate Src-family kinases and enhance HIV-1 replication in an inhibitor-sensitive manner. *PLoS. One* **7**, e32561 (2012).

322. G. H. Renkema, A. Manninen, D. A. Mann, M. Harris, K. Saksela, Identification of the Nef-associated kinase as p21-activated kinase 2. *Current Biology* **9**, 1407-1411 (1999).

323. C. H. Hung *et al.*, HIV-1 Nef assembles a Src family kinase-ZAP-70/Syk-PI3K cascade to downregulate cell-surface MHC-I. *Cell Host Microbe* **1**, 121-133 (2007).

324. A. J. T. a. R. B. M. Schasfoort, *Handbook of Surface Plasmon Resonance*. Handbook of Surface Plasmon Resonance (2008).

325. N. E. Davey *et al.*, The HIV mutation browser: a resource for human immunodeficiency virus mutagenesis and polymorphism data. *PLoS Comput Biol* **10**, e1003951 (2014).

326. T. Schindler *et al.*, Crystal Structure of Hck in Complex with a Src Family–Selective Tyrosine Kinase Inhibitor. *Molecular Cell* **3**, 639-648 (1999).

327. M. Porter, T. Schindler, J. Kuriyan, W. T. Miller, Reciprocal regulation of Hck activity by phosphorylation of Tyr(527) and Tyr(416). Effect of introducing a high affinity intramolecular SH2 ligand. *J Biol Chem* **275**, 2721-2726 (2000).

328. H. R. Dorman *et al.*, Discovery of Non-peptide Small Molecule Allosteric Modulators of the Src-family Kinase, Hck. *Front Chem* **7**, 822 (2019).

329. B. O. Yuanfei Wu, Eric R. Weiss, Elena Popova, Hikaru Yamanaka, Heinrich Göttlinger, Potent Enhancement of HIV-1 Replication by Nef in the Absence of SERINC3 and SERINC5. *mBio* **10**, 1071-1019 (2019).

330. C. Bregnard *et al.*, Comparative proteomic analysis of HIV-1 particles reveals a role for Ezrin and EHD4 in the Nef-dependent increase of virus infectivity. *J Virol* **87**, 3729-3740 (2013).

331. M. Li *et al.*, TIM-mediated inhibition of HIV-1 release is antagonized by Nef but potentiated by SERINC proteins. *Proc Natl Acad Sci U S A* **116**, 5705-5714 (2019).

332. S. Semerdjieva *et al.*, Coordinated regulation of AP2 uncoating from clathrin-coated vesicles by rab5 and hRME-6. *J Cell Biol* **183**, 499-511 (2008).

333. A. G. Tebo, A. Gautier, A split fluorescent reporter with rapid and reversible complementation. *Nat Commun* **10**, 2822 (2019).

334. S. D. Briggs *et al.*, HIV-1 Nef promotes survival of myeloid cells by a Stat3-dependent pathway. *J Biol Chem* **276**, 25605-25611 (2001).

335. A. Jarviluoma *et al.*, High-affinity target binding engineered via fusion of a single-domain antibody fragment with a ligand-tailored SH3 domain. *PLoS One* **7**, e40331 (2012).